INVESTIGATION INTO THE POSSIBILITY OF USING PARTIAL DISCHARGE MEASURING EQUIPMENT TO DIAGNOSE FAULTS ON 3,3 KV MACHINES

by

Dennis Raymond Willemse

Thesis submitted in fulfilment of the requirements for the degree

Magister: Technologiae: Engineering: Electrical

In the

Faculty of Engineering, Information
and Communication Technology

at the

Central University of Technology

Supervisor: Mr. P. Hertzog, M.Tech. (Eng.)
Co-Supervisor: Mr. M. Naude, M.Sc. (Eng.)

BLOEMFONTEIN
April 2004

DECLARATION OF INDEPENDENT WORK

I, DENNIS RAYMOND WILLEMSE, hereby declare that this research project submitted for the degree MAGISTER TECHNOLOGIAE: ENGINEERING: ELECTRICAL, is my own independent work that has not been submitted before to any institution by anyone else or me as part of a qualification.

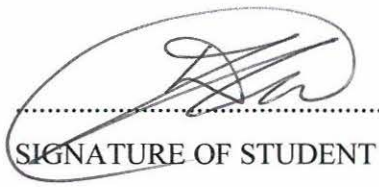

.....

SIGNATURE OF STUDENT

10 Day of APRIL ..2004

ACKNOWLEDGEMENT

I would like to thank the following persons and instances for their help and contribution towards the completion of this project:

My colleagues at Iscor Flat Steel Products for all their technical inputs.

The relevant manufacturers and repairers of electrical machines in Gauteng, for valuable information received from them.

A special thanks to Westward Electric and Iris Power Engineering for the loan of the Partial Discharge equipment.

My wife and family, without whose support, this project would not have been possible.

SYNOPSIS

It is a widely recognised fact that the presence of Partial Discharge activity in machines with an operating voltage exceeding 6,6 kV, enables periodic on-line monitoring of the condition of these machines. Analysis of the discharge activity, can assist maintenance personnel in determining if a winding has become loose, contaminated or if the insulation condition is deteriorating.

However, very little information exists regarding PD activity in machines with an operating voltage of 3,3 kV. Although some studies have been conducted, that dealt with measurement techniques and continuous on-line monitoring of 3,3kV machines, very few investigated the discharge levels or failure mechanisms associated with different types of machines.

Due to the large amount of critical 3,3 kV machines at Iscor Flat Steel Products, it was deemed necessary to investigate the possibility of applying the same techniques to these machines, in order to determine the condition of the windings.

Tests and analysis conducted with a PD Analyser and software manufactured by Iris Power Engineering, indicated that it would be feasible to perform on-line testing of certain 3,3 kV motors.

UITTREKSEL

Dit is alom bekend dat die teenwoordigheid van Gedeeltelike Ontladings aktiwiteite in elektriese masjiene met 'n bedryfspanning van meer as 6,6 kV dit moontlik maak om die toestand van die masjiene aanlyn te bepaal. Wanneer 'n analise gedoen word van die ontladings aktiwiteit, kan die instandhoudingspersoneel bepaal of 'n wikkeling los is, of dit gekontamineer is en of die isolasietoestand besig is om te verswak.

Daar is egter baie min inligting beskikbaar aangaande die Gedeeltelike Ontladings aktiwiteit in masjiene met 'n bedryfspanning van 3,3 kV. Navorsing is al gedoen rondom meet tegnieke en aaneenlopende aanlyn monitering van 3,3 kV masjiene, maar min inligting is beskikbaar oor ontladingsvlakke en falingsmeganismes vir verskillende tipes masjiene.

As gevolg van die groot hoeveelheid kritiese 3,3 kV masjiene by Iscor Flat Steel Products, is daar besluit om die moontlikheid te ondersoek of hierdie tegnieke ook op die masjiene toegepas kan word, sodat die toestand van die wikkelings bepaal kan word.

Toetse en analises wat uitgevoer is met 'n Gedeeltelike Ontladings Analiseerder en sagteware, soos verskaf deur Iris Power Engineering, het aangedui dat dit lewensvatbaar is om aanlyn toetse op sekere 3,3 kV masjiene uit te voer.

ABBREVIATIONS AND SYMBOLS

ECMP	Electrical Condition Monitoring Program
IEEE	Institude of Electrical and Electronic Engineers
Iscor	Iron and Steel Corporation
LPD	Linear Pulse Density
NQN	Normalized Quantity Number
PD	Partial Discharge
PPA	Pulse Phase Analysis
Qm	Peak PD magnitude in Vm at 10pps
RF	Radio Frequency
RTD	Resistance Temperature Detector
SNR	Signal-to-noise ratio
TGA-B	Turbo Generator Analyser Model-B (Specific analyser used)
VPI	Vacuum Pressure Impregnation

TABLE OF CONTENTS

LIST OF FIGURES

Page

LIST OF TABLES

CHAPTER 1 - INTRODUCTION

1.1 Introduction and background

Iscor is a South African company, with its' Flat Steel Products Division based in Vanderbijlpark. For many years, it has successfully operated a **Mechanical Condition Monitoring Program** on all its' critical high voltage motors. This program included vibration analysis, bearing oil sample analysis, thermal scanning etc. In order to ascertain the stator winding condition (and reduce the amount of in service winding failures) of its' high voltage machines, the company has recently introduced an **Electrical Condition Monitoring Program (ECMP).**

This program included the following:

- Installation of on-line Partial Discharge (PD) monitoring equipment on all critical 11 kV machines.
- Acquisition of a TGA analyzer to carry out in-house testing of 11 kV machines.
- Acquisition of the MICAA expert system to be used as a database and training tool.

1.2 The problem and its setting

However, the successful completion of the ECMP on 11 kV machines, still excluded six hundred (also ageing), 3,3 kV machines. All of these machines are an integral part of the plant operation. More than half of the machines are very critical to the plant production processes. Failure of these machines, will lead to reduced production or complete plant shutdown.

A great number of these machines have been in operation for periods exceeding twenty years, without replacement of the stator winding. Because the operational processes will naturally lead to insulation degradation, it can be expected that some of these machines would fail shortly.

1.3 Objective of the research

The purpose of this thesis is to investigate the possibility of using the bus-coupler method to measure PD on 3,3 kV machines, hence to identify all failure mechanisms normally associated with high voltage machines.

1.4 Hypothesis

It is possible to identify failure mechanisms on machines operating at 6,6 kV and above when trending the PD magnitudes, by analysing the graphical representation of PD test results. This method of evaluation shall be used to determine failure mechanisms for 3,3 kV machines. As 3,3 kV machines have a unique winding and insulation arrangement, the suitability of these techniques must be investigated to ensure correct analysis results.

1.5 Research methodology

PD tests will be carried out according to the following conditions:

- Routine testing (after repair of the machine) shall be performed on a test bench, with the aim of studying the effect of load and thus temperature variance.
- Special tests shall also be conducted on the test bench. These machines shall be subjected to accelerated ageing practices and dissected.
- Tests shall be carried out on machines operating in a normal plant environment.

1.6 Assumptions

- The study shall assume that PD measurement is possible and effective, using an Iris Power Engineering PD Analyser and the bus-coupler method of measurement.
- The study shall consider form coil as well as random wound 3,3 kV machines.
- The study shall consider all available 3,3 kV machines (operational and redundant).

CHAPTER 2 – REVIEW OF THE RELATED LITERATURE

2.1 Introduction

Electrical discharges that do not completely bridges the gap between two conductors are called partial discharges [1, p. 5]. Partial discharge measurements have been made on windings of rotating machines for over four decades. Advances made in the last twenty years in electronic noise discrimination techniques has made it possible for engineers to successfully distinguish between PD and noise.

Discharges occur mainly in gas filled cavities inside the insulation, and on the surface of the insulation. The breakdown strength of the cavity depends on its' dimensions and is governed by the type of gas and the gas pressure in the cavity.

Kreuger (using the a-b-c circuit) has discussed partial discharges occurring in gas filled cavities within a dielectric extensively [2, p. 3]. The capacitance of a cavity is represented by a capacitance *c* (Figure 2.1), which is shunted by a breakdown path. The capacitance of the dielectric in series with the cavity is represented by a capacitance *b*. The sound part of the dielectric is represented by a capacitance *a*.

If the circuit is energized with an alternating current voltage, recurring discharging occurs:

- Capacitance *c* is charged,
- Breakdown voltage of the cavity is reached and discharging occurs,
- Capacitance *c* is charged again,
- The cavity discharges again, etc.

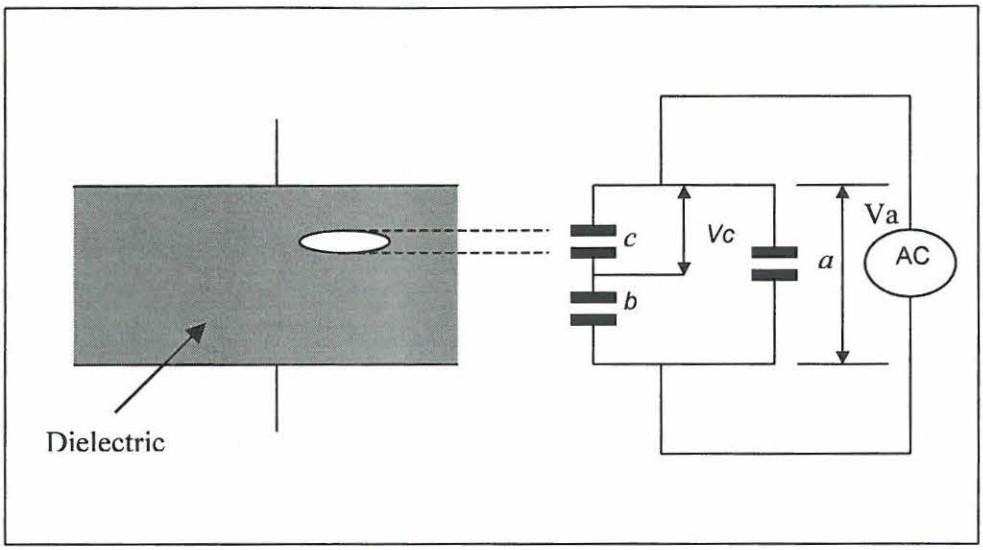

Figure 2.1: Dielectric circuit of insulation

However, recent studies have shown that this approach has limitations that could better be described using electric field theory [9, pp. 239-241]. The resulting electrical field within a dielectric material is the vector sum of two components, namely the Laplacian component and the Poisonian component. The Poisonian induced charge is that component of the induced charge related to the Poisonian field established by the space charge. The Laplacian induced charge is that component of the induced charge related to the Laplacian field associated with the change in conducter potential.

2.2 PD sources in rotating machine windings

Rotating machines have numerous potential sites of PD. Machine design, materials of construction, manufacturing methods, operating conditions and maintenance practices can profoundly affect the quantity, location, characteristics, evolution and significance of PD [1, pp. 7-8]:

- Ground wall delaminations (Figure 2.2) and cavities that develop as a result of machine abuse, thermal ageing, bar vibration and PD erosion may exhibit characteristics that are very different from the characteristics of cavities in new

insulation.

- PD sites may also be present and develop at the interface between the conductors and the ground wall and between the ground wall and the semi-conducting treatment (Figure 2.2), on the surfaces of stator winding elements.
- Other potential sites of PD may occur within girth cracks; mechanical disruptions of insulation caused by overhang heating; sites of impact damage; insulation fractures and abraded areas.
- Slot discharge sites may occur as the result of certain semi-conductive coating conditions that either are present when the machine is new, or develop in operation. These conditions include discontinuities in the semi-conducting slot coating, high resistivity values of the such that it does not function as intended, porosity, separations, migration defects and erosion or abrasion defects.
- Slot discharge sites may also caused by or extinguished by certain types of chemical contamination. It should be noted that because of the wide variation in stator winding constructions, stator bar vibration might not be indicated by PD activity in some machines.
- PD sites may develop at the stress control coating at the slot exit as the result of defects such as electric stress concentrations at the interface between the semi-conducting slot coating and the stress control coating, sites of mechanical damage, or shortened stress control coating.
- PD sites may be present or develop in the stator endwinding beyond the slot because of chemical contamination, floating metal particles, mechanical damage, relative movement of end-winding elements and the spacing between components in the endwinding.
- PD sites external to the stator winding may occur:
  - Near improperly installed RTD cables,
  - On phase connection rings because of vibration, mechanical damage, or relative movement,
  - Within high–voltage bushings,
  - On surfaces of high–voltage bushings, caused by contamination,
  - On phase leads, bus bars, or connection straps,

- Within surge capacit
- Within isolated phase bus duct.

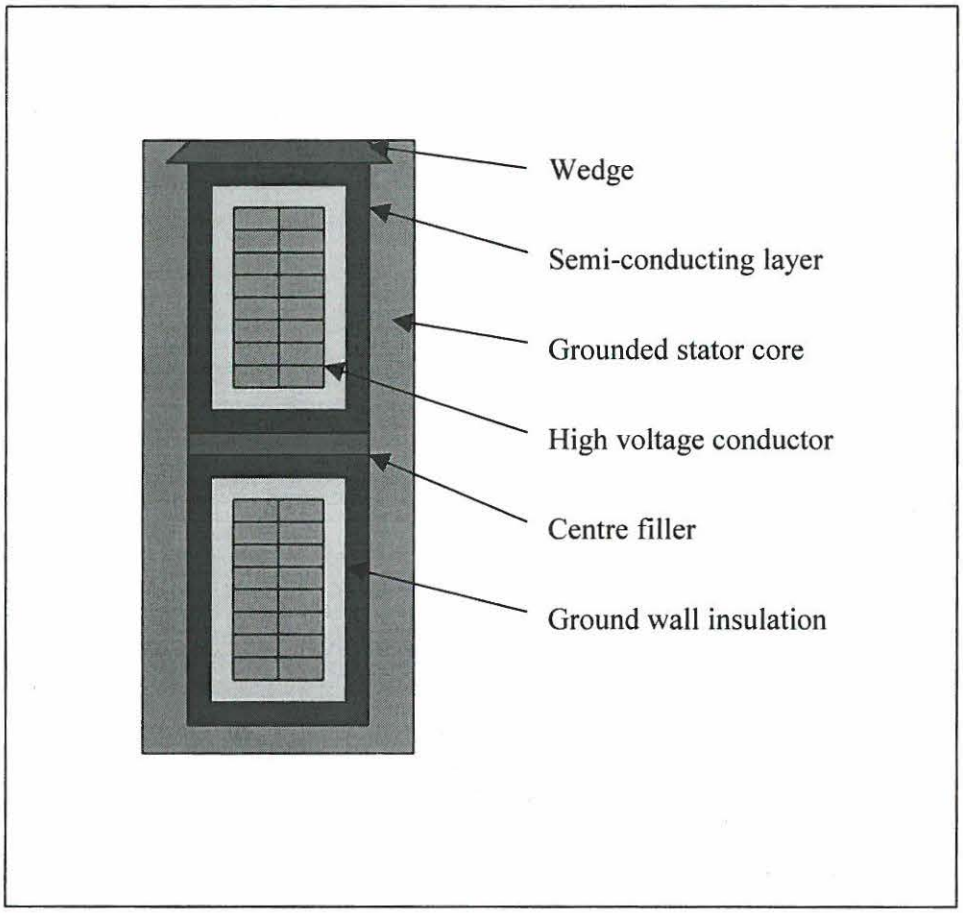

Figure 2.2: Insulation composition of a form coil

2.3 Overview of Partial Discharge detection methods

Partial discharges are accompanied by several physical manifestations: Electrical pulse and resulting radio frequency (RF) pulse, acoustic pulse, light, as well as chemical reactions within the cooling gases that are either air or hydrogen. The following sub-clauses are a summary of how some of these manifestations can be measured, as a

means of quantifying the PD in a stator winding or individual coil or bar [1, pp. 9-12].

2.3.1 Electrical pulse sensing

Because PD involves a flow of electrons and ions across a small distance in a finite period of time, a small current flows every time the PD occurs. The total current will be governed by the transport of a certain number of Pico coulombs of charge. The current flow creates a voltage pulse across the impedance of the insulation system.

One of the primary means of detecting PD is to measure the small voltage pulse that accompanies every PD, or the resulting current pulse. These quantities are measured in circuits remote from the PD. Note that in a typical coil, bar or winding, there may be hundreds of discharges per second, thus many hundreds of electrical pulses may be detected each second.

The voltage pulse can be detected by means of high–voltage capacitors, which are normally connected to the phase terminal or elsewhere in the winding. The capacitor impedance is high at rated power frequency, but is low at the high–frequency signal of the PD voltage pulse.

Alternatively a current transformer, with an high frequency rating, can be installed on the lead that connects the neutral of the machine to the grounding impedance, on the phase leads or in other suitable locations to detect the pulse currents accompanying the PD.

The outputs from the capacitors or current transformer are respectively voltage or current pulses, which can be measured with an oscilloscope, spectrum analyser, or pulse height analyser.

2.3.2 Radio frequency radiation sensing

In addition to creating voltage and current pulses within the stator winding, the discharge spark also creates some RF electromagnetic waves that propagate away from the discharge site. The electromagnetic disturbance created by a PD has RF components from 100 kHz to several hundreds of MHz.

AM radios with a suitable antenna can therefore be used to sense that PD activity is occurring. If a directional RF antenna is used, it is sometimes possible to locate the sites of PD activity within the stator winding.

2.3.3 Power-factor tip up

Because each PD is accompanied by acoustic and RF emissions as well as light, it follows that each PD event absorbs a certain amount of energy. The energy dissipated in the PD pulse must therefore be supplied from the source of power frequency voltage, and it can be considered as an increase in dielectric loss in the stator winding. Thus, an indirect means of measuring the total discharge activity in a coil or winding is to measure the dissipation or power factor of the insulation at low voltage (below the PD inception voltage) and at high voltage (where the presence of any PD will increase the dielectric losses).

A large power–factor tip–up[1] may be indicative of severe PD activity in the coil, bar, and winding. However, especially for coils at or bars with lower tip–up, a correlation between tip–up values and PD activity should not be expected.
Stress control coatings on the end arms of coils or bars can be the cause of increased tip-up, especially for installed windings, in which it is not practical to use guard electrodes.

[1] The power factor at high voltage minus the power factor at low voltage.

2.3.4 Energy/integrated charge transfer

An alternate power frequency approach to that described earlier is the measurement of the energy and integrated charge transfer that results from PD activity. These methods, A and B, are detailed in ASTM D3382–95. In method A, the power loss attributed to the PD activity is calculated from measurements of capacitance and dissipation factor obtained using a conventional high–voltage Capacitance Bridge.

2.3.5 Ozone detection

In air–cooled machines, the presence of discharges on the surface of the coils or bars causes chemical reactions in the adjacent air. One of the by-products of the chemical reactions is ozone. Ozone is a gas with a characteristic odour. The concentration of the ozone increases if there is substantial surface PD activity. Internal PD well within the ground wall insulation or adjacent to the copper conductors in form–windings will not create measurable ozone.

There are several means of measuring the ozone concentration, including inexpensive chemical tubes and electronic sensors. The concentration of ozone is affected by the temperature and humidity of the environment as well as the air–flow rate. It may also be related to machine load and power factor. The sampling location is critical. Though it may be possible to detect ozone during off–line testing, it is primarily useful as an on–line monitoring tool.

2.3.6 Acoustic and ultrasonic detection

Each PD creates a small "shock wave" caused by a rapid increase in temperature of gas in the immediate vicinity of the PD. This small shock wave in turn creates acoustic noise. When many PD pulses are occurring on the surface of the stator coils, "frying bacon," sound results.

The acoustical noise occurs in the frequency range of several hundred Hz to 150 kHz, with most of the acoustical energy occurring around 40 kHz. Directional microphones

can be used to measure the PD sound level, as well as to locate where the surface PD may be occurring. Note that the acoustical noise will not be detected if the PD activity is within the ground-wall unless the activity is especially great.

The method can also be used in conjunction with fibreglass rods that acts as acoustical wave-guides and provide electrical isolation between the component being tested and the detector.

2.3.7 Black-out test

A common means of determining the presence and location of surface discharges is to energize the coil/bar or winding under conditions of complete darkness and conduct a visual inspection from a safe distance.

Alternatively, under conditions of reduced light, ultraviolet detection equipment may be used. In the case of installed windings, the black-out test is primarily useful for detecting and locating surface discharges that involves the stress control coating, air gaps associated with the end arms of coils/bars that are subjected to phase-to-phase voltage, or supports associated with the circuit ring bus.

The blackout test may also be useful for locating girth cracks or slot discharge activity involving individual coils/bars. Some disassembly may be necessary to facilitate the visual inspection. A 50 Hz or 60 Hz variable voltage supply is desirable for applying the test voltage. In order to locate some discharge sources, it will be necessary to be able to energize one phase at a time with the others grounded.

2.4 Measurement techniques used

2.4.1 PD pulse shape

Partial discharge pulses have an extremely fast rise time and short pulse-width. Most PD detection devices only detect the initial pulse, which has a rise time of 1-5 ns, with

corresponding frequency ranges of 50-250 MHz [3, p. 23].

2.4.2 PD sensors

In order to detect the PD pulse, a sensor must be installed near the source of the PD. The sensors used for this research were 80 pF Capacitive Couplers. These couplers block the 50 Hz signal and pass the high frequency PD signal. It is connected to the terminals of the winding, which is close to the line-endwindings where PD could be expected [16, p. 7].

2.4.3 Measurement system

The system used for this research made use of electrical pulse sensing, specifically Directional Time-of-Arrival-Noise Cancellation, and is a product of Iris Power Engineering of Canada. The analysing instrument is called the TGA-B™ (Turbine Generator Analyser-Model B).

Figure 2.3 is a graphical representation of a connection configuration for a directional pulse discrimination system. For this directional installation the machine side coupler (M) was placed as close as possible to the junction between the line-end coil and the supply cable or circuit ring bus.

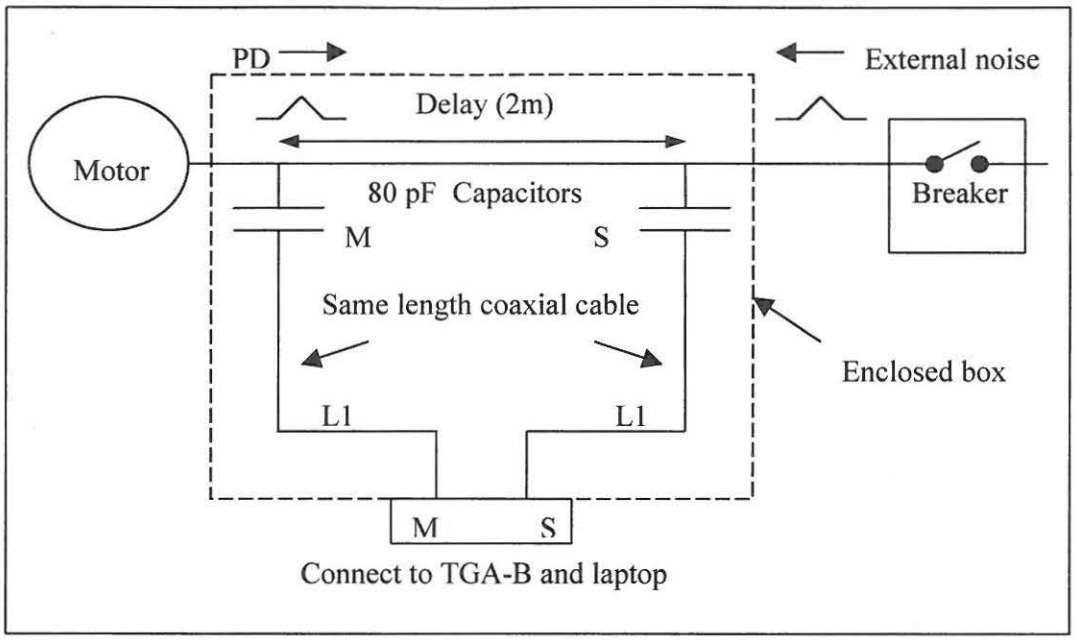

Figure 2.3: Directional Time-of-Arrival Noise Cancellation method

The second system side coupler (S) was placed two meters away from coupler M. The coaxial cables that connected the secondary side of the couplers to the Analyser were of the same length. Calibration involves measuring the delay time[2]. In directional installations, the PD signal and the system noise signal arrives at the two couplers from opposite directions and arrives from the same direction at the end of both coaxial cables.

The TGA-B™ separates the pulses according to the following time-of-arrival criteria:

- L1 represents the time in nanoseconds that it takes a pulse to travel through the coaxial cables. As the coaxial cables are the same length, the travel time L1 is equal from both couplers.
- The TGA-B™ compares the Time–of–Arrival of pulses at the two couplers in a phase. If a pulse is first detected at coupler M (closest to the stator winding), the pulse is assumed to be caused by stator PD and should be counted. However, if a

[2] Delay is the time in nanoseconds it takes a fast rising time pulse to travel along a bus between the two couplers.

pulse is first detected at coupler S (closest to the power system), the pulse is due to noise and should be classified as noise.

- Similarly, arcing or discharges that arrive at coupler S and then at coupler M indicates that noise is occurring within the cable or bus, perhaps from poor connections or PD, and should be counted and classified as bus noise.

The TGA–B™ compares pulse arrival times from the pair of bus couplers per phase, automatically determines which pulses are due to PD from the stator and determines the magnitude, number and phase position of such pulses.

CHAPTER 3 – PD CHARACTERISTICS OF FAILURE MECHANISMS

3.1 Relationship between PD pulse polarity and discharge location

3.1.1 Cavities at the interface between the conductor and the ground-wall insulation

When negative polarity pulses[3] predominate, the source of the PD can be expected to be at or near the copper conductors (Figure 3.1), and may indicate an incomplete bond between the insulation and the copper. In the case of multi–turn coils there may be an inadequate bond between the turn insulation and the ground wall [1, p. 40].

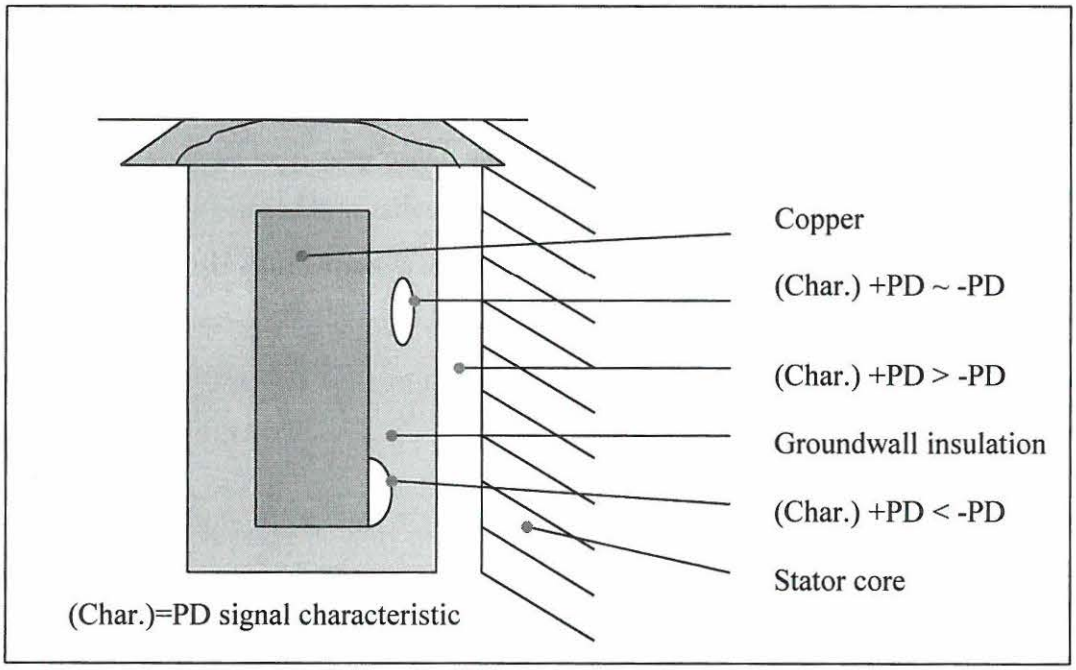

Figure 3.1: Pulse polarity based on cavity location

[3] Negative polarity pulses occur mainly during the positive cycle of the system phase-to-ground voltage waveform.

Unlike a cavity in the bulk of the insulation, metal and dielectric covered electrodes bound this defect. The discharge mechanism as discussed in section 2.1 still apply. However, the system is no longer symmetrical, in the sense that the electrodes are comprised of dissimilar materials. This asymmetry produces a polarity effect, which results in the predominance of negative PD pulses. Such a result can be predicted from gas discharge theory and some consideration of the charge mobility on the electrodes [5, p. 5].

On the insulating surface, the mobility of the positive ions is much lower than that for negative species. Consequently, when the conductor is at high voltage, PD will occur preferentially on the positive half–cycle of the phase-to-ground voltage waveform, as negative species will be pushed out into the gas gap towards the positively charged insulating surface.

The conductor is at a higher voltage potential than the insulating material surrounding it during the positive half cycle of the phase-to-ground voltage waveform with the result that the predominance of negative ions on the conductor surface migrate through the gap (caused by the void) towards the more positively charged insulation surface.

The negative PD pulses refer to the direction of flow of current, which is negatively charged ions.

Observation of negative polarity dependence usually indicates that the bond between the conductor stack and the ground wall insulation is deteriorated.

3.1.2 Cavities near iron core

When positive polarity PD pulses[4] predominate in magnitude, the source of the PD

[4] Positive polarity PD pulses occur mainly during the negative half–cycle of the system phase-to-ground voltage waveform.

likely involves the external semi–conducting coating on the slot section or the stress control coating of the coil. In the case of air-cooled machines, such discharges may be accompanied by the production of ozone [1, p. 40].

This phenomenon is a surface discharge, which takes place between the surface of the stator coil and the iron core. Discharges in the slot can result from two principal processes. In one mechanism degradation of the semicon coating, due to coil movement causing abrasion or lack of adhesion of the semicon coating due to chemical attack, can result in isolated patches of semicon coating or bare patches of the stator insulation [5, p. 5].

These areas will tend to charge up and depending upon the dimensions of the gas gap, can result in a discharge. Alternatively, or in concert with the above mechanism, excessive bar movement due to weakening of the slot support system can also cause slot discharge. This particular phenomenon is extremely dangerous for stator insulation.

Again, this geometry is asymmetric and hence a polarity effect will be observed. In this case there will be a predominance of positive PD pulses. This is because, unlike the above situation for the defect at the conductor/insulation interface, the metallic electrode is grounded. Consequently, the relatively immobile positive space charge on the surface of the stator insulation will result in localised breakdown occurring predominantly on the positive half–cycle.

The iron core is at a higher voltage potential, relative to the insulating material (which surrounds the conductor) adjacent to it, during the negative half-cycle of the phase-to-ground voltage waveform, with the result that the mobile negative ions in the iron core migrate towards the more positively charged insulation material.

3.1.3 Voids in the bulk of the insulation

A partial discharge will occur across a void within the insulation material when both an over voltage in the void exists and a free electron or ion is present. When the voltage

across the void exceeds the breakdown voltage of that insulation material (which is some composition of air) the partial discharge occur and the voltage across the gap will stabilize at a level required to sustain the discharge activity. During this process the charges within the void will redistribute according to the applied voltage. As the ac voltage cycle reverses polarity, these charges will cause another over voltage, but in the opposite polarity, resulting in another partial discharge, but the flow of electric charges (current) is in the opposite direction. If both sides of the void consist of the same insulation material, then the charge distribution will be equal during the positive and negative cycles of the voltage waveform. These partial discharge pulses will clump at the classic positions for the phase-to-ground dependant pulses, which is negative pulses at 45° for the positive half-cycle of the phase-to-ground voltage and positive pulses at 225° for the negative half-cycle of the phase-to-ground voltage.

3.1.4 Endwinding discharges

Contamination or inadequate spacing between endwindings of two different phases can lead to partial discharge in that area. Unlike the previously described discharge pulses that are phase-to-ground voltage dependant, this discharge mechanism is phase-to-phase voltage dependant. There is a 30° phase shift between the phase-to-ground voltage and the phase-to-phase voltage, with the result that the discharge activities will be dominant at 15° and 75° (45°+ and -30°) and 195° and 255° (225°+ and -30°) when the phase-to-ground voltage is taken as the reference voltage.

3.2 Load effect

If test data are taken at load conditions that differ by at least 40%, it may be possible to ascertain the effects of magnetic forces on coil vibration. For loose windings PD can be extremely load dependant, with the positive PD increasing with the load. This is due to the increase in magnetic forces ($F \propto I^2$) causing an increase in coil movement and thus surface (positive) PD activity. The effect is most significant with loose thermoset windings such as epoxy-mica insulated windings [1, p. 41][3, p. 63] & [13, p. 3].

3.3 Temperature effect

The operating temperature of the machine can greatly affect the results from a partial discharge test. Various materials respond differently to changes in temperature [1, p. 42].

3.3.1 Negative temperature effect

The sizes of voids within a stator winding are usually inversely proportional to the operating temperature. As the temperature increases the copper and ground wall material expand, closing voids and thus decreasing PD. The greater the temperature effect, the more the internal delamination [3, p. 64].

3.3.2 Positive temperature effect

It may also be possible that positive PD actually increases with temperature. This phenomenon is frequently an indication of deterioration of the semicon/grading coating. As the temperature of the stator winding increases, the resistance of the coatings increases, and results in an increase in surface (positive) PD activity [3, p. 64].

3.4 Specific failure mechanisms

The following sub-paragraphs are a discussion of the phase-angles at which discharges would occur for specific failure mechanisms of machines with a stator voltage of 6,6 kV and higher.

3.4.1 Thermal deterioration

Thermal deterioration results from operating an insulation system for long periods near its design maximum, or for shorter periods above the design limit. Its' discharge position is known as the ***classical position*** of PD. In general negative PD pulses normally occur between 0° and 90° of the ac cycle and positive PD occur between 180°

and 270°, while most PD mechanisms will produce a peak in partial discharge activity at about 45° and 225° [4, p. 4] & [6, pp. 5-8].

Voids are distributed throughout the insulation and may discharge regardless of the "direction" of electrical stress across them. Therefore, a more or less equal distribution of positive and negative discharges at the classic position is indicative of general thermal deterioration or ageing. The extent of the change in PD with temperature, is dependant on the degree of delamination that may be present. There is little change in PD with load.

3.4.2 Phase-to-phase PD activity

Several PD sources may be found in the endwinding part of the winding of a rotating machine. Most of the discharge phenomena experienced on the endwinding, give rise to surface discharges. Since the fields in the endwinding are phase-to-phase dependent and the electrical fields in the slot area are phase-to-ground voltage, it is possible to distinguish between discharge activity occurring in the slot part and the endwinding part, by using the Pulse Phase Analysis plot. Phase-to-phase dependant PD will be shifted by ± 30° [7, p. 576]. Figure 3.2 and Figure 3.3 could explain this 30° shift in the phase angle of the discharges [8, p. 17].

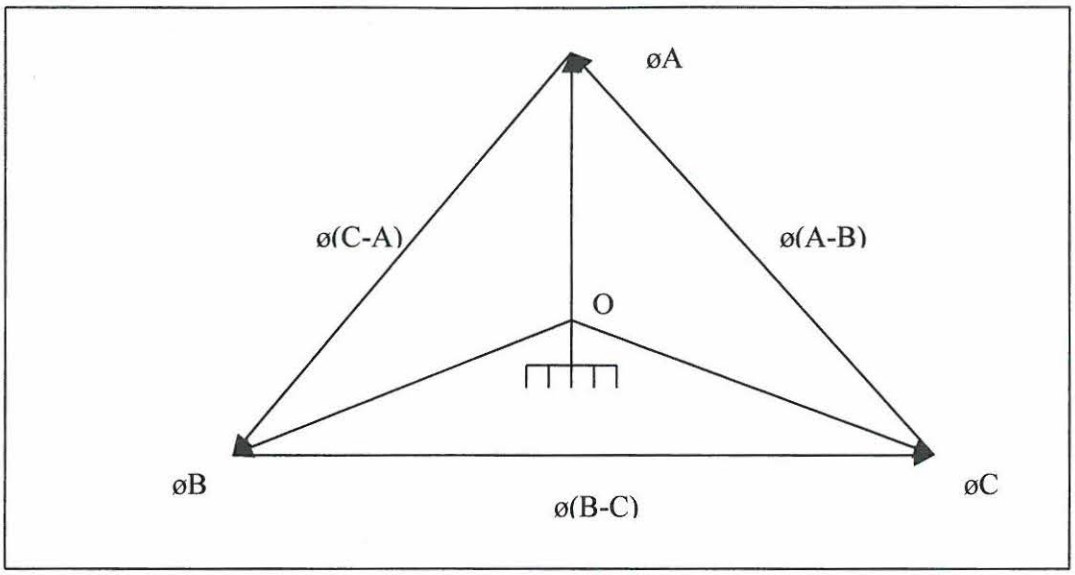

Figure 3.2: Three- phase vector diagram of a rotating machine

Figure 3.2 shows the classical vector diagram of a three phase rotating machine. Three vectors, øA, øB and øC, electrically rotated 120° apart, represents the line to ground voltages of phases A, B and C. The phase-to-phase dependant voltages are represented by the vectors ø(A-B), ø(B-C) and ø(C-A). By shifting the phase-to-phase vectors to originate in point O, and by concentrating on phase vectors related to phase-A, Figure 3.3 may be created.

Figure 3.3 shows the electrical field between phases C and A in the endwinding area, represented by vector ø(C-A), to be shifted +30° from the phase-to-ground field in the slot of phase A, represented by vector øA. The electrical field between phases B and A, represented by vector ø(A-B), is shifted -30° from øA.

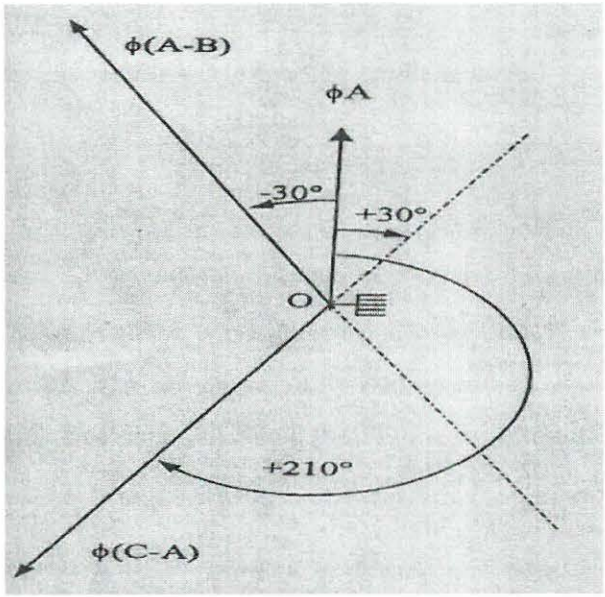

Figure 3.3: Multiple vector diagram

3.4.3 Loose Coils

Unattended loose coils will lead to abrasion of the surface coatings of the coil. Damaged surface coatings may lead to discharges in the slot. As a result, discharge that occur from loose coils are predominantly surface type PD within the slot portion of the core and therefore positive and centred at 225°. If the stator coils become loose in the slot, the positive polarity PD pulses can be expected to have at least twice the magnitude and ten times the repetition rate of the negative polarity pulses [1, p. 40]. The condition is more pronounced during on–line tests at high load. Loose coils have a negative temperature effect.

3.4.4 Electrical slot discharge

Slot discharge is the term given to discharges that occur between the surface of the coil and the stator iron. The PD pattern for slot discharge is similar to loose coils, with positive PD at 225° predominating with a negative temperature effect. There is no noticeable load effect [3, p. 70].

3.4.5 Inadequate spacing between coils

This source of PD, results in activity that is phase-to-phase dependent and therefore 30° shifted from the classic positions. Since this activity is frequently isolated to a specific area of the winding, the PD pattern may reveal which phases are involved. This is only possible if the two affected phases both have detectable endwinding activity and their respective 30° phase shifts correspond to what would be expected according to the machine rotation. Since the PD may occur between the top and bottom coil in a slot, visual verification of the activity may be difficult [3, p. 70].

3.4.6 Improper impregnation

When resin, tapes impregnation processes and other factors come into play during the winding manufacturing, voids may be left entrapped within the winding. These voids are scattered throughout the insulation without dominance of voids at either the copper or the core. There is no noticeable polarity predominance of the PD activity centered at 45° and 225°. This mechanism has a negative temperature effect but no changes with load [3, p. 70].

3.4.7 Semicon/grading coating interface deterioration

PD that occurs at the semicon/grading coating interface, is surface type activity that is phase-to-ground voltage dependant. The activity is predominantly positive and centered at 225°. The materials involved in this area, are primarily conductive by design and conductivity changes with temperature. Therefore, an increase in temperature can lead to an increase in PD activity. If a PD pattern is predominantly positive, centered at 225°, and increases with temperature, it is most likely from the semicon/grading coating interface deterioration [3, p. 71].

CHAPTER 4 – INTERPRETING TGA RESULTS

The TGA software has been specially designed to facilitate interpreting the partial discharge activity in the stator winding, i.e. determining the condition of the stator winding insulation [6, pp. 5-4]. Since the trend in PD activity over time, and the relative activity between identical machines is the key to interpreting results, special plots have been created.

4.1 PD view software

The PD View software contains the following two standard graphical presentations of the PD data captured:

4.1.1 Pulse height analysis

The main display presented by the PD View software, after completion of each PD test per phase, shows 2x two–dimensional plots (Figure 4.1).

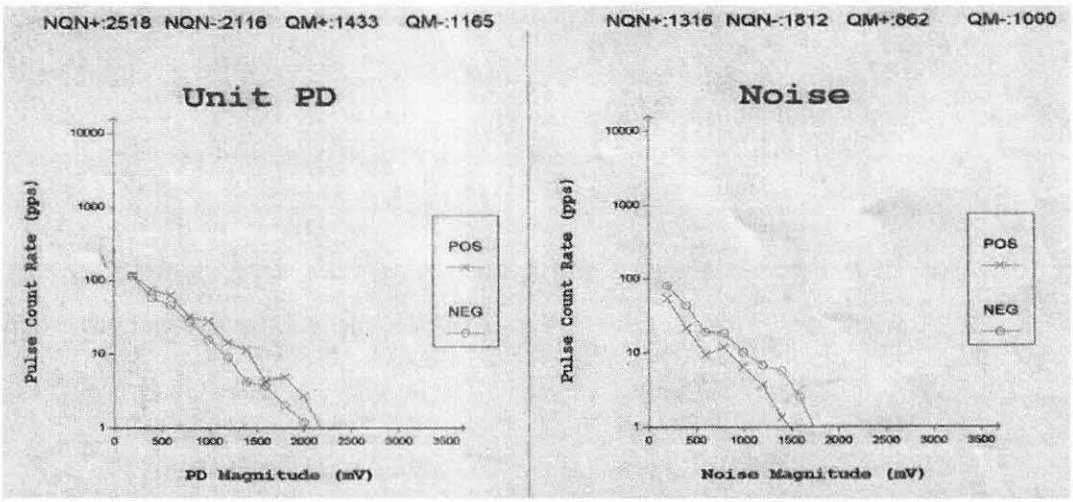

Figure 4.1: Pulse height analysis of PD

Each of these plots is referred to as a pulse height analysis. The plots show the number

of partial discharges per second (vertical scale), versus the magnitude or height of the pulses (horizontal scale), as recorded by the TGA during the most recent test on a specific coupler.

The left plot is the pulse height analysis for all the partial discharge activity in the indicated phase of the winding. The right plot shows the total electrical noise from the power system.

Two lines are plotted on each pulse height analysis graph. One line indicates the partial discharge activity from positive partial discharge pulse. The other line is the negative partial discharge activity.

Qmax (QM) is called the peak PD magnitude – it is a statistical value, defined as the magnitude corresponding to a partial discharge repetition rate of 10 pulses per second. Qmax relates to how severe the deterioration is in the worst spot of the winding.

NQN is called the total PD activity – it is another statistical value, which is a normalised quantity number, which is proportional to the total amount of deterioration monitored and is similar to the power factor tip-up test.

Qmax indicates PD at the worst place whilst NQN indicates how widespread the PD activities are.

Polarity predominance is present when there is a clear separation of the positive and negative graphs or a ratio of +Qmax/-Qmax > 1.5 or –Qmax/+Qmax > 1.5.

4.1.2 Pulse phase analysis

The second type of plot (Figure 4.2) is three-dimensional. These plots show the number (vertical scale) and magnitude (scale coming out of the page) of the PD versus the ac phase angle (horizontal scale).

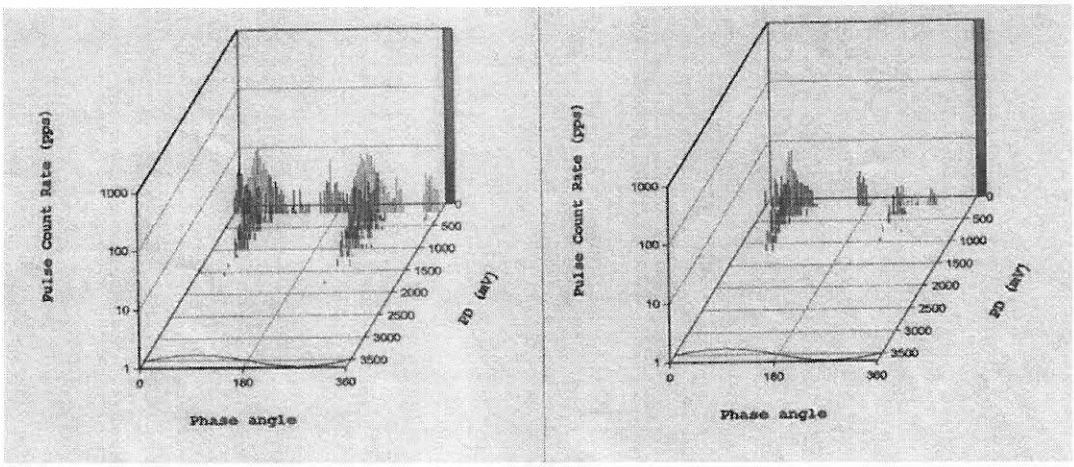

Figure 4.2: Pulse phase analysis of PD

During data collection, each cycle is divided into 100 phase windows to enable displaying of data relative to the specific phase-to-ground voltage reference.

4.2 Advance view software

The Advance View data contains a variety of plots and allows for data manipulation, which can enhance PD interpretation. For this thesis, only the Polar plot and the Linear Pulse Density plot were considered.

4.2.1 Polar plot

The Pulse Phase data can with the help of the Advance View software be displayed as a polar plot (Figure 4.3). This makes the recognition of the phase angle of the discharges much easier. Discharge angles can also be measured more accurately.

The classical pulse positions are at 45° and 225°. Phase-to-phase PD activities are usually 30° shifted from the classical positions. Pulses at phase-to-ground zero crossings, 0° or 180° are usually from a source that is affected by mechanical vibration, such as a loose connection. There is however some controversy about the cause for discharges at the zero crossings.

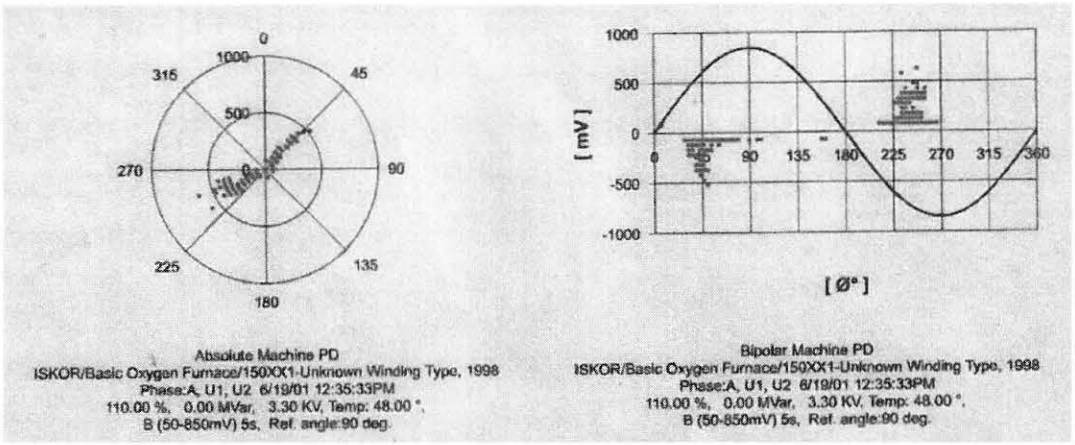

Figure 4.3: Polar plot of PD

4.2.2 Trend plots

The first comparison made during any test analysis and evaluation is to compare the results of the current test with any previous test results. If the operating parameters (load, temperature, voltage, etc.), is the same as those of the previous test, then a direct comparison can be made between the two test results. If the PD is increasing between test results, there is most likely a decline in the condition of the stator winding insulation system (Figure 4.4).

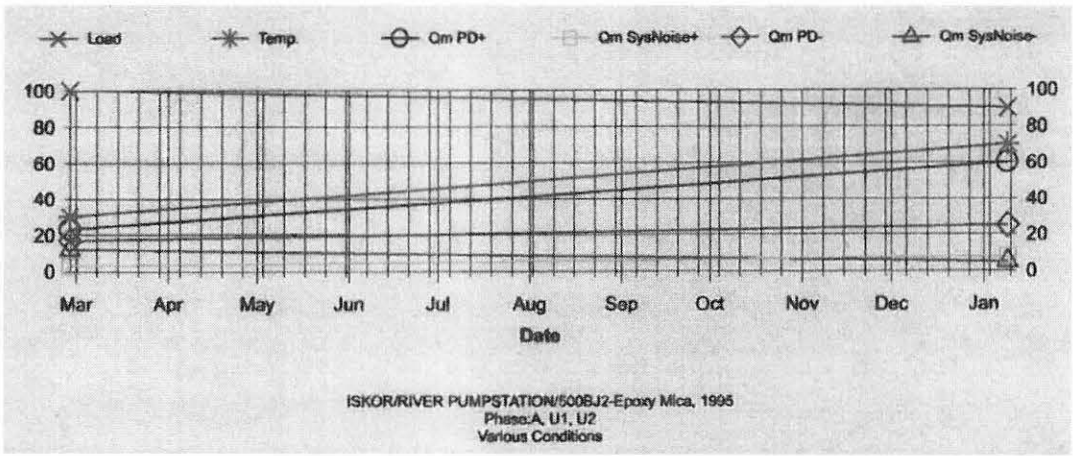

Figure 4.4: Trend plot of PD

4.2.3 Linear pulse density plot

The Linear pulse density plot (Figure 4.5) presents PD pulse magnitude, and pulse repetition rate, as a function of reference phase angle and thus provides a means of Pulse phase analysis.

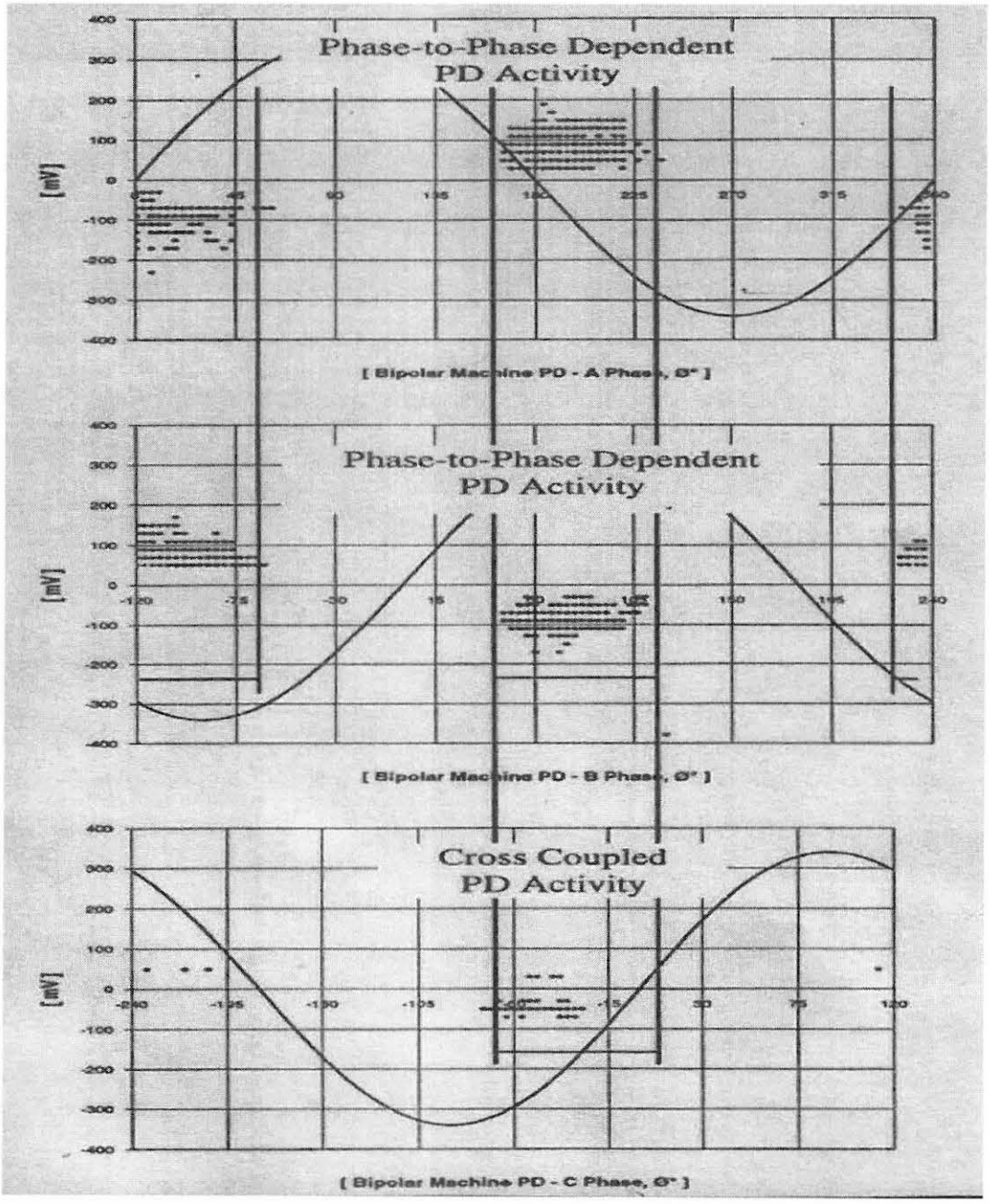

Figure 4.5: Linear pulse density plot

In pulse phase analysis, the reference voltage usually chosen for a given measurement is the phase-to-ground voltage of the phase subjected to on-line testing. By creating a linear pulse density plot for each phase of a given machine, with the reference phase-to-ground voltage shifted 120° between phases based on phase rotation, the discharge activity will be present in the time domain. Phase-to-phase PD should then be easily recognizable. Due to the fact that the phase rotation for the tests conducted for this research was not always known, linear pulse density plots for both A-B-C and A-C-B rotations were included where possible.

CHAPTER 5 – COIL CONSTRUCTION AND INSULATING SYSTEMS

5.1 Coil construction

5.1.1 Form wound windings

Form wound windings (Figure 5.1) consist of preformed square conductors, with multiple insulation layers. The bare conductor strands are normally covered with an insulating film to serve as strand insulation. A certain amount of strands are then bundled together and insulated to provide dedicated turn insulation. The turns are again bound together by insulation that provides the ground wall insulation. All of these sub-parts of the insulation system will contain Mica in some or other form.

Mica is a mineral silicate, appearing in nature in a form that can be split into ever-thinner sheets. It is the best insulating material found. All quality insulating systems for medium-voltage motor coils contains Mica and usually fibreglass, since neither material is damaged by Partial Discharges from voltage stress.

The slot portion of the coil is normally taped (or painted) with a semi-conductive material that grounds the coil in the slot [11, p. 6]. It is important that the resistivity values are within the specific band for the motor operation conditions. The coil must thus provide a low-resistance connection between the coil and the stator slot to prevent electrical discharge.

With the objective of controlling the stress voltage at the end of the core, a painting (or tape) of silicon carbide is normally applied on the ground wall insulation, overlapping the semicon [11, p. 6] & [12, p. 1]. This non-linear grading coating, allows the voltage on the surface of the coil in the endwinding to gradually taper off to the minimal voltage at the semi-conductive coating, thus eliminating discharge at the semi-conductive coating.

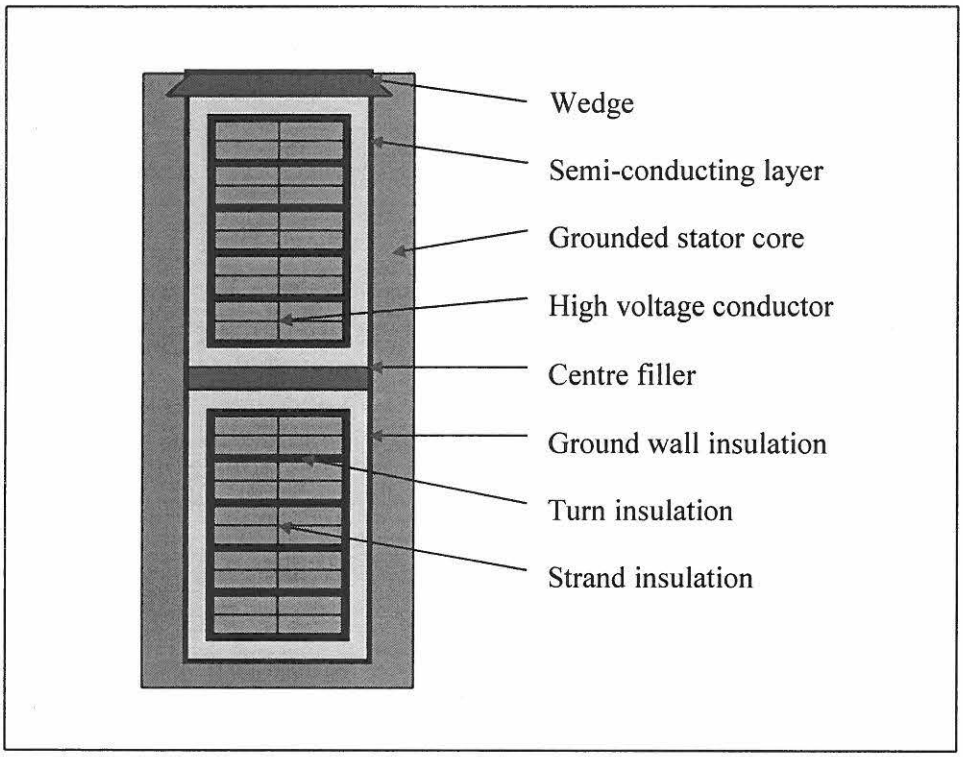

Figure 5.1: Construction of a Form coil

5.1.2 Random wound windings

In contrast with form wound windings, random wound windings (Figure 5.2) have less turn insulation (enamel coating), irregular turn arrangements in slot (hence the name "random") and relatively large and frequent air gaps between the turns/strands are more difficult to fill with resin [10, p. 3].

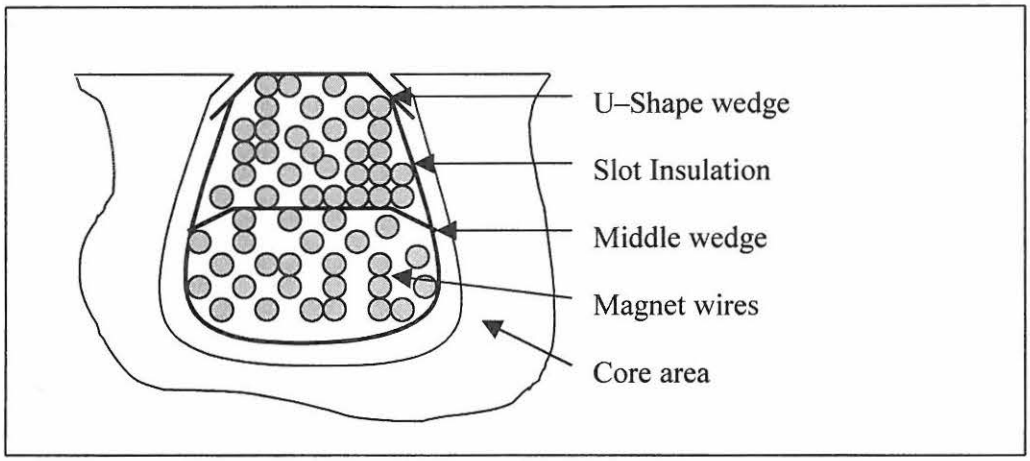

Figure 5.2: Construction of a Random wound coil

5.2 Insulating Systems

5.2.1 Dip

This process is normally used for random wound machines. The machines are dipped into an insulating varnish consisting of resinous material and a thinner. The thinner reduces the viscosity of the resinous material to improve its coating and impregnation capabilities. During the baking cure of the varnish, the thinner, which is an aromatic, evaporates, leaving a tough insulating film that improves the dielectric, mechanical and moisture resistance. However, when the varnish evaporates, voids in the insulation remain. These voids can allow partial discharges to develop, which can then result in coil failure.

5.2.2 Vacuum pressure impregnation

This is currently the most used impregnation system. The great advantage of the VPI system is the removal of all the air from the insulation layers during the vacuum cycle. All air spaces are filled with resin as it is introduced into the tank to flood the winding. Pressure is introduced to force the resin into all unfilled spaces in the insulation and coil structure. The pressure is also used to return the excess resin to the storage tank and the

coils, now filled with resin, are cured at an elevated temperature in an oven.

5.2.3 Resin-rich (B-stage) system

An alternative to the VPI system is the resin-rich insulation system. The Mica tapes are made with partially cured (or B-stage) tapes. The tapes contains a surplus of resin, hence the name Resin-Rich [14, p. 211].

Coils manufactured with the Resin-Rich system are cured in a hot press to manufacturing tolerances. The temperature of the press is hot enough to cause the resin to flow, hopefully filling all air spaces to eliminate voids or air pockets in the coils. Excess resin usually flows axially into the end-winding region of the coil.

One advantage of the Resin-Rich system is that the resin viscosity needed for good impregnation is not a factor in the design of the insulation system.

CHAPTER 6 – METHODS AND TECHNIQUES

6.1 Devising a method of testing 3,3 kV machines for research purposes

An investigation into existing literature regarding PD measurement on 3,3 kV machines have shown that due to the low levels of discharge activity encountered, an instrument was developed by Iris Power Engineering for continuous monitoring [17, pp. 1-6][19, p. 2][20, pp. 1-6] & [18, pp. 1-13] called the Motortrac system. Purchasing a Motortrac system was not an economically viable option and performing Partial Discharge testing on 3,3 kV machines (for research purposes) came down to three possible options:

- Installing PD bus-couplers on all machines earmarked for testing:
  - This idea was rejected outright because of the high cost it would entail. The PD couplers were very expensive in relation to the machines that they were intended to protect (especially if there were insufficient prove of their success on 3,3 kV machines).
- Installing bus-couplers on a machine before testing, and removing it afterwards. This idea were rejected due to the following time constraints:
  - Time required for installing the couplers before a test and removing them afterwards (Normally a day).
  - Obtaining down time from the plant for the installation and removal of the couplers on-site.
- To build a portable PD test kit that could be connected into a circuit, perform tests, and be removed from the circuit again.

It was decided to proceed with option three.

6.1.1 Constructing a portable test kit to perform temporary PD testing

Portable test kits, which contained two epoxy-mica capacitors (placed two meters apart) per phase, were designed and constructed by the author. Figure 6.1 shows the original

test kit, which was later redesigned (Figure 6.2) to improve safety and operating conditions.

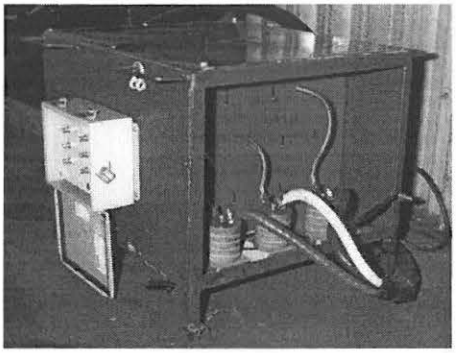

Figure 6.1: Original portable test kit

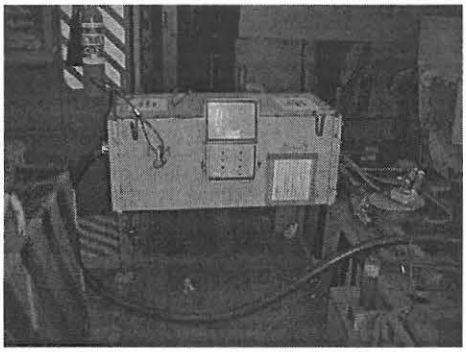

Figure 6.2: Improved portable test kit

6.2 Testing techniques

In order to study the effect of load, temperature variance, accelerated ageing and contaminants on the machines, the following type testing was performed:

- Routine tests were performed on repaired machines at the Test Floor, with the aim of studying the effect of load and consequent temperature variance.
- Special tests were also performed on redundant machines at the Test Floor. These machines were subjected to accelerated ageing practices and, in some cases, dissected.
- Machines, operating under normal operating conditions, were also tested on-site.

6.2.1 Routine PD testing at the Test Floor

6.2.1.1 Testing procedures

The machine is connected to a hydraulic dynamometer, and taken through the following testing cycles as indicated in Table 6.1 to determine any possible failure mechanism:

Table 6.1: Testing cycles to determine possible failure mechanisms

Test cycle	Test type	Test procedure[5]	Purpose of test
1	Start-up test at no-load.	Measure PD while the stator winding is still cold.	To determine the base PD, mainly caused by applied voltage, of the machine.
2	Full load test at cold conditions.	Measure PD while the machine is 100% loaded and the stator winding temperature is still below 35°C.	This is PD caused by the applied voltage as well as the increase in load. A substantial increase in PD will be the first indication of possible loose coils.
3	Full load test at hot conditions.	Measure PD while the machine is 100% loaded and the stator winding temperature is above 70°C.	To measure the PD at normal operating conditions.
4	No load test at hot conditions.	Measure PD with the load removed but with the stator winding temperature still above 70°C.	If the PD magnitude decreases it could indicate possible movement of coils.

6.2.2 Special PD testing at the Test Floor

Two redundant 3,3 kV machines were subjected to extreme thermal stresses. These machines were coupled to a hydraulic dynamometer and overloaded in order to study the effect of increased temperature and load on the discharge activity.

[5] These rules were adhered to as best possible, taking into account the maximum loading capacity of the Test Floor and the heat dissipation characteristics of the machine under test.

6.2.3 Tests conducted in the plant environment

Some machines in the plant at Iscor Flat Steel Products are subjected to severe environmental and over-load conditions. Several machines were tested to determine the PD levels of machines under operational conditions.

The following procedures were followed for on-site testing:

- A date is set with the plant for the intended PD testing of a specific machine.
- All the required test equipment (Portable test kit, analyser, computer, etc.) is transported to the plant.
- The machine is switched off, the required safety procedures are completed and the portable test kit is connected into the supply circuit.
- The machine is then powered up to normal operating conditions. This sometimes required that the machine be operated for at least one hour at normal load, in order to get as close as possible to normal operating temperature.
- PD tests are then performed on all three phases.
- After completion of the test, the test kit is removed from the circuit, and the machine is reconnected directly to the supply again.

Analysis of machines tested in a plant environment is normally a question of noting the discharge magnitude at the phase angle and temperature that it occurred, as the operating conditions can seldom be varied).

6.3 PD analysis method

6.3.1 PD analysis principles for electrical machines with design operating voltages of 6,6 kV and above

The PD analysis principles for higher voltage machines has been discussed in detail in CHAPTER 3 – PD CHARACTERISTICS OF FAILURE MECHANISMS. These

principles will now be used for the analyses of 3,3 kV motors. Two flow charts summarise these principles where:

- Classic PD is phase-to ground pulses, which occur all along coils as they pass along the length of the slots in the iron core (slot PD). This type of PD is centred at 45° for negative pulses and 225° for the positive pulses [3, p. 50].
- Non-classic PD pulses centred at other positions of the phase cycle may be caused other voltage references [3, p. 50]:
    - Phase-to-phase voltage dependant PD pulses will be ± 30° phase shifted from the classic position.
    - Cross-coupling PD activity is high frequency pulses that may capacitively couple from one phase to another across the endwinding and can be detected by observing PD pulses shifted ± 60° or 120° from the classic positions.
    - Pulses occurring at 0° and 180° are usually from a source that is affected by mechanical vibration, such as a loose connection.

6.3.1.1 Classic PD flowchart [3, p. 59]

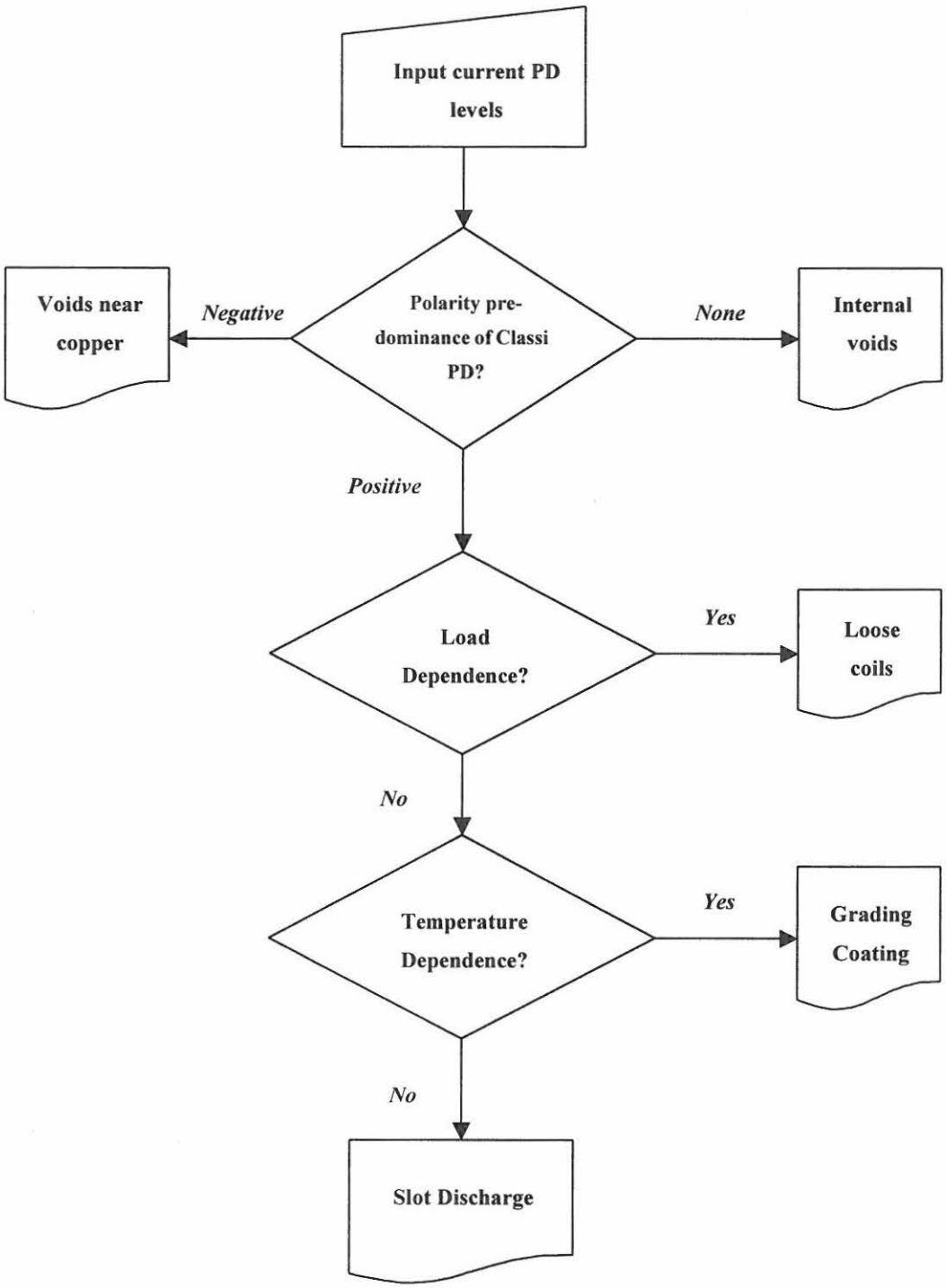

6.3.1.2 Non-classic PD flowchart [3, p. 60]

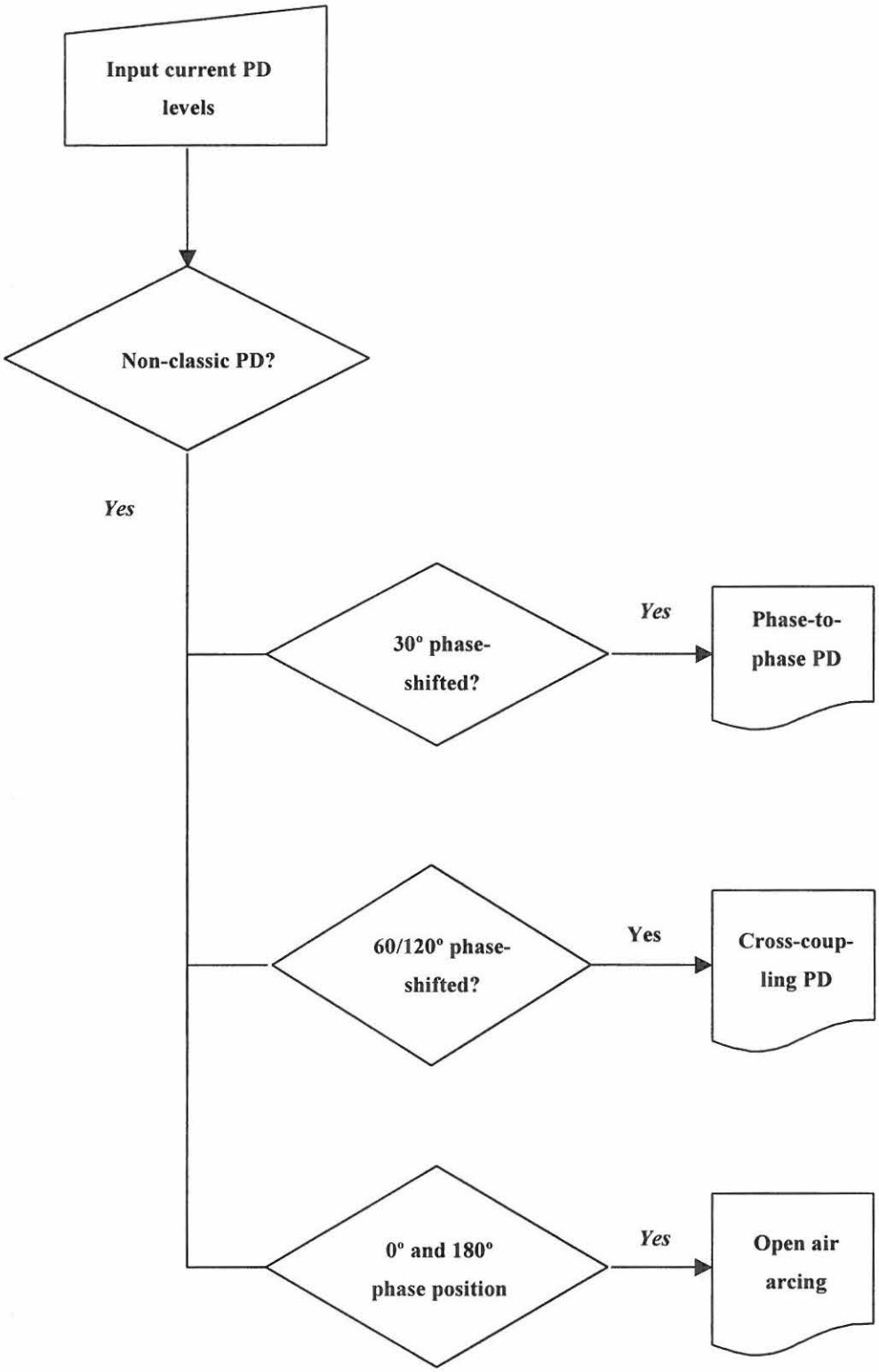

6.3.2 Analysis Matrix

The aim of the techniques described in 6.1, is to obtain data that could be successfully analysed in order to determine developing failure mechanisms experienced by the machines under test. An analysis matrix (Table 6.2) were compiled by using PD analysis principles of higher voltage machines to assist in determining areas of discharge in a stator winding,

Table 6.2: Analysis matrix

Condition	Phase-A	Phase-B	Phase-C
Can the graphical data be analysed?			
If not, supply reason?			
Are any discharges occurring at the classical discharge position (45°/225°)?			
Does this classical PD have polarity predominance?			
Are the negative discharges predominant?			
Are the positive discharges predominant?			
Is the positive discharges load dependant?			
Is the positive discharges temperature dependant?			
Is the discharge angle shifted by 30° from the 45°/225° axis?			
Does the two dimensional plot indicate a "hump", as normally associated with phase-phase PD?			
Is the relationship between the affected phases, clearly visible on the LPD plot (for the correct phase rotation)?			
Are the discharges shifted by 60°/120° from the 45°/225° axis?			
Are the discharges occurring at the 0°/180°?			

6.3.2.1 Explanation of matrix abbreviations

- **Yes** – The discharge angle; temperature dependency; load dependency, etc. can clearly be distinguished from studying the graphs.
- **No** – The graph does not correspond with the question asked.
- **n/a** – The question has no relevance to the graph in question.
- **n/c** – The graph might correspond with the question asked, but without any certainty.

6.3.3 Discharge Magnitudes

In order to correctly analyse the data gathered it is essential that the discharge magnitudes, measured at different loads and temperatures, be available. Table 6.3 is an example of how this data would be presented to assist analysis:

Table 6.3: Discharge magnitudes at different loads and temperatures

Load and temperature	Phase-A		Phase-B		Phase-C	
PD measured at no-load, with the temperature of the stator winding at *x*°C *(Temp. for phases A-B-C)*	+NQN	-NQN	+NQN	-NQN	+NQN	-NQN
	+Qmax	-Qmax	+Qmax	-Qmax	+Qmax	-Qmax
PD measured at *x*% load, with the temperature of the stator winding at *x*°C *(Temp. for phases A-B-C)*	+NQN	-NQN	+NQN	-NQN	+NQN	-NQN
	+Qmax	-Qmax	+Qmax	-Qmax	+Qmax	-Qmax
PD measured at *x*% load, with the temperature of the stator winding at *x*°C	+NQN	-NQN	+NQN	-NQN	+NQN	-NQN
	+Qmax	-Qmax	+Qmax	-Qmax	+Qmax	-Qmax

Table 6.3: (cont.)

Load and temperature	Phase-A		Phase-B		Phase-C	
(Temp. for phases A-B-C)						
PD measured at no-load,	+NQN	-NQN	+NQN	-NQN	+NQN	-NQN
with the temperature of the						
stator winding at *x*°C	+Qmax	-Qmax	+Qmax	-Qmax	+Qmax	-Qmax
(Temp. for phases A-B-C)						

CHAPTER 7 – PD TESTING AT THE TEST FLOOR

7.1 Introduction

PD testing was performed and results analysed on a machine with unknown winding configuration, random wound machines and form coil wound machines.

7.2 PD test results and analysis data

7.2.1 Winding type: Form coil

7.2.1.1 Impregnation method – unknown insulation system

7.2.1.1.1 Motor # 150XX3

Table 7.1: Nameplate data for motor # 150XX3

Make	Power	Stator Voltage	Stator Current	# Poles
TECO	150 kW	3300 V	n/a	4-pole

Table 7.2: Discharge magnitudes for motor # 150XX3

Load and temperature	Phase-A		Phase-B		Phase-C	
PD measured at no-load,	÷NQN	-NQN	+NQN	-NQN	+NQN	-NQN
with the temperature of	141	74	98	19	29	17
the stator winding at	+Qmax	-Qmax	+Qmax	-Qmax	+Qmax	-Qmax
21°C, 22°C and 25°C	75	49	83	0	8	9
respectively.						
PD measured at 100%	+NQN	-NQN	+NQN	-NQN	+NQN	-NQN
load, with the temperature	160	67	126	94	36	14

Table 7.2: (Cont.)

Load and temperature	Phase-A		Phase-B		Phase-C	
of the stator winding at	+Qmax	-Qmax	+Qmax	-Qmax	+Qmax	-Qmax
36°C, 32°C and 28°C	95	49	79	71	21	9
respectively.						
PD measured at 100%	+NQN	-NQN	+NQN	-NQN	+NQN	-NQN
load, with the temperature	363	339	576	348	1751	1539
of the stator winding at	+Qmax	-Qmax	+Qmax	-Qmax	+Qmax	-Qmax
58°C, 59°C and 60°C	181	138	235	203	n/a	n/a
respectively.						
PD measured at no-load,	+NQN	-NQN	+NQN	-NQN	+NQN	-NQN
with the temperature of	280	215	366	310	167	91
the stator winding at	+Qmax	-Qmax	+Qmax	-Qmax	+Qmax	-Qmax
59°C, 57°C and 56°C	160	121	322	282	0	0
respectively.						

(See Appendixes A1-A5, for graphical representation of discharges)

Table 7.3: Analysis matrix for motor # 150XX3

Condition	Phase-A	Phase-B	Phase-C
Can the graphical data be analysed?	Yes	Yes	Yes
If not, supply reason?	n/a		
Are any discharges occurring at the classical discharge position (45°/225°)?	Yes	Yes	No
Does this classical PD have polarity predominance?	No	Yes	n/c
Are the negative discharges predominant?	n/a	No	n/a
Are the positive discharges predominant?	n/a	Yes	n/a
Is the positive discharges load dependant?	n/a	No	n/a
Is the positive discharges temperature dependant?	n/a	Yes	n/a
Is the discharge angle shifted by 30° from the	Yes	Yes	No

Table 7.3: (Cont.)

Condition	Phase-A	Phase-B	Phase-C
45°/225° axis?			
Does the two dimensional plot indicate a "hump", as normally associated with phase-phase PD?	n/c	Yes	Yes
Is the relationship between the affected phases, clearly visible on the LPD plot (for the correct phase rotation)?	No	No	No
Are the discharges shifted by 60°/120° from the 45°/225° axis?	No	n/c	n/c
Are the discharges occurring at the 0°/180°?	No	No	No

Table 7.4: Winding configuration

Winding type	Impregnation type	Coils	Turns/ coil	Conductor size	Slot width	Con.
Form	?	?	?	?	?	?

Observations

The machine was opened for inspection, and found to have a Form coil winding.

Conclusion

- The majority of the discharges appear to be occurring in the slot on the surface of the coil.
- There are also signs of phase-to-phase related discharges:
  - Phase-to-phase discharges can occur on the endwinding due to contamination. Contamination can lead to tracking which will eventually lead to a phase-to-phase failure.
  - Inadequate spacing/ insulation between coils can lead to discharges between coils causing a build-up of ozone.

- It is however not possible to determine if this is occurring between coils in the slot or on the endwinding.

7.2.1.2 Impregnation method: Dip (Isonel)

7.2.1.2.1 Motor # 400BA2

Table 7.5: Nameplate data for motor # 400BA2

Make	Power	Stator Voltage	Stator Current	Speed
English Electric	**400 hp**	**3300 V**	**62 A**	**1474 r/min**

Table 7.6: Discharge magnitudes for motor # 400BA2

Load and temperature	Phase-A		Phase-B		Phase-C	
PD measured at 125% load, with the temperature of the stator winding at 33°C, 34°C and 34°C respectively.	+NQN	-NQN	+NQN	-NQN	+NQN	-NQN
	47	42	6	3	14	11
	+Qmax	-Qmax	+Qmax	-Qmax	+Qmax	-Qmax
	26	23	4	3	7	6

(See Appendixes A77-A81, for graphical representation of discharges)

Table 7.7: Analysis matrix for motor # 400BA2

Condition	Phase-A	Phase-B	Phase-C
Can the graphical data be analysed?	Yes	Yes	Yes
If not, supply reason?	n/a		
Are any discharges centred at the classical discharge position of (45°/225°)?	No	No	No

Table 7.7: (Cont.)

Condition	Phase-A	Phase-B	Phase-C
Does this classical PD have polarity predominance?	n/a	n/a	n/a
Are the negative discharges predominant?	n/a	n/a	n/a
Are the positive discharges predominant?	n/a	n/a	n/a
Is the positive discharges load dependant?	n/a	n/a	n/a
Is the positive discharges temperature dependant?	n/a	n/a	n/a
Is the discharge angle shifted by 30° from the 45°/225° axis?	Yes	No	Yes
Does the two dimensional plot indicate a "hump", as normally associated with phase-phase PD?	No	No	No
Is the relationship between the affected phases, clearly visible on the LPD plot (for the correct phase rotation)?	Yes	Yes	Yes
Are the discharges shifted by 60°/120° from the 45°/225° axis?	No	No	No
Are the discharges occurring at the 0°/180°?	No	No	No

Table 7.8: Winding configuration for motor # 400BA2

Winding type	Impregnation type	Coils	Turns/ coil	Conductor size	Slot width	Con.
Form coil	Dip (Isonel)	36	15	6.15x2.8	9.8	Star

Observation

The machine had been rewound according to the winding data listed in the winding configuration table.

Conclusion

Discharges are definitely phase-to-phase, and it is affecting all three phases:

- Phase-to-phase discharges can occur on the endwinding due to contamination. Contamination can lead to tracking which will eventually lead to a phase-to-phase failure.
- Inadequate spacing/ insulation between coils can lead to discharges between coils causing a build-up of ozone.
- It is however not possible to determine if this is occurring between coils in the slot or on the endwinding.

7.2.1.3 Impregnation method: Resin rich insulation system

7.2.1.3.1 Motor # 160BF1

Table 7.9: Nameplate data for motor # 160BF1

Make	Power	Stator Voltage	Stator Current	Speed
Siemens	160 kW	3300 V	37 A	1471 r/min

Table 7.10: Discharge magnitudes for motor # 160BF1

Load and temperature	Phase-A		Phase-B		Phase-C	
PD measured at 100% load, with the temperature of the stator winding at 69°C, 68°C and 68°C respectively.	+NQN	-NQN	+NQN	-NQN	+NQN	-NQN
	3	3	5	6	1	6
	+Qmax	-Qmax	+Qmax	-Qmax	+Qmax	-Qmax
	0	2	3	3	0	4

(See Appendixes A11-A14, for graphical representation of discharges)

Table 7.11: Analysis matrix for motor # 160BF1

Condition	Phase-A	Phase-B	Phase-C
Can the graphical data be analysed?	No	No	No
If not, supply reason?	Magnitude too low		

Table 7.12: Winding configuration for motor # 160BF1

Winding type	Impregnation type	Coils	Turns/ coil	Conductor size	Slot width	Con.
Form Coil	Resin Rich	48	14	4.25x1.96	12.5	Star

Observations

N/A

Conclusion

Discharge magnitudes at 100% load and temperature are too low to analyse.

7.2.1.3.2 Motor # 160BF3

Table 7.13: Nameplate data for motor # 160BF3

Make	Power	Stator Voltage	Stator Current	Speed
Siemens	160 kW	3300 V	37 A	1471 r/min

Table 7.14: Discharge magnitudes for motor # 160BF3

Load and temperature	Phase-A		Phase-B		Phase-C	
PD measured at 100% load, with the temperature of the stator winding at 85°C, 85°C and 83°C respectively.	+NQN	-NQN	+NQN	-NQN	+NQN	-NQN
	5	n/a	12	10	n/a	n/a
	+Qmax	-Qmax	+Qmax	-Qmax	+Qmax	-Qmax
	0	0	0	0	0	0

(See Appendixes A15-A18, for graphical representation of discharges)

Table 7.15: Analysis matrix for motor # 160BF3

Condition	Phase-A	Phase-B	Phase-C
Can the graphical data be analysed?	No	No	No
If not, supply reason?	Magnitude too low		

Table 7.16: Winding configuration for motor # 160BF3

Winding type	Impregnation type	Coils	Turns/ coil	Conductor size	Slot width	Con.
Form Coil	Resin Rich	48	14	4.25x1.96	12.5	Star

Observations

N/a

Conclusion

Discharge magnitudes at 100% load and temperature are too low to analyse.

7.2.1.3.3 Motor # 160BF11

Table 7.17: Nameplate data for motor # 160BF11

Make	Power	Stator Voltage	Stator Current	Speed
Siemens	160 kW	3300 V	37 A	1471 r/min

Table 7.18: Discharge magnitudes for motor # 160BF11

Load and temperature	Phase-A		Phase-B		Phase-C	
PD measured at 100% load, with the temperature of the stator winding at 72°C, 73°C and 74°C respectively.	**+NQN**	**-NQN**	**+NQN**	**-NQN**	**+NQN**	**-NQN**
	n/a	n/a	n/a	n/a	5	2
	+Qmax	**-Qmax**	**+Qmax**	**-Qmax**	**+Qmax**	**-Qmax**
	0	0	0	0	3	0

(See Appendixes A19-A21, for graphical representation of discharges)

Table 7.19: Analysis matrix for motor # 160BF11

Condition	Phase-A	Phase-B	Phase-C
Can the graphical data be analysed?	No	No	No
If not, supply reason?	Magnitude too low		

Table 7.20: Winding configuration for motor # 160BF11

Winding type	Impregnation type	Coils	Turns/ coil	Conductor size	Slot width	Con.
Form Coil	Resin Rich	48	14	4.25x1.96	12.5	Star

Observations

N/a

Conclusion

Discharge magnitudes at 100% load and temperature are too low to analyse.

7.2.1.3.4 Motor # 200DP2

Table 7.21: Nameplate data for motor # 200DP2

Make	Power	Stator Voltage	Stator Current	Speed
Siemens	200 kW	3300 V	44.5 A	1477 r/min

Table 7.22: Discharge magnitudes for motor # 200DP2

Load and temperature	Phase-A		Phase-B		Phase-C	
PD measured at no-load, with the temperature of the stator winding at 25°C, 26°C and 27°C respectively.	+NQN	-NQN	+NQN	-NQN	+NQN	-NQN
	7	3	7	11	23	2
	+Qmax	-Qmax	+Qmax	-Qmax	+Qmax	-Qmax
	5	0	7	10	16	2
PD measured at 100% load, with the temperature of the stator winding at 40°C, 37°C and 31°C respectively.	+NQN	-NQN	+NQN	-NQN	+NQN	-NQN
	23	n/a	19	37	92	n/a
	+Qmax	-Qmax	+Qmax	-Qmax	+Qmax	-Qmax
	0	0	0	32	87	0
PD measured at 100% load, with the temperature of the stator winding at 69°C, 69°C and 70°C respectively.	+NQN	-NQN	+NQN	-NQN	+NQN	-NQN
	28	17	18	22	75	18
	+Qmax	-Qmax	+Qmax	-Qmax	+Qmax	-Qmax
	12	11	14	14	50	12
PD measured at no-load, with the temperature of the stator winding at 62°C, 65°C and 68°C respectively.	+NQN	-NQN	+NQN	-NQN	+NQN	-NQN
	20	5	18	22	75	19
	+Qmax	-Qmax	+Qmax	-Qmax	+Qmax	-Qmax
	10	4	12	13	50	12

(See Appendixes A32-A36, for graphical representation of discharges)

Table 7.23: Analysis matrix for motor # 200DP2

Condition	Phase-A	Phase-B	Phase-C
Can the graphical data be analysed?	Yes	Yes	Yes
If not, supply reason?	n/a		
Are any discharges centred at the classical discharge position of (45°/225°)?	Yes	No	No
Does this classical PD have polarity predominance?	Yes	n/a	n/a
Are the negative discharges predominant?	No	n/a	n/a
Are the positive discharges predominant?	Yes	n/a	n/a
Is the positive discharges load dependant?	No	n/a	n/a
Is the positive discharges temperature dependant?	Yes	n/a	n/a
Is the discharge angle shifted by 30° from the 45°/225° axis?	No	Yes	Yes
Does the two dimensional plot indicate a "hump", as normally associated with phase-phase PD?	Yes	Yes	n/c
Is the relationship between the affected phases, clearly visible on the LPD plot (for the correct phase rotation)?	n/c	n/c	n/c
Are the discharges shifted by 60°/120° from the 45°/225° axis?	No	n/c	n/c
Are the discharges occurring at the 0°/180°?	No	n/c	n/c

Table 7.24: Winding configuration for motor # 200DP2

Winding type	Impregnation type	Coils	Turns/ coil	Conductor size	Slot width	Con.
Form Coil	Resin Rich	48	10	2X(3.9X1.3)		Star

Observations

- This machine still has its' original Siemens winding. The winding data could not be obtained from the manufacturer. The data shown in the winding configuration column above were obtained from the data sheet of an identical machine.
- The graphical representation of discharge activity for phases-B&C are very unusual.

Conclusion

Discharges appear to be phase-to-phase related, with the possibility that phases-B&C are discharging to air.

7.2.1.3.5 Conclusion summary for resin rich motors tested at the Test Floor

- Discharge values are very low.
- Motor # 200DP2 is the only machine with discharge levels that could be analysed (only phase-to-phase discharges were visible).
- The winding condition of these type of motors could not be determined by means of PD measurement.

7.2.1.4 Impregnation method: Vpi insulation system

7.2.1.4.1 Motor # 185CD1

Table 7.25: Nameplate data for motor # 185CD1

Make	Power	Stator Voltage	Stator Current	Speed
GEC	185 kW	3300 V	39.7 A	1488 r/min

Table 7.26: Discharge magnitudes for motor # 185CD1

Load and temperature	Phase-A		Phase-B		Phase-C	
PD measured at no-load, with the temperature of the stator winding at 27°C, 29°C and 30°C respectively.	+NQN	-NQN	+NQN	-NQN	+NQN	-NQN
	5	5	69	2	1	12
	+Qmax	-Qmax	+Qmax	-Qmax	+Qmax	-Qmax
	0	0	0	0	0	0
PD measured at 100% load, with the temperature of the stator winding at 41°C, 43°C and 45°C respectively.	+NQN	-NQN	+NQN	-NQN	+NQN	-NQN
	6	7	71	2	n/a	7
	+Qmax	-Qmax	+Qmax	-Qmax	+Qmax	-Qmax
	0	0	0	0	0	0
PD measured at 100% load, with the temperature of the stator winding at 79°C, 80°C and 82°C respectively.	+NQN	-NQN	+NQN	-NQN	+NQN	-NQN
	n/a	13	57	26	26	4
	+Qmax	-Qmax	+Qmax	-Qmax	+Qmax	-Qmax
	0	0	40	0	29	0
PD measured at no-load, with the temperature of	+NQN	-NQN	+NQN	-NQN	+NQN	-NQN
	n/a	n/a	54	47	15	16

Table 7.26: (Cont.)

Load and temperature	Phase-A		Phase-B		Phase-C	
the stator winding at 81°C, 80°C and 80°C respectively.	+Qmax	-Qmax	+Qmax	-Qmax	+Qmax	-Qmax
	0	0	17	23	9	10

(See Appendixes A27-A31, for graphical representation of discharges)

Table 7.27: Analysis matrix for motor # 185CD1

Condition	Phase-A	Phase-B	Phase-C
Can the graphical data be analysed?	Yes	Yes	Yes
If not, supply reason?		n/a	
Are any discharges centred at the classical discharge position of (45°/225°)?	No	Yes	No
Does this classical PD have polarity predominance?	No	Yes	No
Are the negative discharges predominant?	n/a	No	n/a
Are the positive discharges predominant?	n/a	Yes	n/a
Is the positive discharges load dependant?	n/a	No	n/a
Is the positive discharges temperature dependant?	n/a	Yes	n/a
Is the discharge angle shifted by 30° from the 45°/225° axis?	n/a	No	n/a
Does the two dimensional plot indicate a "hump", as normally associated with phase-phase PD?	No	No	No
Is the relationship between the affected phases, clearly visible on the LPD plot (for the correct phase rotation)?	Yes	Yes	Yes
Are the discharges shifted by 60°/120° from the 45°/225° axis?	No	No	Yes
Are the discharges occurring at the 0°/180°?	Yes	No	No

Table 7.28: Winding configuration for motor # 185CD1

Winding type	Impregnation type	Coils	Turns/ coil	Conductor size	Slot width	Con.
Form coil	VPI	n/a	n/a	7.5x2.12	10.6	n/a

Observations

This machine still has its' original GEC winding. The winding data could not be obtained from the manufacturer. The data shown in the winding configuration column above, were obtained from the data sheet of an identical machine.

Conclusion

Most of the discharge activity is definitely phase-to-phase related (As can be seen from the LPD plot).

- Phase-to-phase discharges can occur on the endwinding due to contamination. Contamination can lead to tracking which will eventually lead to a phase-to-phase failure.
- Inadequate spacing/ insulation between coils can lead to discharges between coils causing a build-up of ozone.
- It is however not possible to determine if this is occurring between coils in the slot or on the endwinding.

7.2.1.4.2 Motor # 220AA5

Table 7.29: Nameplate data for motor # 220AA5

Make	Power	Stator Voltage	Stator Current	Speed
Siemens	220 kW	3300 V	49 A	1478 r/min

Table 7.30: Discharge magnitudes for motor # 220AA5

Load and temperature	Phase-A		Phase-B		Phase-C	
PD measured at no-load, with the temperature of the stator winding at 15°C, 15°C and 15°C respectively.	+NQN	-NQN	+NQN	-NQN	+NQN	-NQN
	1	n/a	1	n/a	4	5
	+Qmax	-Qmax	+Qmax	-Qmax	+Qmax	-Qmax
	0	0	0	0	3	4
PD measured at 100% load, with the temperature of the stator winding at 25°C, 23°C and 20°C respectively.	+NQN	-NQN	+NQN	-NQN	+NQN	-NQN
	1	n/a	n/a	n/a	4	5
	+Qmax	-Qmax	+Qmax	-Qmax	+Qmax	-Qmax
	0	0	0	0	3	4
PD measured at 150% load, with the temperature of the stator winding at 48°C, 55°C and 60°C respectively.	+NQN	-NQN	+NQN	-NQN	+NQN	-NQN
	9	10	77	66	23	18
	+Qmax	-Qmax	+Qmax	-Qmax	+Qmax	-Qmax
	7	6	25	49	13	12

(See Appendixes A37-A41, for graphical representation of discharges)

Table 7.31: Analysis matrix for motor # 220AA5

Condition	Phase-A	Phase-B	Phase-C
Can the graphical data be analysed?	Yes	Yes	Yes
If not, supply reason?	n/a		
Are any discharges centred at the classical discharge position of (45°/225°)?	No	Yes	n/c
Does this classical PD have polarity predominance?	n/a	Yes	n/a
Are the negative discharges predominant?	n/a	No	n/a
Are the positive discharges predominant?	n/a	Yes	n/a

Table 7.31: (Cont.)

Condition	Phase-A	Phase-B	Phase-C
Is the positive discharges load dependant?	n/a	No	n/a
Is the positive discharges temperature dependant?	n/a	Yes	n/a
Is the discharge angle shifted by 30° from the 45°/225° axis?	No	Yes	n/c
Does the two dimensional plot indicate a "hump", as normally associated with phase-phase PD?	No	No	No
Is the relationship between the affected phases, clearly visible on the LPD plot (for the correct phase rotation)?	Yes	Yes	n/c
Are the discharges shifted by 60°/120° from the 45°/225° axis?	n/c	No	No
Are the discharges occurring at the 0°/180°?	No	No	Yes

Table 7.32: Winding configuration for motor # 220AA5

Winding type	Impregnation type	Coils	Turns/ coil	Conductor size	Slot width	Con.
Form Coil	VPI (Epoxy)	48	10	2x(3.54x1.4)	9.6	Star

Observations

This machine has been rewound with the data indicated in the winding configuration column.

Conclusion

Discharges appear to be phase-to-phase related.

- Phase-to-phase discharges can occur on the endwinding due to contamination.

Contamination can lead to tracking which will eventually lead to a phase-to-phase failure.

- Inadequate spacing/ insulation between coils can lead to discharges between coils causing a build-up of ozone.
- It is however not possible to determine if this is occurring between coils in the slot or on the endwinding.

7.2.1.4.3 Motor # 250BB4

Table 7.33: Nameplate data for motor # 250 BB4

Make	Power	Stator Voltage	Stator Current	Speed
AEI	250 hp	3300 V	40.4 A	1470 r/min

Table 7.34: Discharge magnitudes for motor # 250BB4

Load and temperature	Phase-A		Phase-B		Phase-C	
PD measured at no-load, with the temperature of the stator winding at 20°C, 19°C and 20°C respectively.	+NQN	-NQN	+NQN	-NQN	+NQN	-NQN
	4	4	n/a	n/a	5	n/a
	+Qmax	-Qmax	+Qmax	-Qmax	+Qmax	-Qmax
	3	0	0	0	4	0
PD measured at 100% load, with the temperature of the stator winding at 30°C, 26°C and 24°C respectively.	+NQN	-NQN	+NQN	-NQN	+NQN	-NQN
	4	3	5	n/a	6	1
	+Qmax	-Qmax	+Qmax	-Qmax	+Qmax	-Qmax
	0	0	5	0	5	0
PD measured at 150% load, with the	+NQN	-NQN	+NQN	-NQN	+NQN	-NQN
	10	9	68	60	28	16

Table 7.34: (Cont.)

Load and temperature	Phase-A		Phase-B		Phase-C	
temperature of the stator winding at 51°C, 59°C and 53°C respectively.	+Qmax	-Qmax	+Qmax	-Qmax	+Qmax	-Qmax
	6	5	25	28	18	12

(See Appendixes A47-A51, for graphical representation of discharges)

Table 7.35: Analysis matrix for motor # 250BB4

Condition	Phase-A	Phase-B	Phase-C
Can the graphical data be analysed?	Yes	Yes	Yes
If not, supply reason?		n/a	
Are any discharges centred at the classical discharge position of (45°/225°)?	No	No	Yes
Does this classical PD have polarity predominance?	n/a	n/a	Yes
Are the negative discharges predominant?	n/a	n/a	No
Are the positive discharges predominant?	n/a	n/a	Yes
Is the positive discharges load dependant?	n/a	n/a	No
Is the positive these discharges temperature dependant?	n/a	n/a	Yes
Is the discharge angle shifted by 30° from the 45°/225° axis?	Yes	Yes	No
Does the two dimensional plot indicate a "hump", as normally associated with phase-phase PD?	No	No	No
Is the relationship between the affected phases, clearly visible on the LPD plot (for the correct phase rotation)?	No	No	No
Are the discharges shifted by 60°/120° from the 45°/225° axis?	No	No	No
Are the discharges occurring at the 0°/180°?	No	No	No

Table 7.36: Winding configuration for motor # 250BB4

Winding type	Impregnation type	Coils	Turns/ coil	Conductor size	Slot width	Con.
Form Coil	VPI	60	14	2.33x3.55	11.1	n/a

Observations

The machine had been rewound according to the winding data listed in the winding configuration table.

Conclusion

Discharges appears to be phase-phase related, with some possible slot discharge.

- Phase-to-phase discharges can occur on the endwinding due to contamination. Contamination can lead to tracking which will eventually lead to a phase-to-phase failure.
- Inadequate spacing/ insulation between coils can lead to discharges between coils causing a build-up of ozone.
- It is however not possible to determine if this is occurring between coils in the slot or on the endwinding.

7.2.1.4.4 Motor # 300AA3

Table 7.37: Nameplate data for motor # 300AA3

Make	Power	Stator Voltage	Stator Current	Speed
GEC	300 kW	3300 V	66 A	1482 r/min

Table 7.38: Discharge magnitudes for motor # 300AA3

Load and temperature	Phase-A		Phase-B		Phase-C	
PD measured at no-load, with the temperature of the stator winding at 18°C, 21°C and 22°C respectively.	+NQN	-NQN	+NQN	-NQN	+NQN	-NQN
	18	12	n/a	2	1	2
	+Qmax	-Qmax	+Qmax	-Qmax	+Qmax	-Qmax
	11	9	0	2	0	2
PD measured at 100% load, with the temperature of the stator winding at 23°C, 23°C and 23°C respectively.	+NQN	-NQN	+NQN	-NQN	+NQN	-NQN
	28	14	n/a	n/a	13	5
	+Qmax	-Qmax	+Qmax	-Qmax	+Qmax	-Qmax
	17	8	0	0	9	4
PD measured at 100% load, with the temperature of the stator winding at *x*°C.	+NQN	-NQN	+NQN	-NQN	+NQN	-NQN
	137	143	27	12	14	21
	+Qmax	-Qmax	+Qmax	-Qmax	+Qmax	-Qmax
	39	73	8	6	9	16
PD measured at no-load, with the temperature of the stator winding at *x*°C.	+NQN	-NQN	+NQN	-NQN	+NQN	-NQN
	52	61	5	4	18	18
	+Qmax	-Qmax	+Qmax	-Qmax	+Qmax	-Qmax
	37	38	5	0	8	5

(See Appendixes A57-A61, for graphical representation of discharges)

Table 7.39: Analysis matrix for motor # 300AA3

Condition	Phase-A	Phase-B	Phase-C
Can the graphical data be analysed?	Yes	Yes	Yes
If not, supply reason?	n/a		
Are any discharges centred at the classical discharge position of (45°/225°)?	Yes	No	No
Does this classical PD have polarity	Yes	n/a	n/a

Table 7.39: (Cont.)

Condition	Phase-A	Phase-B	Phase-C
predominance?			
Are the negative discharges predominant?	Yes	n/a	n/a
Are the positive discharges predominant?	No	n/a	n/a
Is the positive discharges load dependant?	n/c	n/a	n/a
Is the positive discharges temperature dependant?	Yes	n/a	n/a
Is the discharge angle shifted by 30° from the 45°/225° axis?	n/c	No	No
Does the two dimensional plot indicate a "hump", as normally associated with phase-phase PD?	Yes	Yes	n/c
Is the relationship between the affected phases, clearly visible on the LPD plot (for the correct phase rotation)?	Yes	Yes	Yes
Are the discharges shifted by 60°/120° from the 45°/225° axis?	No	Yes	No
Are the discharges occurring at the 0°/180°?	No	No	Yes

Table 7.40: Winding configuration for motor # 300AA3

Winding type	Impregnation type	Coils	Turns/ coil	Conductor size	Slot width	Con.
Form coil	VPI	60	8	6.76x2.52	10.4	Star

Observations

- The machine was not fitted with temperature sensors. Temperature readings were measured externally.
- This machine still has its' original GEC winding. The winding data could not be obtained from the manufacturer. The data shown in the winding configuration

column above, were obtained from the data sheet of an identical machine.

Conclusion

Most of the discharge activity is definitely phase-to-phase related (As can be seen from the LPD plot). All three phases are discharging to each other, with some cross-coupling.

- Phase-to-phase discharges can occur on the endwinding due to contamination. Contamination can lead to tracking which will eventually lead to a phase-to-phase failure.
- Inadequate spacing/ insulation between coils can lead to discharges between coils causing a build-up of ozone.
- It is however not possible to determine if this is occurring between coils in the slot or on the endwinding.

7.2.1.4.5 Motor # 305AA2

Table 7.41: Nameplate data for motor # 305AA2

Make	Power	Stator Voltage	Stator Current	Speed
GEC	380 kW	3300 V	66 A	1482 r/min

Table 7.42: Discharge magnitudes for motor # 305AA2

Load and temperature	Phase-A		Phase-B		Phase-C	
PD measured at no-load,	+NQN	-NQN	+NQN	-NQN	+NQN	-NQN
with the temperature of	83	144	222	163	431	317
the stator winding at	+Qmax	-Qmax	+Qmax	-Qmax	+Qmax	-Qmax
x°C.	53	86	110	83	206	157
PD measured at 100%	+NQN	-NQN	+NQN	-NQN	+NQN	-NQN

Table 7.42: (Cont.)

Load and temperature	Phase-A		Phase-B		Phase-C	
load, with the temperature of the stator winding at x°C.						
	+Qmax	**-Qmax**	**+Qmax**	**-Qmax**	**+Qmax**	**-Qmax**
PD measured at 100% load, with the temperature of the stator winding at x°C.	**+NQN**	**-NQN**	**+NQN**	**-NQN**	**+NQN**	**-NQN**
	122	220	445	314	787	463
	+Qmax	**-Qmax**	**+Qmax**	**-Qmax**	**+Qmax**	**-Qmax**
	58	94	211	143	390	234
PD measured at no-load, with the temperature of the stator winding at x°C.	**+NQN**	**-NQN**	**+NQN**	**-NQN**	**+NQN**	**-NQN**
	+Qmax	**-Qmax**	**+Qmax**	**-Qmax**	**+Qmax**	**-Qmax**

(See Appendixes A62-A66, for graphical representation of discharges)

Table 7.43: Analysis matrix for motor # 305AA2

Condition	Phase-A	Phase-B	Phase-C
Can the graphical data be analysed?	Yes	Yes	Yes
If not, supply reason?	n/a		
Are any discharges centred at the classical discharge position of (45°/225°)?	No	Yes	Yes
Does this classical PD have polarity predominance?	n/a	Yes	Yes
Are the negative discharges predominant?	n/a	No	No
Are the positive discharges predominant?	n/a	Yes	Yes
Is the positive discharges load dependant?	n/a	n/c	n/c
Is the positive discharges temperature dependant?	n/a	Yes	Yes
Is the discharge angle shifted by 30° from the 45°/225° axis?	No	n/c	No

Table 7.43: (Cont.)

Condition	Phase-A	Phase-B	Phase-C
Does the two dimensional plot indicate a "hump", as normally associated with phase-phase PD?	No	No	No
Is the relationship between the affected phases, clearly visible on the LPD plot (for the correct phase rotation)?	Yes	Yes	Yes
Are the discharges shifted by 60°/120° from the 45°/225° axis?	Yes	No	No
Are the discharges occurring at the 0°/180°?	No	No	No

Table 7.44: Winding configuration for motor # 305AA2

Winding type	Impregnation type	Coils	Turns/ coil	Conductor size	Slot width	Con.
Form coil	VPI	72	6	4(3.98x2)	11.9	Star

Observations

- The machine had been rewound according to the winding data listed in the winding configuration table.
- Temperature was not measured during the test. It is however a logical deduction that the temperature would have risen after the machine was under load for 20 minutes.

Conclusion

The bulk of the discharges appear to be occurring in the slot portion, on the surface of the coil, with some discharging phase-to-phase.

7.2.1.4.6 Motor # 380AB1

Introduction

Motor # 380AB1 is the primary driver for a Coal Crusher at the Coal Plant. The machine was tested in the plant on 9th February 2002. Analysis of the graphical representation of the discharges indicated possible end-winding discharge between phase-B and phase-C (See Appendix C35). A bearing failure caused the machine to be removed from service and dismantled at Iscor's Electrical Workshop. Figure 7.1 shows what the machine looked like after dismantling.

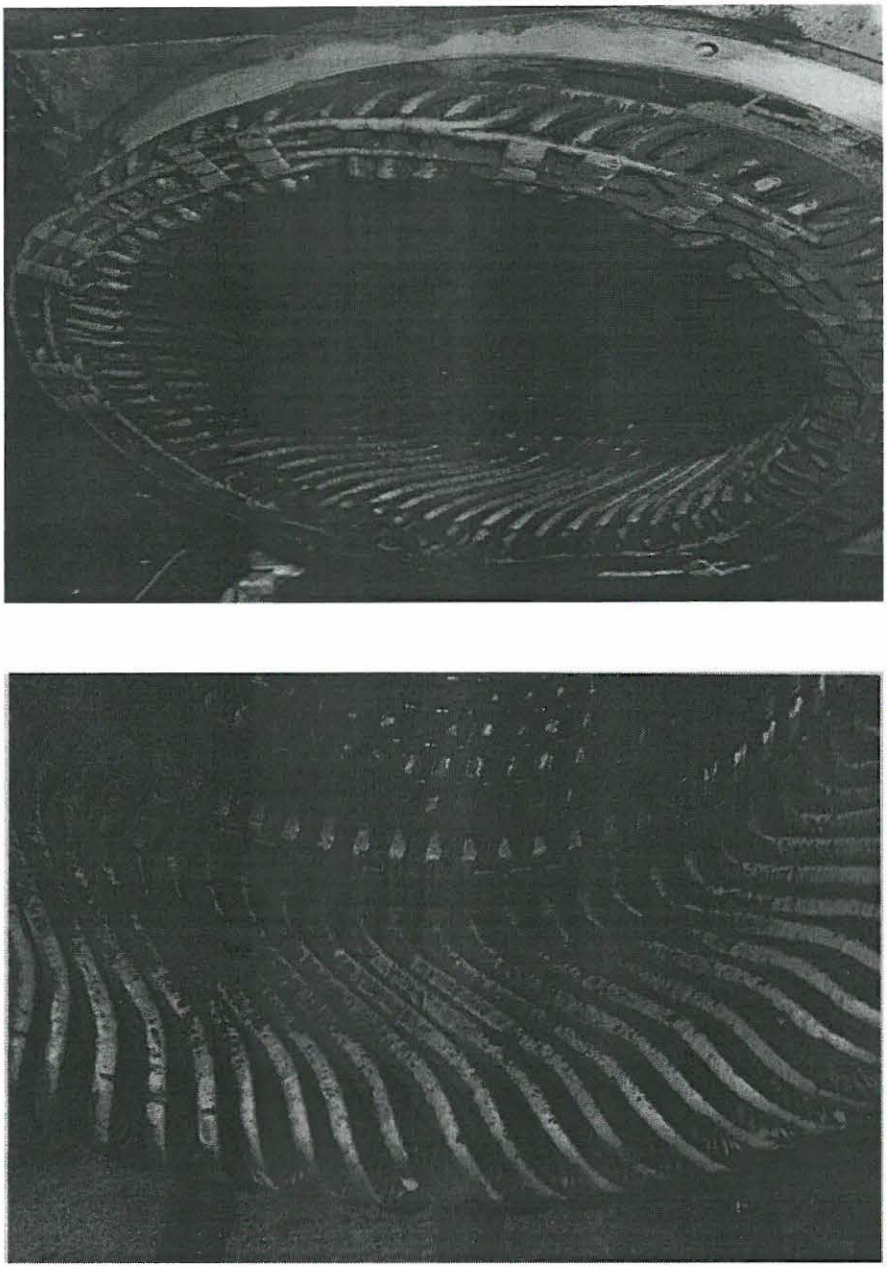

Figure 7.1: End-winding of motor # 380AB1

The motor was severely contaminated with carbon dust. The bearing failure caused the rotor to rub, damaging parts of the stator insulation.

The machine was cleaned and tested at the Test Floor with the following results:

Table 7.45: Nameplate data for motor # 380AB1

Make	Power	Stator Voltage	Stator Current	Speed
GEC	380Kw	3300V	66A	1482 r/min

Table 7.46: Discharge magnitudes for motor # 380AB1

Load and temperature	Phase-A		Phase-B		Phase-C	
PD measured at no-load, with the temperature of the stator winding at 28°C, 28°C and 28°C respectively.	+NQN	-NQN	+NQN	-NQN	+NQN	-NQN
	158	135	141	132	216	151
	+Qmax	-Qmax	+Qmax	-Qmax	+Qmax	-Qmax
	74	68	93	89	57	76
PD measured at 100% load, with the temperature of the stator winding at 48°C, 41°C and 36°C respectively.	+NQN	-NQN	+NQN	-NQN	+NQN	-NQN
	398	292	234	203	290	166
	+Qmax	-Qmax	+Qmax	-Qmax	+Qmax	-Qmax
	192	142	123	94	148	123
PD measured at 100% load, with the temperature of the stator winding at 71°C, 73°C and 73°C respectively.	+NQN	-NQN	+NQN	-NQN	+NQN	-NQN
	489	345	836	472	893	667
	+Qmax	-Qmax	+Qmax	-Qmax	+Qmax	-Qmax
	236	180	559	375	455	330
PD measured at no-load, with the temperature of the stator winding at *x*°C.	+NQN	-NQN	+NQN	-NQN	+NQN	-NQN
	n/a	n/a	n/a	n/a	n/a	n/a
	+Qmax	-Qmax	+Qmax	-Qmax	+Qmax	-Qmax
	n/a	n/a	n/a	n/a	n/a	n/a

(See Appendixes A67-A71, for graphical representation of discharges)

Table 7.47: Analysis matrix for motor # 380AB1

Condition	Phase-A	Phase-B	Phase-C
Can the graphical data be analysed?	Yes	Yes	Yes
If not, supply reason?	n/a		
Are any discharges centred at the classical discharge position of (45°/225°)?	Yes	Yes	Yes
Does this classical PD have polarity predominance?	Yes	Yes	Yes
Are the negative discharges predominant?	No	No	No
Are the positive discharges predominant?	Yes	Yes	Yes
Is the positive discharges load dependant?	n/c	n/c	n/c
Is the positive discharges temperature dependant?	Yes	Yes	Yes
Is the discharge angle shifted by 30° from the 45°/225° axis?	Yes	Yes	Yes
Does the two dimensional plot indicate a "hump", as normally associated with phase-phase PD?	No	No	No
Is the relationship between the affected phases, clearly visible on the LPD plot (for the correct phase rotation)?	No	No	No
Are the discharges shifted by 60°/120° from the 45°/225° axis?	No	No	No
Are the discharges occurring at the 0°/180°?	No	No	No

Table 7.48: Winding configuration for motor # 380AB1

Winding type	Impregnation type	Coils	Turns/ coil	Conductor size	Slot width	Con.
Form coil	VPI	72	6	8x2x2(top)	11.9	Star

Observations

The positive discharges of phases-B&C are shifted with 30° from the classical position.

Conclusion

- The bulk of the discharges appear to be occurring in the slot portion, with some discharging phase-to-phase.
- Discharge levels seemed to have increased substantially since the previous measurement in the plant.
- After the machine was cleaned, there was no sign of the endwinding "humps" normally associated with endwinding contamination.
- Although the LPD plots indicate phase-to-phase discharges, the linear plots do not show any "humps".

7.2.1.4.7 Motor # 380XX1

Table 7.49: Nameplate data for motor # 380XX1

Make	Power	Stator Voltage	Stator Current	# Poles
Hertz	380 kW	3300 V	n/a	4-pole

Table 7.50: Discharge magnitudes for motor # 380XX1

Load and temperature	Phase-A		Phase-B		Phase-C	
PD measured at no-load, with the temperature of the stator winding at 25°C, 27°C and 28°C respectively.	+NQN	-NQN	+NQN	-NQN	+NQN	-NQN
	342	406	504	459	51	29
	+Qmax	-Qmax	+Qmax	-Qmax	+Qmax	-Qmax
	227	192	306	271	33	25
PD measured at 100% load, with the temperature of the stator winding at 41°C, 37°C and 33°C respectively.	+NQN	-NQN	+NQN	-NQN	+NQN	-NQN
	221	167	537	403	49	28
	+Qmax	-Qmax	+Qmax	-Qmax	+Qmax	-Qmax
	155	112	308	235	29	19
PD measured at 100% load, with the temperature of the stator winding at 82°C, 67°C and 79°C respectively.	+NQN	-NQN	+NQN	-NQN	+NQN	-NQN
	240	328	952	795	100	97
	+Qmax	-Qmax	+Qmax	-Qmax	+Qmax	-Qmax
	136	200	540	463	72	56
PD measured at no-load, with the temperature of the stator winding at 77°C, 78°C and 75°C respectively.	+NQN	-NQN	+NQN	-NQN	+NQN	-NQN
	235	332	1174	836	101	92
	+Qmax	-Qmax	+Qmax	-Qmax	+Qmax	-Qmax
	154	195	741	571	54	53

(See Appendixes A72-A76, for graphical representation of discharges)

Table 7.51: Analysis matrix for motor # 380XX1

Condition	Phase-A	Phase-B	Phase-C
Can the graphical data be analysed?	Yes	Yes	Yes
If not, supply reason?	n/a		

Table 7.51: (Cont.)

Condition	Phase-A	Phase-B	Phase-C
Are any discharges centred at the classical discharge position of (45°/225°)?	No	Yes	No
Does this classical PD have polarity predominance?	n/a	No	n/a
Are the negative discharges predominant?	n/a	No	n/a
Are the positive discharges predominant?	n/a	Yes	n/a
Is the positive discharges load dependant?	n/a	No	n/a
Is the positive discharges temperature dependant?	n/a	Yes	n/a
Is the discharge angle shifted by 30° from the 45°/225° axis?	No	Yes	No
Does the two dimensional plot indicate a "hump", as normally associated with phase-phase PD?	No	No	No
Is the relationship between the affected phases, clearly visible on the LPD plot (for the correct phase rotation)?	Yes	Yes	No
Are the discharges shifted by 60°/120° from the 45°/225° axis?	No	No	n/c
Are the discharges occurring at the 0°/180°?	Yes	No	No

Table 7.52: Winding configuration for motor # 380XX1

Winding type	Impregnation type	Coils	Turns/ coil	Conductor size	Slot width	Con.
Form coil	VPI	72	7	2(5.2x3)	13	Star

Observations

The machine was newly manufactured according to the data indicated in the winding

configuration table.

Conclusion

Discharges are definitely phase-to-phase related. The bulk of the discharges are occurring between phases-A&B:

- Phase-to-phase discharges can occur on the endwinding due to contamination. Contamination can lead to tracking which will eventually lead to a phase-to-phase failure.
- Inadequate spacing/ insulation between coils can lead to discharges between coils causing a build-up of ozone.
- It is however not possible to determine if this is occurring between coils in the slot or on the endwinding.

7.2.1.4.8 Motor # 400KW GEC

Table 7.53: Nameplate data for motor # 400KW GEC

Make	Power	Stator Voltage	Stator Current	Speed
GEC	400 kW	3300 V	85 A	1480 r/min

Table 7.54: Discharge magnitudes for motor # 400KW GEC

Load and temperature	Phase-A		Phase-B		Phase-C	
PD measured at no-load,	+NQN	-NQN	+NQN	-NQN	+NQN	-NQN
with the temperature of	21	64	56	13	69	46
the stator winding at	+Qmax	-Qmax	+Qmax	-Qmax	+Qmax	-Qmax
41°C.	0	48	0	0	50	42
PD measured at 100%	+NQN	-NQN	+NQN	-NQN	+NQN	-NQN
load, with the	34	24	77	29	94	96

Table 7.54: (Cont.)

Load and temperature	Phase-A		Phase-B		Phase-C	
temperature of the stator	+Qmax	-Qmax	+Qmax	-Qmax	+Qmax	-Qmax
winding at 53°C, 46°C and 42°C respectively.	34	0	54	0	62	63
PD measured at 100%	+NQN	-NQN	+NQN	-NQN	+NQN	-NQN
load, with the	48	30	118	91	109	79
temperature of the stator	+Qmax	-Qmax	+Qmax	-Qmax	+Qmax	-Qmax
winding at 70°C, 74°C and 80°C respectively.	25	8	51	46	66	53

(See Appendixes A90-A94, for graphical representation of discharges)

Table 7.55: Analysis matrix for motor # 400KW GEC

Condition	Phase-A	Phase-B	Phase-C
Can the graphical data be analysed?	Yes	Yes	Yes
If not, supply reason?	n/a		
Are any discharges centred at the classical discharge position of (45°/225°)?	Yes	Yes	Yes
Does this classical PD have polarity predominance?	Yes	Yes	Yes
Are the negative discharges predominant?	No	No	No
Are the positive discharges predominant?	Yes	Yes	Yes
Is the positive discharges load dependant?	No	No	No
Is the positive discharges temperature dependant?	Yes	Yes	Yes
Is the discharge angle shifted by 30° from the 45°/225° axis?	No	No	No
Does the two dimensional plot indicate a "hump", as normally associated with phase-phase PD?	Yes	No	No
Is the relationship between the affected phases,	No	No	No

Table 7.55: (Cont.)

Condition	Phase-A	Phase-B	Phase-C
clearly visible on the LPD plot (for the correct phase rotation)?			
Are the discharges shifted by 60°/120° from the 45°/225° axis?	No	No	No
Are the discharges occurring at the 0°/180°?	No	No	No

Table 7.56: Winding configuration for motor # 400KW GEC

Winding type	Impregnation type	Coils	Turns/ coil	Conductor size	Slot width	Con.
Form coil	VPI	60	7	7.3x3.35	9.5	n/a

Observation

This machine still has its' original GEC winding. The winding data could not be obtained from the manufacturer. The data shown in the Winding configuration column above, were obtained from the data sheet of an identical machine.

Conclusion

Discharges appear to be occurring in the slot portion of the winding.

7.2.1.4.9 Motor # 585AA2

Table 7.57: Nameplate data for motor # 585AA2

Make	Power	Stator Voltage	Stator Current	Speed
Brown Boveri	585 hp	3300 V	95 A	980 r/min

Table 7.58: Discharge magnitudes for motor # 585AA2

Load and temperature	Phase-A		Phase-B		Phase-C	
PD measured at no-load, with the temperature of the stator winding at 26°C, 28°C and 28°C respectively.	+NQN	-NQN	+NQN	-NQN	+NQN	-NQN
	202	76	152	52	n/a	71
	+Qmax	-Qmax	+Qmax	-Qmax	+Qmax	-Qmax
	129	45	84	37	54	35
PD measured at 70% load, with the temperature of the stator winding at 35°C, 40°C and 43°C respectively.	+NQN	-NQN	+NQN	-NQN	+NQN	-NQN
	297	191	179	80	226	148
	+Qmax	-Qmax	+Qmax	-Qmax	+Qmax	-Qmax
	142	68	95	38	117	76

(See Appendixes A95-A99, for graphical representation of discharges)

Table 7.59: Analysis matrix for motor # 585AA2

Condition	Phase-A	Phase-B	Phase-C
Can the graphical data be analysed?	Yes	Yes	Yes
If not, supply reason?	n/a		
Are any discharges centred at the classical discharge position of (45°/225°)?	Yes	Yes	Yes
Does this classical PD have polarity predominance?	Yes	Yes	Yes
Are the negative discharges predominant?	No	No	No
Are the positive discharges predominant?	Yes	Yes	Yes
Is the positive discharges load dependant?	n/a	n/a	n/a
Is the positive discharges temperature dependant?	Yes	Yes	Yes
Is the discharge angle shifted by 30° from the 45°/225° axis?	Yes	Yes	Yes

Table 7.59: (Cont.)

Condition	Phase-A	Phase-B	Phase-C
Does the two dimensional plot indicate a "hump", as normally associated with phase-to-phase PD?	No	No	No
Is the relationship between the affected phases, clearly visible on the LPD plot (for the correct phase rotation)?	No	No	No
Are the discharges shifted by 60°/120° from the 45°/225° axis?	No	No	No
Are the discharges occurring at the 0°/180°?	No	No	No

Table 7.60: Winding configuration for motor # 585AA2

Winding type	Impregnation type	Coils	Turns/ coil	Conductor size	Slot width	Con.
Form coil	VPI	72	16	2(4.8x1.2)	n/a	n/a

Observation

- Only the positive part of the discharges at full-load, are shifted with 30° from the classical position.
- The machine had been rewound according to the winding data listed in the winding configuration table.

Conclusion

The bulk of the discharges appear to be occurring in the slot portion, close to the surface of the coil.

7.2.1.4.10 Conclusion summary for vpi motors tested at the Test Floor

- All the motors tested showed some indication of PD activity.
- Most machines show signs of phase-to-phase related PD.
- A fair amount of motors show discharges in the slot on the surface of the coil. This could be due to the absence of semi conducting tape on the coils.
- The PD activity in these motors could be an indication of the condition of the motor, as far as:
  - Slot discharges, and
  - Phase-to-phase discharges is concerned.

7.2.2 Winding type: Random wound

7.2.2.1 Motor # 160BB3

Table 7.61: Nameplate data for motor # 160BB3

Make	Power	Stator Voltage	Stator Current	Speed
AEI	160 kW	3300 V	33 A	1482 r/min

Table 7.62: Discharge magnitudes for motor # 160BB3

Load and temperature	Phase-A		Phase-B		Phase-C	
PD measured at no-load, with the temperature of the stator winding at 24°C, 26°C and 33°C respectively.	+NQN	-NQN	+NQN	-NQN	+NQN	-NQN
	313	354	705	534	191	191
	+Qmax	-Qmax	+Qmax	-Qmax	+Qmax	-Qmax
	204	216	332	235	122	142
PD measured at 100% load, with the temperature of the stator winding at 40°C, 39°C and 35°C respectively.	+NQN	-NQN	+NQN	-NQN	+NQN	-NQN
	272	272	1041	965	426	301
	+Qmax	-Qmax	+Qmax	-Qmax	+Qmax	-Qmax
	179	192	736	656	175	168
PD measured at 150% load, with the temperature of the stator winding at 50°C, 60°C and 58°C respectively.	+NQN	-NQN	+NQN	-NQN	+NQN	-NQN
	272	265	1314	1747	577	388
	+Qmax	-Qmax	+Qmax	-Qmax	+Qmax	-Qmax
	161	143	689	738	275	220
PD measured at no-load, with the temperature of	+NQN	-NQN	+NQN	-NQN	+NQN	-NQN
	n/a	n/a	1420	1533	n/a	n/a

Table 7.62: (Cont.)

Load and temperature	Phase-A		Phase-B		Phase-C	
the stator winding at	+Qmax	-Qmax	+Qmax	-Qmax	+Qmax	-Qmax
60°C.	n/a	n/a	757	530	n/a	n/a

(See Appendixes A6-A10, for graphical representation of discharges)

Table 7.63: Analysis matrix for motor # 160BB3

Condition	Phase-A	Phase-B	Phase-C
Can the graphical data be analysed?	Yes	Yes	Yes
If not, supply reason?	n/a		
Are any discharges centred at the classical discharge position of (45°/225°)?	n/c	No	Yes
Does this classical PD have polarity predominance?	n/a	n/a	Yes
Are the negative discharges predominant?	n/a	n/a	No
Are the positive discharges predominant?	n/a	n/a	Yes
Is the positive discharges load dependant?	n/a	n/a	Yes
Is the positive discharges temperature dependant?	n/a	n/a	Yes
Is the discharge angle shifted by 30° from the 45°/225° axis?	n/a	Yes	Yes
Does the two dimensional plot indicate a "hump", as normally associated with phase-phase PD?	No	No	No
Is the relationship between the affected phases, clearly visible on the LPD plot (for the correct phase rotation)?	No	Yes	Yes
Are the discharges shifted by 60°/120° from the 45°/225° axis?	n/c	No	No
Are the discharges occurring at the 0°/180°?	n/c	No	No

Table 7.64: Winding configuration for motor # 160BB3

Winding type	Impregnation type	Coils	Turns/ coil	Conductor size	Slot width	Con.
Random	Dip	60	22	4x1.25 & 1x1.35	n/a	Star

Observations

- Phase-C experienced a drastic increase in PD between no-load and full-load, with only a 2°C rise in temperature.
- Discharges occurring at 135° and 315° on phase-A, appears to be cross-coupled from phases-B & C.

Conclusion

- Most of the discharge activity is definitely phase-to-phase related. The bulk of the discharges are occurring between phases-B&C, with cross-coupling to phase-A.
  - Phase-to-phase discharges can occur on the endwinding due to contamination. Contamination can lead to tracking which will eventually lead to a phase-to-phase failure.
  - Inadequate spacing/ insulation between coils can lead to discharges between coils causing a build-up of ozone.
  - It is however not possible to determine if this is occurring between coils in the slot or on the endwinding.
- Phase-C experienced a sudden increase in positive discharges between no-load and full-load, which has the appearance of a loose coil. This phenomenon could however be influenced by the fact that the temperature sensing devices are positioned per phase and not per slot (It is also uncertain what the discharge activity of a loose random wound coil, would be).

7.2.2.2 Motor # 175BD3

Table 7.65: Nameplate data for motor # 175BD3

Make	Power	Stator Voltage	Stator Current	Speed
GEC	130 kW	3300 V	29 A	1487 r/min

Table 7.66: Discharge magnitudes for motor # 175BD3

Load and temperature	Phase-A		Phase-B		Phase-C	
PD measured at no-load, with the temperature of the stator winding at 22°C, 24°C and 23°C respectively.	+NQN	-NQN	+NQN	-NQN	+NQN	-NQN
	991	759	2404	2547	1929	1186
	+Qmax	-Qmax	+Qmax	-Qmax	+Qmax	-Qmax
	600	501	1266	1408	1223	738
PD measured at 100% load, with the temperature of the stator winding at 30°C, 35°C and 40°C respectively.	+NQN	-NQN	+NQN	-NQN	+NQN	-NQN
	1196	795	2343	2573	2102	1541
	+Qmax	-Qmax	+Qmax	-Qmax	+Qmax	-Qmax
	575	509	1312	1411	1090	828
PD measured at 100% load, with the temperature of the stator winding at 95°C, 92°C and 90°C respectively.	+NQN	-NQN	+NQN	-NQN	+NQN	-NQN
	515	376	457	434	1300	1156
	+Qmax	-Qmax	+Qmax	-Qmax	+Qmax	-Qmax
	391	358	233	257	878	719
PD measured at no-load, with the temperature of the stator winding at 83°C, 80°C and 75°C respectively.	+NQN	-NQN	+NQN	-NQN	+NQN	-NQN
	539	542	722	505	1635	1282
	+Qmax	-Qmax	+Qmax	-Qmax	+Qmax	-Qmax
	391	384	481	371	955	617

(See Appendixes A22-A26, for graphical representation of discharges)

Table 7.67: Analysis matrix for motor # 175BD3

Condition	Phase-A	Phase-B	Phase-C
Can the graphical data be analysed?	Yes	Yes	Yes
If not, supply reason?		n/a	
Are any discharges centred at the classical discharge position of (45°/225°)?	Yes	Yes	Yes
Does this classical PD have polarity predominance?	No	No	No
Are the negative discharges predominant?	n/a	n/a	n/a
Are the positive discharges predominant?	n/a	n/a	n/a
Is the positive discharges load dependant?	n/a	n/a	n/a
Is the positive discharges temperature dependant?	n/a	n/a	n/a
Is the discharge angle shifted by 30° from the 45°/225° axis?	n/c	Yes	No
Does the two dimensional plot indicate a "hump", as normally associated with phase-phase PD?	No	No	No
Is the relationship between the affected phases, clearly visible on the LPD plot (for the correct phase rotation)?	n/c	n/c	n/c
Are the discharges shifted by 60°/120° from the 45°/225° axis?	n/c	No	No
Are the discharges occurring at the 0°/180°?	No	Yes	No

Table 7.68: Winding configuration for motor # 175BD3

Winding type	Impregnation type	Coils	Turns/ coil	Conductor size	Slot width	Con.
Random	Dip	30	38	1.5, 1.4, 1.0	n/a	Δ

Observations

- This machine has been rewound with the data indicated in the winding configuration column.
- The machine experienced very high discharge levels.

Conclusion

The bulk of the discharges appear to be occurring in the slot portion of the winding, between the conductors and the core.

7.2.2.3 Motor # 240AB3

Table 7.69: Nameplate data for motor # 240AB3

Make	Power	Stator Voltage	Stator Current	Speed
AEI	240 kW	3300 V	48 A	1482 r/min

Table 7.70: Discharge magnitudes for motor # 240AB3

Load and temperature	Phase-A		Phase-B		Phase-C	
PD measured at no-load, with the temperature of the stator winding at 25°C external.	+NQN	-NQN	+NQN	-NQN	+NQN	-NQN
	3	1	5	3	13	n/a
	+Qmax	-Qmax	+Qmax	-Qmax	+Qmax	-Qmax
	3	0	3	3	4	4
PD measured at 100% load, with the temperature of the stator winding not measured.	+NQN	-NQN	+NQN	-NQN	+NQN	-NQN
	5	4	12	5	2	4
	+Qmax	-Qmax	+Qmax	-Qmax	+Qmax	-Qmax
	4	0	10	0	0	0
PD measured at 100% load, with the temperature of the stator winding at 43°C external.	+NQN	-NQN	+NQN	-NQN	+NQN	-NQN
	24	25	43	40	49	44
	+Qmax	-Qmax	+Qmax	-Qmax	+Qmax	-Qmax
	13	12	26	22	26	26
PD measured at no-load, with the temperature of the stator winding not measured.	+NQN	-NQN	+NQN	-NQN	+NQN	-NQN
	25	24	48	49	83	53
	+Qmax	-Qmax	+Qmax	-Qmax	+Qmax	-Qmax
	16	14	21	34	47	37

(See Appendixes A42-A46, for graphical representation of discharges)

Table 7.71: Analysis matrix for motor # 240AB3

Condition	Phase-A	Phase-B	Phase-C
Can the graphical data be analysed?	Yes	Yes	Yes
If not, supply reason?	n/a		
Are any discharges centred at the classical discharge position of (45°/225°)?	n/c	No	n/c

Table 7.71: (Cont.)

Condition	Phase-A	Phase-B	Phase-C
Does this classical PD have polarity predominance?	n/a	n/a	n/a
Are the negative discharges predominant?	n/a	n/a	n/a
Are the positive discharges predominant?	n/a	n/a	n/a
Is the positive discharges load dependant?	n/a	n/a	n/a
Is the positive discharges temperature dependant?	n/a	n/a	n/a
Is the discharge angle shifted by 30° from the 45°/225° axis?	No	Yes	Yes
Does the two dimensional plot indicate a "hump", as normally associated with phase-phase PD?	Yes	Yes	Yes
Is the relationship between the affected phases, clearly visible on the LPD plot (for the correct phase rotation)?	n/c	n/c	n/c
Are the discharges shifted by 60°/120° from the 45°/225° axis?	No	No	No
Are the discharges occurring at the 0°/180°?	No	No	No

Table 7.72: Winding configuration for motor # 240AB3

Winding type	Impregnation type	Coils	Turns/ coil	Conductor size	Slot width	Con.
Random	Unknown	60	30	2x064 & 2x060	n/a	n/a

Observations

This machine still has its' original AEI winding. The winding data could not be obtained from the manufacturer. The data shown in the winding configuration column

above, were obtained from the data sheet of an identical machine.

Conclusion

Discharge activity appears to be phase-to-phase related.

- Phase-to-phase discharges can occur on the endwinding due to contamination. Contamination can lead to tracking which will eventually lead to a phase-to-phase failure.
- Inadequate spacing/ insulation between coils can lead to discharges between coils causing a build-up of ozone.
- It is however not possible to determine if this is occurring between coils in the slot or on the endwinding.

7.2.2.4 Motor # 250BC3

Table 7.73: Nameplate data for motor # 250BC3

Make	Power	Stator Voltage	Stator Current	Speed
Hawker Siddeley	250 hp	3300 V	43.7 A	1488 r/min

Table 7.74: Discharge magnitudes for motor # 250BC3

Load and temperature	Phase-A		Phase-B		Phase-C	
PD measured at no-load, with the temperature of the stator winding at 23°C, 24°C and 27°C respectively.	+NQN	-NQN	+NQN	-NQN	+NQN	-NQN
	8	10	n/a	n/a	5	n/a
	+Qmax	-Qmax	+Qmax	-Qmax	+Qmax	-Qmax
	0	0	0	0	7	0
PD measured at 100%	+NQN	-NQN	+NQN	-NQN	+NQN	-NQN

Load and temperature	Phase-A		Phase-B		Phase-C	
load, with the temperature of the stator winding at 37°C, 34°C and 32°C respectively.	1	2	n/a	n/a	10	n/a
	+Qmax	-Qmax	+Qmax	-Qmax	+Qmax	-Qmax
	0	0	0	0	12	0
PD measured at 150% load, with the temperature of the stator winding at 85°C, 79°C and 87°C respectively.	**+NQN**	**-NQN**	**+NQN**	**-NQN**	**+NQN**	**-NQN**
	62	61	72	86	117	67
	+Qmax	**-Qmax**	**+Qmax**	**-Qmax**	**+Qmax**	**-Qmax**
	28	31	35	36	63	43

(See Appendixes A52-A56, for graphical representation of discharges)

Table 7.75: Analysis matrix for motor # 250BC3

Condition	Phase-A	Phase-B	Phase-C
Can the graphical data be analysed?	Yes	Yes	Yes
If not, supply reason?	n/a		
Are any discharges centred at the classical discharge position of (45°/225°)?	No	Yes	No
Does this classical PD have polarity predominance?	n/a	No	n/a
Are the negative discharges predominant?	n/a	n/a	n/a
Are the positive discharges predominant?	n/a	n/a	n/a
Is the positive discharges load dependant?	n/a	n/a	n/a
Is the positive discharges temperature dependant?	n/a	n/a	n/a
Is the discharge angle shifted by 30° from the 45°/225° axis?	No	No	No
Does the two dimensional plot indicate a "hump", as normally associated with phase-phase PD?	No	Yes	No

Table 7.75: (Cont.)

Condition	Phase-A	Phase-B	Phase-C
Is the relationship between the affected phases, clearly visible on the LPD plot (for the correct phase rotation)?	n/c	n/c	n/c
Are the discharges shifted by 60°/120° from the 45°/225° axis?	n/c	No	n/c
Are the discharges occurring at the 0°/180°?	No	No	No

Table 7.76: Winding configuration for motor # 250BC3

Winding type	Impregnation type	Coils	Turns/ coil	Conductor size	Slot width	Con.
Random	Dip	48	11	6x1.7	n/a	Star

Observations

This machine still has its' original Hawker Siddeley winding. The winding data could not be obtained from the manufacturer. The data shown in the winding configuration column above, were obtained from the data sheet of an identical machine.

Conclusion

- Some discharge activity appears to be phase-to-phase related.
  - Phase-to-phase discharges can occur on the endwinding due to contamination. Contamination can lead to tracking which will eventually lead to a phase-to-phase failure.
  - Inadequate spacing/ insulation between coils can lead to discharges between coils causing a build-up of ozone.
  - It is however not possible to determine if this is occurring between coils in the slot or on the endwinding.
- Discharge patterns appear to be random.

7.2.2.5 Motor # 400CE1

Table 7.77: Nameplate data for motor # 400CE1

Make	Power	Stator Voltage	Stator Current	Speed
Hawker Siddeley	400 hp	3300 V	80 A	738 r/min

Table 7.78: Discharge magnitudes for motor # 400CE1

Load and temperature	Phase-A		Phase-B		Phase-C	
PD measured at no-load, with the temperature of the stator winding at 25°C, 26°C and 27°C respectively.	+NQN	-NQN	+NQN	-NQN	+NQN	-NQN
	170	163	229	225	189	167
	+Qmax	-Qmax	+Qmax	-Qmax	+Qmax	-Qmax
	93	93	124	115	93	93
PD measured at 100% load, with the temperature of the stator winding at 30°C, 32°C and 30°C respectively.	+NQN	-NQN	+NQN	-NQN	+NQN	-NQN
	153	157	238	165	112	109
	+Qmax	-Qmax	+Qmax	-Qmax	+Qmax	-Qmax
	53	53	104	89	57	57
PD measured at 100% load, with the temperature of the stator winding at 51°C, 51°C and 51°C respectively.	+NQN	-NQN	+NQN	-NQN	+NQN	-NQN
	375	350	1525	1219	n/a	n/a
	+Qmax	-Qmax	+Qmax	-Qmax	+Qmax	-Qmax
	194	161	915	919	n/a	n/a
PD measured at no-load, with the temperature of the stator winding at	+NQN	-NQN	+NQN	-NQN	+NQN	-NQN
	552	412	1826	1508	803	730
	+Qmax	-Qmax	+Qmax	-Qmax	+Qmax	-Qmax

Table 7.78: (Cont.)

Load and temperature	Phase-A		Phase-B		Phase-C	
50°C, 49°C and 47°C respectively.	259	231	1022	1033	344	344

(See Appendixes A82-A85, for graphical representation of discharges)

Table 7.79: Analysis matrix for motor # 400CE1

Condition	Phase-A	Phase-B	Phase-C
Can the graphical data be analysed?	Yes	Yes	Yes
If not, supply reason?	n/a		
Are any discharges centred at the classical discharge position of (45°/225°)?	Yes	Yes	Yes
Does this classical PD have polarity predominance?	Yes	Yes	Yes
Are the negative discharges predominant?	No	No	No
Are the positive discharges predominant?	Yes	Yes	Yes
Is the positive discharges load dependant?	n/c	n/c	n/c
Is the positive discharges temperature dependant?	Yes	Yes	Yes
Is the discharge angle shifted by 30° from the 45°/225° axis?	n/c	n/c	n/c
Does the two dimensional plot indicate a "hump", as normally associated with phase-phase PD?	Yes	Yes	Yes
Is the relationship between the affected phases, clearly visible on the LPD plot (for the correct phase rotation)?	No	No	No
Are the discharges shifted by 60°/120° from the 45°/225° axis?	No	No	No
Are the discharges occurring at the 0°/180°?	No	No	No

Table 7.80: Winding configuration for motor # 400CE1

Winding type	Impregnation type	Coils	Turns/ coil	Conductor size	Slot width	Con.
Random	Dip	36	12	1.6 x 10	n/a	n/a

Observation

- Discharges are occurring around the classical position, with some discharges possibly 30° shifted.
- The machine had been rewound according to the winding data listed in the winding configuration table.

Conclusion

The bulk of the discharges appear to be occurring in the slot portion, with some discharging phase-to-phase.

7.2.2.6 Conclusion summary for random wound motors tested at the Test Floor

- Random wound motors are experiencing very high levels of PD activity.
- The majority of the discharges are occurring within the coil, possibly between the conductors and the core and between the individual conductors.
- There are also indications of phase-to-phase discharges.

7.2.3 Winding type: Unknown

7.2.3.1 Motor # 400CH1

Table 7.81: Nameplate data for motor # 400CH1

Make	Power	Stator Voltage	Stator Current	Speed
GEC	400 kW	3300 V	89 A	989 r/min

Table 7.82: Discharge magnitudes for motor # 400CH1

Load and temperature	Phase-A		Phase-B		Phase-C	
PD measured at no-load, with the temperature of the stator winding at *x*°C.	+NQN	-NQN	+NQN	-NQN	+NQN	-NQN
	n/a	2	27	n/a	n/a	6
	+Qmax	-Qmax	+Qmax	-Qmax	+Qmax	-Qmax
	0	0	30	0	0	6
PD measured at 100% load, with the temperature of the stator winding at 21°C, 21°C and 24°C respectively.	+NQN	-NQN	+NQN	-NQN	+NQN	-NQN
	n/a	n/a	29	25	15	16
	+Qmax	-Qmax	+Qmax	-Qmax	+Qmax	-Qmax
	0	0	24	24	0	0
PD measured at 100% load, with the temperature of the stator winding at 34°C, 34°C and 34°C respectively.	+NQN	-NQN	+NQN	-NQN	+NQN	-NQN
	60	49	40	23	36	30
	+Qmax	-Qmax	+Qmax	-Qmax	+Qmax	-Qmax
	34	29	33	0	33	31
PD measured at no-load, with the temperature of	+NQN	-NQN	+NQN	-NQN	+NQN	-NQN
	96	95	48	33	28	26

Table 7.82: (Cont.)

Load and temperature	Phase-A		Phase-B		Phase-C	
the stator winding at	+Qmax	-Qmax	+Qmax	-Qmax	+Qmax	-Qmax
34°C.	62	57	36	0	31	29

(See Appendixes A86-A89, for graphical representation of discharges)

Table 7.83: Analysis matrix for motor # 400CH1

Condition	Phase-A	Phase-B	Phase-C
Can the graphical data be analysed?	Yes	Yes	Yes
If not, supply reason?		n/a	
Are any discharges centred at the classical discharge position of (45°/225°)?	n/c	Yes	Yes
Does this classical PD have polarity predominance?	n/a	No	No
Are the negative discharges predominant?	n/a	n/a	n/a
Are the positive discharges predominant?	n/a	n/a	n/a
Is the positive discharges load dependant?	n/a	n/a	n/a
Is the positive discharges temperature dependant?	n/a	n/a	n/a
Is the discharge angle shifted by 30° from the 45°/225° axis?	n/c	n/c	n/c
Does the two dimensional plot indicate a "hump", as normally associated with phase-phase PD?	No	No	No
Is the relationship between the affected phases, clearly visible on the LPD plot (for the correct phase rotation)?	No	No	No
Are the discharges shifted by 60°/120° from the 45°/225° axis?	No	No	No
Are the discharges occurring at the 0°/180°?	No	No	No

Table 7.84: Winding configuration for motor # 400CH1

Winding type	Impregnation type	Coils	Turns/ coil	Conductor size	Slot width	Con.
n/a	n/a	n/a	n/a	n/a	n/a	n/a

Observation

No winding data was available for this machine type.

Conclusion

Discharges appear to be occurring in the slot portion of the winding.

CHAPTER 8 – PD TESTING OF SPECIAL MACHINES

8.1 Introduction

Two redundant 3,3 kV machines were donated to the project by Iscor Flat Steel Products for the purpose of studying the effect of increased temperature and load on the discharge activity. To be able to subject these machines to extreme thermal stresses, the machines were coupled to a hydraulic dynamometer located in the Test Floor and overloaded.

8.2 Testing of motor # 250BB3

This machine was originally built by AEI, but rewound in February 1999 by an independent repair facility. It operated for two months in the plant, prior to be decommissioned.

The machine was subjected to different overload cycles over a period of three days as displayed in Table 8.1:

Table 8.1: Load cycle for motor # 250BB3

Day 1 – 13/04/1999						
Load %	**Time**	**Temp.(°C)**	**+NQN**	**-NQN**	**+Qmax**	**-Qmax**
100	17:22	28	95	68	47	33
170	21:31	134	2491	200	1233	0
Day 2 – 14/04/1999						
Load %	**Time**	**Temp.(°C)**	**+NQN**	**-NQN**	**+Qmax**	**-Qmax**
100	10:06	31	402	173	194	128
175	11:30	149	2312	210	1186	223

Table 8.1: (Cont.)

Day 3 – 15/04/1999						
Load %	**Time**	**Temp.(°C)**	**+NQN**	**-NQN**	**+Qmax**	**-Qmax**
100	14:10	33	416	268	267	147
200	14:39	173	2136	229	1075	257

(See Appendixes B1-B7, for graphical representation of discharges)

Table 8.2: Analysis matrix for motor # 250BB3

Condition	Phase-A	Phase-B	Phase-C
Can the graphical data be analysed?	Yes	Yes	Yes
If not, supply reason?	n/a		
Are any discharges centred at the classical discharge position of (45°/225°)?	Yes	Yes	Yes
Does this classical PD have polarity predominance?	Yes	Yes	Yes
Are the negative discharges predominant?	No	No	No
Are the positive discharges predominant?	Yes	Yes	Yes
Is the positive discharges load dependant?	No	No	No
Is the positive discharges temperature dependant?	Yes	Yes	Yes
Is the discharge angle shifted by 30° from the 45°/225° axis?	n/c	n/c	n/c
Does the two dimensional plot indicate a "hump", as normally associated with phase-to-phase PD?	No	No	No
Is the relationship between the affected phases, clearly visible on the LPD plot (for the correct phase rotation)?	No	No	No
Are the discharges shifted by 60°/120° from the 45°/225° axis?	No	No	No
Are the discharges occurring at the 0°/180°?	No	No	No

Physical inspection of the stator winding by means of dissection

After completion of the three-day testing, the machine was dismantled, and the line-end coils were removed for inspection, which revealed the following:

- The rewind and VPI of this machine was poorly done. There was poor impregnation of the epoxy and the coils were not manufactured to the correct size. This resulted in the coils being forced into the slots. Which caused the coils to skew in the slot (Figure 8.1). It also left gaps (in some areas), of up to 0.8mm between the coil and the slot surface.
- There was visible black discharge residue on the surface of the slot filler between the top and bottom coils (Figure 8.2 & Figure 8.3). The discharge area was almost at the end of the slot.
- The machine was not fitted with neither semicon nor stress grading tapes.

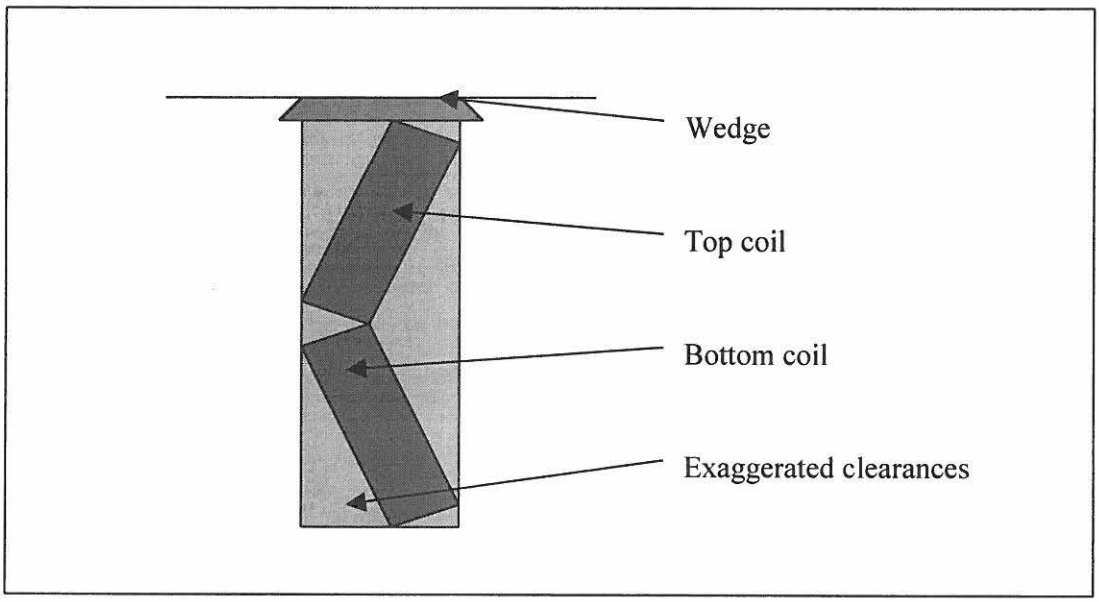

Figure 8.1: Skew coils of motor # 250BB3

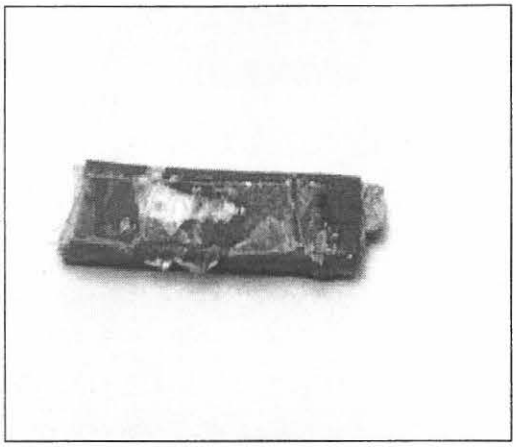

Figure 8.2: Centre filler for motor # 250BB3

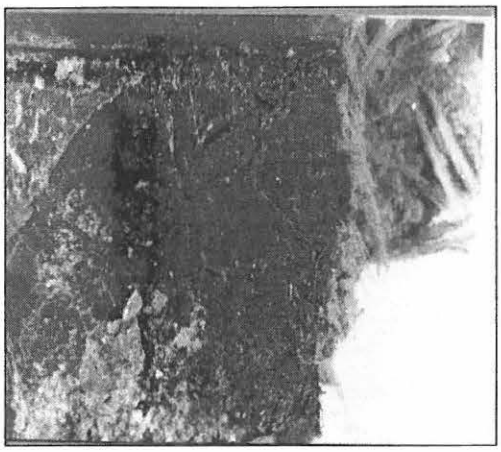

Figure 8.3: Enlarged view of centre filler

Conclusion

- The machine exhibited a dramatic increase in positive discharges with an increase in temperature (while the negative discharges showed a marginal increase). This is a classic example of electrical slot discharge due to the non-existence of the semicon.
- The phase-to-phase related discharges (as shown by the LPD plot) are substantiated by the discharge residue on the slot filler (Figure 8.2), indicating that some discharge has occurred in the slot, between the line-end coil and a coil of another phase in the same slot.

8.3 Testing of motor # 250CG2

This machine was still fitted with its' original winding and operated in the plant since 1983. After initial loading of the machine, it was found that phase-B was emitting the most discharge, and it was decided to focus on this phase.

It was therefore decided to increase the temperature in increments (Table 8.3), while observing the effect on the PD. The dynamometer experienced difficulty in sufficiently

overloading the machine to cause excessive temperature rise. To solve this problem the cooling circuit of the machine was interrupted at 100% load conditions.

Table 8.3: Relationship between PD and temperature of motor # 250CG2

Time	Temp.(°C)	+NQN	-NQN	+Qmax	-Qmax
20:21	37	34	15	18	10
20:36	47	36	16	21	11
20:52	52	35	22	19	10
21:10	65	43	30	24	12
21:21	70	50	36	25	20
21:29	75	51	41	25	20
21:37	80	55	45	27	23
21:46	85	67	50	32	23
21:55	90	80	61	37	27
22:05	95	172	120	84	55
22:14	100	173	149	79	58
22:24	105	229	171	152	159
22:36	111	237	184	149	79
22:46	115	259	172	168	80
22:57	120	295	211	159	94
23:10	125	289	214	160	94
23:23	130	351	206	184	142
23:38	136	390	211	198	140
23:52	141	433	350	284	258
00:03	145	553	302	353	159
00:19	150	650	391	381	302
00:39	155	577	255	397	141

Relationship between temperature and discharge activity

As can be seen from Figure 8.4, there is a steady rise in PD activity with an increase in temperature. Both the positive and negative discharge magnitudes are increasing with the change in positive discharges being consistently more than the negative, with an increase in temperature *(See Appendixes B8-B22 for graphical representation of discharges).*

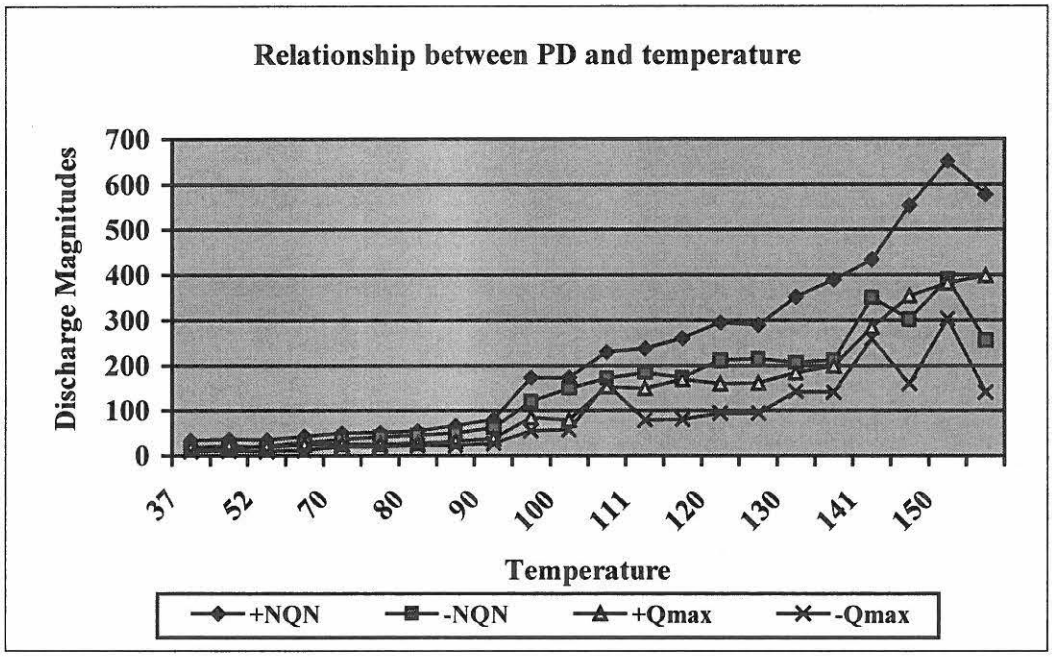

Figure 8.4: Relationship between PD and temperature

Physical inspection of the stator winding by means of dissection

After completion of the three-day testing, the machine was dismantled and the end-windings cut off for inspection, which revealed the following:

- The stator winding was well manufactured, with very few cavities in the insulation.
- The endwinding were forced close together (Figure 8.5).

- Removal of the line-end coils showed discharge activity between one line-end coil and the phase adjacent to it (Figure 8.6 and Figure 8.7).

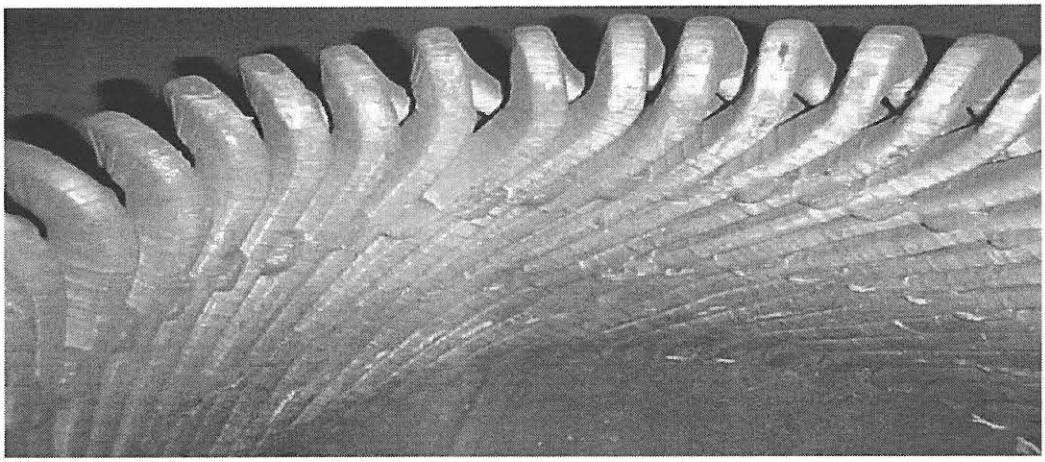

Figure 8.5: End-winding of motor # 250CG2

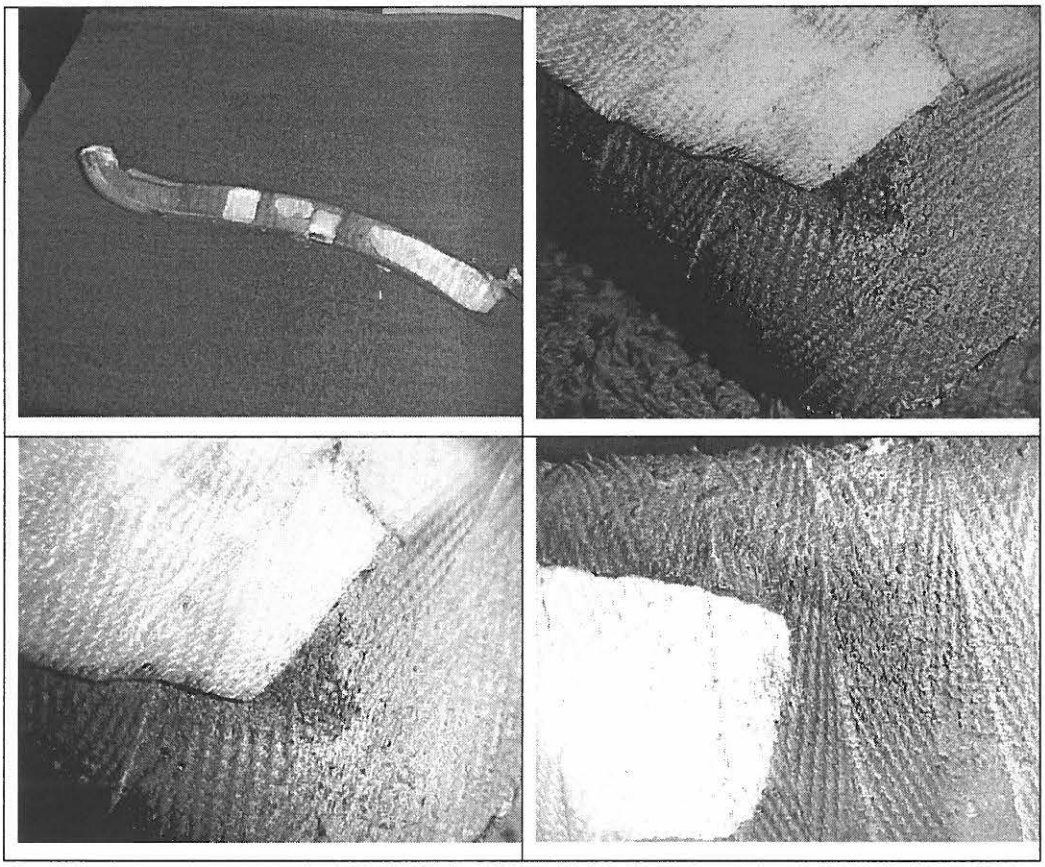

Figure 8.6: Enlargements of PD activity on line-end coil for motor # 250CG2

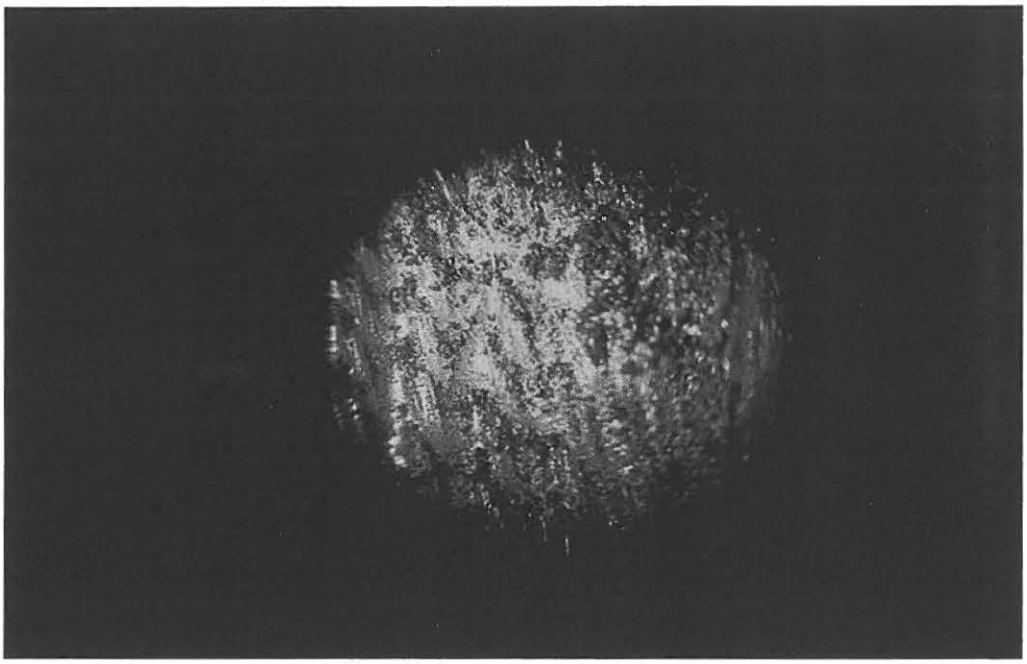

Figure 8.7: 30X enlargement of PD activity on line-end coil of motor # 250CG2

Conclusion

- The machine exhibited an increase in both positive and negative discharges with increased temperature. This is also electrical slot discharge due to the non-existence of the semicon layer.
- There is physical evidence of phase-to-phase related discharges.

CHAPTER 9 – PD TESTING IN A PLANT ENVIRONMENT

9.1 Introduction

Some machines in the plant at Iscor Flat Steel Products are subjected to severe environmental and over-load conditions. Several machines were tested in order to determine levels of PD activity that a 3,3 kV machine would experience in a plant environment under operational conditions.

Figure 9.1 is an example of the inaccessibility of some of the machines that were tested.

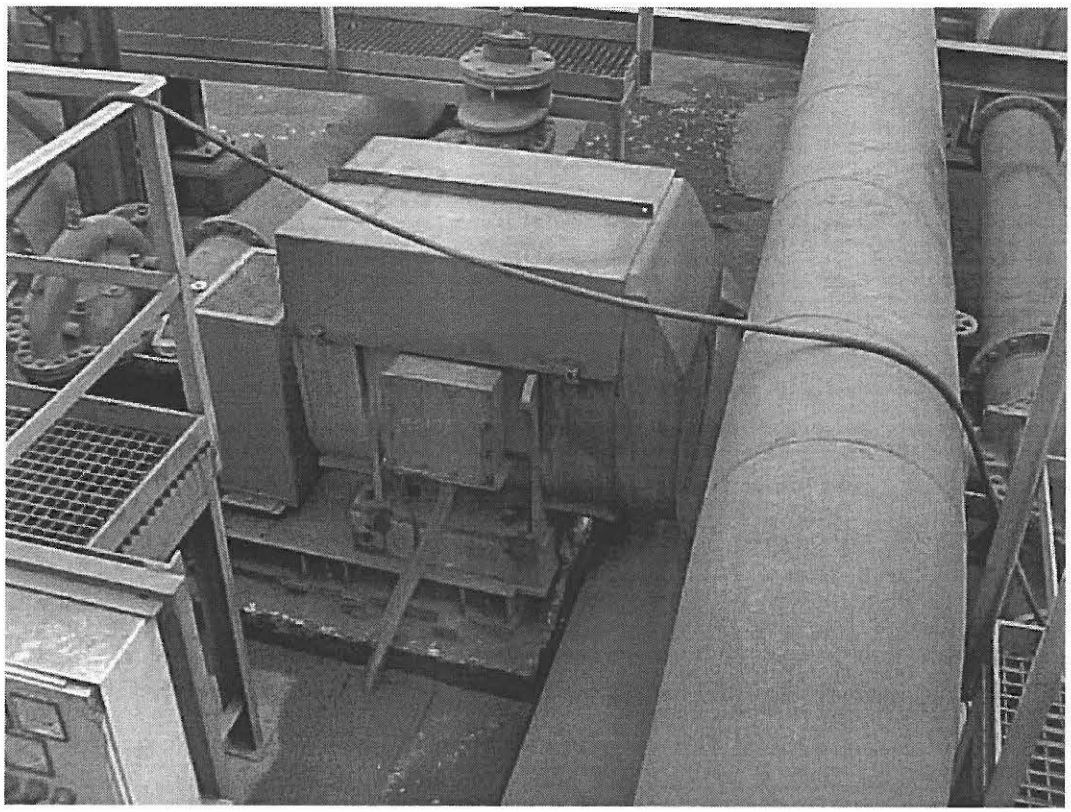

Figure 9.1: Motor # 150CL3

9.2 Plant testing

9.2.1 Motors tested with very low PD values

9.2.1.1 Motor # 150CL2

Table 9.1: Nameplate data for motor # 150CL2

Make	Power	Stator Voltage	Stator Current	Speed
AEI	150 kW	3300 V	31 A	1483 r/min

Table 9.2: Discharge magnitudes for motor # 150CL2

Load and temperature	Phase-A		Phase-B		Phase-C	
PD measured at 100% load, with the temperature of the stator winding unknown.	+NQN	-NQN	+NQN	-NQN	+NQN	-NQN
	n/a	n/a	n/a	n/a	n/a	n/a
	+Qmax	-Qmax	+Qmax	-Qmax	+Qmax	-Qmax
	0	0	0	0	n/a	n/a

(See Appendixes C1-C2, for graphical representation of discharges)

9.2.1.2 Motor # 160BF1

Table 9.3: Nameplate data for motor # 160BF1

Make	Power	Stator Voltage	Stator Current	Speed
Siemens	160 kW	3300 V	37 A	1471 r/min

Table 9.4: Discharge magnitudes for motor # 160BF1

Load and temperature	Phase-A		Phase-B		Phase-C	
PD measured at 90 % load, with the temperature of the stator winding at 45°C.	+NQN	-NQN	+NQN	-NQN	+NQN	-NQN
	n/a	n/a	2	n/a	n/a	n/a
	+Qmax	-Qmax	+Qmax	-Qmax	+Qmax	-Qmax
	0	0	0	0	0	0

(See Appendixes C7, for graphical representation of discharges)

9.2.1.3 Motor # 160BF3

Table 9.5: Nameplate data for motor # 160BF3

Make	Power	Stator Voltage	Stator Current	Speed
Siemens	160 kW	3300 V	37 A	1471 r/min

Table 9.6: Discharge magnitudes for motor # 160BF3

Load and temperature	Phase-A		Phase-B		Phase-C	
PD measured at 90% load, with the temperature of the stator winding at 34°C, 36°C and 42 °C respectively.	+NQN	-NQN	+NQN	-NQN	+NQN	-NQN
	n/a	n/a	n/a	n/a	n/a	n/a
	+Qmax	-Qmax	+Qmax	-Qmax	+Qmax	-Qmax
	0	0	0	0	0	0

(See Appendixes C13, for graphical representation of discharges)

9.1.1.1 Motor # 160BF8

Table 9.7: Nameplate data for motor # 160BF8

Make	Power	Stator Voltage	Stator Current	Speed
Siemens	160 kW	3300 V	37 A	1471 r/min

Table 9.8: Discharge magnitudes for motor # 160BF8

Load and temperature	Phase-A		Phase-B		Phase-C	
PD measured at 70% load, with the temperature of the stator winding at 30°C.	+NQN	-NQN	+NQN	-NQN	+NQN	-NQN
	n/a	n/a	n/a	n/a	n/a	n/a
	+Qmax	-Qmax	+Qmax	-Qmax	+Qmax	-Qmax
	0	0	0	0	0	0

(See Appendixes C14, for graphical representation of discharges)

9.2.1.4 Motor # 160BF10

Table 9.9: Nameplate data for motor # 160BF10

Make	Power	Stator Voltage	Stator Current	Speed
Siemens	160 kW	3300 V	37 A	1471 r/min

Table 9.10: Discharge magnitudes for motor # 160BF10

Load and temperature	Phase-A		Phase-B		Phase-C	
PD measured at 70% load, with the temperature of the stator winding at 54°C.	+NQN	-NQN	+NQN	-NQN	+NQN	-NQN
	n/a	n/a	n/a	n/a	n/a	n/a
	+Qmax	-Qmax	+Qmax	-Qmax	+Qmax	-Qmax
	0	0	0	0	0	0

(See Appendixes C15-C17, for graphical representation of discharges)

9.2.1.5 Motor # 250BC1

Table 9.11: Nameplate data for motor # 250BC1

Make	Power	Stator Voltage	Stator Current	Speed
Hawker Siddeley	250 hp	3300 V	43.7 A	1488 r/min

Table 9.12: Discharge magnitudes for motor # 250BC1

Load and temperature	Phase-A		Phase-B		Phase-C	
PD measured at 70% load, with the temperature of the stator winding at 45°C, 48°C and 51°C respectively.	+NQN	-NQN	+NQN	-NQN	+NQN	-NQN
	n/a	n/a	n/a	n/a	n/a	n/a
	+Qmax	-Qmax	+Qmax	-Qmax	+Qmax	-Qmax
	0	0	0	0	0	0

(See Appendixes C23, for graphical representation of discharges)

9.2.1.6 Motor # 250BC2

Table 9.13: Nameplate data for motor # 250BC2

Make	Power	Stator Voltage	Stator Current	Speed
Hawker Siddeley	250 hp	3300 V	43.7 A	1488 r/min

Table 9.14: Discharge magnitudes for motor # 250BC2

Load and temperature	Phase-A		Phase-B		Phase-C	
PD measured at 95% load, with the temperature of the stator winding at 29°C.	+NQN	-NQN	+NQN	-NQN	+NQN	-NQN
	n/a	n/a	n/a	n/a	n/a	n/a
	+Qmax	-Qmax	+Qmax	-Qmax	+Qmax	-Qmax
	0	0	0	0	0	0

(See Appendixes C24, for graphical representation of discharges)

9.2.1.7 Motor # 250BC3

Table 9.15: Nameplate data for motor # 250BC3

Make	Power	Stator Voltage	Stator Current	Speed
Hawker Siddeley	250 hp	3300 V	43.7 A	1488 r/min

Table 9.16: Discharge magnitudes for motor # 250BC3

Load and temperature	Phase-A		Phase-B		Phase-C	
PD measured at 70%	+NQN	-NQN	+NQN	-NQN	+NQN	-NQN
load, with the	n/a	n/a	n/a	n/a	n/a	n/a
temperature of the stator	+Qmax	-Qmax	+Qmax	-Qmax	+Qmax	-Qmax
winding at 30°C, 33°C	0	0	0	0	0	0
and 36°C respectively.						

(See Appendixes C25, for graphical representation of discharges)

9.2.1.8 Motor # 250BC4

Table 9.17: Nameplate data for motor # 250BC4

Make	Power	Stator Voltage	Stator Current	Speed
Hawker Siddeley	250 hp	3300 V	43.7 A	1488 r/min

Table 9.18: Discharge magnitudes for motor # 250BC4

Load and temperature	Phase-A		Phase-B		Phase-C	
PD measured at 75%	+NQN	-NQN	+NQN	-NQN	+NQN	-NQN
load, with the	4	n/a	8	1	6	n/a
temperature of the stator	+Qmax	-Qmax	+Qmax	-Qmax	+Qmax	-Qmax
winding at 53°C, 58°C	3	0	6	0	4	0
and 60°C respectively.						

(See Appendixes C26, for graphical representation of discharges)

9.2.1.9 Motor # 435AA3

Table 9.19: Nameplate data for motor # 435AA3

Make	Power	Stator Voltage	Stator Current	Speed
AEI	435 hp	3300 V	68 A	988 r/min

Table 9.20: Discharge magnitudes for motor # 435AA3

Load and temperature	Phase-A		Phase-B		Phase-C	
PD measured at 90% load, with the temperature of the stator winding at 36°C.	+NQN	-NQN	+NQN	-NQN	+NQN	-NQN
	n/a	2	1	1	1	n/a
	+Qmax	-Qmax	+Qmax	-Qmax	+Qmax	-Qmax
	0	2	0	0	0	0

(See Appendixes C37-C40, for graphical representation of discharges)

9.2.1.10 Conclusion summary

These motors exhibited no or very low levels of PD activity.

9.2.2 Motors tested with significant PD values

9.2.2.1 Motor # 150CL3

Table 9.21: Nameplate data for motor # 150CL3

Make	Power	Stator Voltage	Stator Current	Speed
AEI	150 kW	3300 V	31 A	1483 r/min

Table 9.22: Discharge magnitudes for motor # 150CL3

Load and temperature	Phase-A		Phase-B		Phase-C	
PD measured at 100% load, with the temperature of the stator winding unknown.	+NQN	-NQN	+NQN	-NQN	+NQN	-NQN
	26	22	401	434	181	158
	+Qmax	**-Qmax**	**+Qmax**	**-Qmax**	**+Qmax**	**-Qmax**
	0	0	158	193	100	88

(See Appendixes C3-C6, for graphical representation of discharges)

Table 9.23: Analysis matrix for motor # 150CL3

Condition	Phase-A	Phase-B	Phase-C
Can the graphical data be analysed?	Yes	Yes	Yes
If not, supply reason?	n/a		
Are any discharges centred at the classical discharge position of (45°/225°)?	No	No	No
Does this classical PD have polarity predominance?	n/a	n/a	n/a
Are the negative discharges predominant?	n/a	n/a	n/a

Table 9.23: (Cont.)

Condition	Phase-A	Phase-B	Phase-C
Are the positive discharges predominant?	n/a	n/a	n/a
Is the discharge angle shifted by 30° from the 45°/225° axis?	No	Yes	Yes
Does the two dimensional plot indicate a "hump", as normally associated with phase-phase PD?	Yes	Yes	n/c
Is the relationship between the affected phases, clearly visible on the LPD plot (for the correct phase rotation)?	Yes	Yes	Yes
Are the discharges shifted by 60°/120° from the 45°/225° axis?	No	No	No
Are the discharges occurring at the 0°/180°?	No	No	n/c

Conclusion

The PD appears to be phase-to-phase related:

- Phase-to-phase discharges can occur on the endwinding due to contamination. Contamination can lead to tracking which will eventually lead to a phase-to-phase failure.
- Inadequate spacing/ insulation between coils can lead to discharges between coils causing a build-up of ozone.
- It is however not possible to determine if this is occurring between coils in the slot or on the endwinding.

9.2.2.2 Motor # 160BF2

Table 9.24: Nameplate data for motor # 160BF2

Make	Power	Stator Voltage	Stator Current	Speed
Siemens	160 kW	3300 V	37 A	1471 r/min

Table 9.25: Discharge magnitudes for motor # 160BF2

Load and temperature	Phase-A		Phase-B		Phase-C	
PD measured at 90% load, with the temperature of the stator winding at 52°C, 55°C and 56 °C respectively.	+NQN	-NQN	+NQN	-NQN	+NQN	-NQN
	42	50	41	46	50	31
	+Qmax	-Qmax	+Qmax	-Qmax	+Qmax	-Qmax
	21	25	20	21	42	24

(See Appendixes C8-C12, for graphical representation of discharges)

Table 9.26: Analysis matrix for motor # 160BF2

Condition	Phase-A	Phase-B	Phase-C
Can the graphical data be analysed?	Yes	Yes	Yes
If not, supply reason?	n/a		
Are any discharges centred at the classical discharge position of (45°/225°)?	No	No	Yes
Does this classical PD have polarity predominance?	n/a	n/a	Yes
Are the negative discharges predominant?	n/a	n/a	No
Are the positive discharges predominant?	n/a	n/a	Yes
Is the discharge angle shifted by 30° from the	Yes	No	n/c

Table 9.26: (Cont.)

Condition	Phase-A	Phase-B	Phase-C
45°/225° axis?			
Does the two dimensional plot indicate a "hump", as normally associated with phase-phase PD?	No	No	n/c
Is the relationship between the affected phases, clearly visible on the LPD plot (for the correct phase rotation)?	Yes	Yes	Yes
Are the discharges shifted by 60°/120° from the 45°/225° axis?	No	Yes	No
Are the discharges occurring at the 0°/180°?	n/c	No	No

Conclusion

The PD appears to be phase-to-phase related.

- Phase-to-phase discharges can occur on the endwinding due to contamination. Contamination can lead to tracking which will eventually lead to a phase-to-phase failure.
- Inadequate spacing/ insulation between coils can lead to discharges between coils causing a build-up of ozone.
- It is however not possible to determine if this is occurring between coils in the slot or on the endwinding.

9.2.2.3 Motor # 180CC4

Table 9.27: Nameplate data for motor # 180CC4

Make	Power	Stator Voltage	Stator Current	Speed
Harland	180 hp	3300 V	29 A	980 r/min

Table 9.28: Discharge magnitudes for motor # 180CC4

Load and temperature	**Phase-A**		**Phase-B**		**Phase-C**	
PD measured at 100% load, with the temperature of the stator winding at 28°C.	**+NQN**	**-NQN**	**+NQN**	**-NQN**	**+NQN**	**-NQN**
	66	38	15	30	21	32
	+Qmax	**-Qmax**	**+Qmax**	**-Qmax**	**+Qmax**	**-Qmax**
	32	35	12	28	13	12

(See Appendixes C18-C22, for graphical representation of discharges)

Table 9.29: Analysis matrix for motor # 180CC4

Condition	**Phase-A**	**Phase-B**	**Phase-C**
Can the graphical data be analysed?	Yes	Yes	Yes
If not, supply reason?	n/a		
Are any discharges occurring at the classical discharge position (45°/225°)?	No	No	No
Does this classical PD have polarity predominance?	n/a	n/a	n/a
Are the negative discharges predominant?	n/a	n/a	n/a
Are the positive discharges predominant?	n/a	n/a	n/a
Is the discharge angle shifted by 30° from the 45°/225° axis?	Yes	Yes	Yes
Does the two dimensional plot indicate a "hump", as normally associated with phase-phase PD?	Yes	Yes	Yes
Is the relationship between the affected phases, clearly visible on the LPD plot (for the correct phase rotation)?	Yes	Yes	Yes
Are the discharges shifted by 60°/120° from the 45°/225° axis?	No	No	No
Are the discharges occurring at the 0°/180°?	No	No	No

Conclusion

Phase-to-phase related PD:

- Phase-to-phase discharges can occur on the endwinding due to contamination. Contamination can lead to tracking which will eventually lead to a phase-to-phase failure.
- Inadequate spacing/ insulation between coils can lead to discharges between coils causing a build-up of ozone.
- It is however not possible to determine if this is occurring between coils in the slot or on the endwinding.

9.2.2.4 Motor # 305AA2

Table 9.30: Nameplate data for motor # 305AA2

Make	Power	Stator Voltage	Stator Current	Speed
GEC	380 kW	3300 V	83 A	983 r/min

Table 9.31: Discharge magnitudes for motor # 305AA2

Load and temperature	Phase-A		Phase-B		Phase-C	
PD measured at 45% load, with the temperature of the stator winding at 55°C, 51°C and 55°C respectively.	+NQN	-NQN	+NQN	-NQN	+NQN	-NQN
	140	183	172	232	626	484
	+Qmax	-Qmax	+Qmax	-Qmax	+Qmax	-Qmax
	76	101	121	146	387	289

(See Appendixes C27-C31, for graphical representation of discharges)

Table 9.32: Analysis matrix for motor # 305AA2

Condition	Phase-A	Phase-B	Phase-C
Can the graphical data be analysed?	Yes	Yes	Yes
If not, supply reason?	n/a		
Are any discharges centred at the classical discharge position of (45°/225°)?	No	No	Yes
Does this classical PD have polarity predominance?	n/a	n/a	Yes
Are the negative discharges predominant?	n/a	n/a	No
Are the positive discharges predominant?	n/a	n/a	Yes
Is the discharge angle shifted by 30° from the 45°/225° axis?	No	No	No
Does the two dimensional plot indicate a "hump", as normally associated with phase-phase PD?	No	No	No
Is the relationship between the affected phases, clearly visible on the LPD plot (for the correct phase rotation)?	Yes	Yes	Yes
Are the discharges shifted by 60°/120° from the 45°/225° axis?	No	No	No
Are the discharges occurring at the 0°/180°?	Yes	No	No

Conclusion

Phase-to-phase related PD:

- Phase-to-phase discharges can occur on the endwinding due to contamination. Contamination can lead to tracking which will eventually lead to a phase-to-phase failure.
- Inadequate spacing/ insulation between coils can lead to discharges between coils causing a build-up of ozone.

- It is however not possible to determine if this is occurring between coils in the slot or on the endwinding.

9.2.2.5 Motor # 380AB1

Table 9.33: Nameplate data for motor # 380AB1

Make	Power	Stator Voltage	Stator Current	Speed
GEC	380 kW	3300 V	83 A	983 r/min

Table 9.34: Discharge magnitudes for motor # 380AB1

Load and temperature	Phase-A		Phase-B		Phase-C	
PD measured at 65% load, with the temperature of the stator winding at 61°C.	+NQN	-NQN	+NQN	-NQN	+NQN	-NQN
	129	118	88	62	150	124
	+Qmax	-Qmax	+Qmax	-Qmax	+Qmax	-Qmax
	71	63	38	30	97	73

(See Appendixes C32-C36, for graphical representation of discharges)

Table 9.35: Analysis matrix for motor # 380AB1

Condition	Phase-A	Phase-B	Phase-C
Can the graphical data be analysed?	Yes	Yes	Yes
If not, supply reason?	n/a		
Are any discharges centred at the classical discharge position of (45°/225°)?	Yes	Yes	Yes
Does this classical PD have polarity predominance?	No	Yes	No
Are the negative discharges predominant?	n/a	No	n/a

Table 9.35: (Cont.)

Condition	Phase-A	Phase-B	Phase-C
Are the positive discharges predominant?	n/a	Yes	n/a
Is the discharge angle shifted by 30° from the 45°/225° axis?	No	No	No
Does the two dimensional plot indicate a "hump", as normally associated with phase-phase PD?	No	No	No
Is the relationship between the affected phases, clearly visible on the LPD plot (for the correct phase rotation)?	No	No	No
Are the discharges shifted by 60°/120° from the 45°/225° axis?	No	No	No
Are the discharges occurring at the 0°/180°?	No	No	No

Conclusion

The bulk of the discharges appear to be occurring in the slot portion of the coil.

9.2.2.6 Motor # 435AA5

Table 9.36: Nameplate data for motor # 435AA5

Make	Power	Stator Voltage	Stator Current	Speed
AEI	435 hp	3300 V	68 A	988 r/min

Table 9.37: Discharge magnitudes for motor # 435AA5

Load and temperature	Phase-A		Phase-B		Phase-C	
PD measured at 100% load, with the temperature of the stator winding at 38°C, 40°C and 40°C respectively.	+NQN	-NQN	+NQN	-NQN	+NQN	-NQN
	3	8	17	15	24	15
	+Qmax	-Qmax	+Qmax	-Qmax	+Qmax	-Qmax
	3	6	11	11	14	7

(See Appendixes C41-C45, for graphical representation of discharges)

Table 9.38: Analysis matrix for motor # 435AA5

Condition	Phase-A	Phase-B	Phase-C
Can the graphical data be analysed?	Yes	Yes	Yes
If not, supply reason?	n/a		
Are any discharges centred at the classical discharge position of (45°/225°)?	No	Yes	Yes
Does this classical PD have polarity predominance?	n/a	Yes	Yes
Are the negative discharges predominant?	n/a	No	No
Are the positive discharges predominant?	n/a	Yes	Yes
Is the discharge angle shifted by 30° from the 45°/225° axis?	n/a	No	No
Does the two dimensional plot indicate a "hump", as normally associated with phase-phase PD?	No	No	No
Is the relationship between the affected phases, clearly visible on the LPD plot (for the correct phase rotation)?	n/c	n/c	n/c

Table 9.38: (Cont.)

Condition	Phase-A	Phase-B	Phase-C
Are the discharges shifted by 60°/120° from the 45°/225° axis?	n/c	No	No
Are the discharges occurring at the 0°/180°?	n/c	No	No

Conclusion

- The bulk of the discharges appear to be occurring in the slot portion of the coil.
- The LPD plot indicates phase-to-phase related PD between phases-A&C.

9.2.2.7 Motor # 500BJ1

Table 9.39: Nameplate data for motor # 500BJ1

Make	Power	Stator Voltage	Stator Current	Speed
Siemens	500 kW	3300 V	114 A	1450 r/min

Table 9.40: Discharge magnitudes for motor # 500BJ1

Load and temperature	Phase-A		Phase-B		Phase-C	
PD measured at 80% load, with the temperature of the stator winding at 43°C.	+NQN	-NQN	+NQN	-NQN	+NQN	-NQN
	1025	690	219	333	412	323
	+Qmax	-Qmax	+Qmax	-Qmax	+Qmax	-Qmax
	672	442	139	184	236	198

(See Appendixes C46-C50, for graphical representation of discharges)

Table 9.41: Analysis matrix for motor # 500BJ1

Condition	Phase-A	Phase-B	Phase-C
Can the graphical data be analysed?	Yes	Yes	Yes
If not, supply reason?	n/a		
Are any discharges centred at the classical discharge position of (45°/225°)?	Yes	No	Yes
Does this classical PD have polarity predominance?	No	n/a	Yes
Are the negative discharges predominant?	No	n/a	No
Are the positive discharges predominant?	n/a	n/a	Yes
Is the discharge angle shifted by 30° from the 45°/225° axis?	n/a	n/a	No
Does the two dimensional plot indicate a "hump", as normally associated with phase-phase PD?	n/c	No	No
Is the relationship between the affected phases, clearly visible on the LPD plot (for the correct phase rotation)?	Yes	Yes	n/c
Are the discharges shifted by 60°/120° from the 45°/225° axis?	No	Yes	No
Are the discharges occurring at the 0°/180°?	No	No	No

Conclusion

PD appears to be occurring on the surface of the coil, with some phase-to-phase related activity. The machine was opened for inspection and the coils were found to be skewed in the slots, which left 0.5mm cavities between some of the coils and the core.

9.2.2.8 Motor # 500BJ2

Table 9.42: Nameplate data for motor # 500BJ2

Make	Power	Stator Voltage	Stator Current	Speed
Siemens	500 kW	3300 V	114 A	1450 r/min

Table 9.43: Discharge magnitudes for motor # 500BJ2

Load and temperature	Phase-A		Phase-B		Phase-C	
PD measured at 100% load, with the temperature of the stator winding at 30°C.	+NQN	-NQN	+NQN	-NQN	+NQN	-NQN
	34	18	n/a	25	n/a	20
	+Qmax	-Qmax	+Qmax	-Qmax	+Qmax	-Qmax
	23	17	32	24	15	12

(See Appendixes C51-C55, for graphical representation of discharges)

Table 9.44: Analysis matrix for motor # 500BJ2

Condition	Phase-A	Phase-B	Phase-C
Can the graphical data be analysed?	Yes	Yes	Yes
If not, supply reason?	n/a		
Are any discharges centred at the classical discharge position of visible on the LPD plot (for the correct phase rotation)?	n/c	n/c	n/c
Does this classical PD have polarity predominance?	Yes	Yes	Yes
Are the negative discharges predominant?	No	No	No
Are the positive discharges predominant?	Yes	Yes	Yes

Table 9.44: (Cont.)

Condition	Phase-A	Phase-B	Phase-C
Is the discharge angle shifted by 30° from the 45°/225° axis?	Yes	Yes	Yes
Does the two dimensional plot indicate a "hump", as normally associated with phase-phase PD?	Yes	Yes	Yes
Is the relationship between the affected phases, clearly visible on the LPD plot (for the correct phase rotation)?	n/c	n/c	n/c
Are the discharges shifted by 60°/120° from the 45°/225° axis?	No	No	No
Are the discharges occurring at the 0°/180°?	No	No	No

Conclusion

This machine operates in a very humid environment. The unusual discharge patterns as well as the "humps" on the 2D plot, indicates possible end-winding discharges.

9.2.2.9 Motor # 500BJ3

Table 9.45: Nameplate data for motor # 500BJ3

Make	Power	Stator Voltage	Stator Current	Speed
Siemens	500 kW	3300 V	114 A	1450 r/min

Table 9.46: Discharge magnitudes for motor # 500BJ3

Load and temperature	Phase-A		Phase-B		Phase-C	
PD measured at 100% load, with the temperature of the stator winding at 67°C, 63°C and 60°C respectively.	+NQN	-NQN	+NQN	-NQN	+NQN	-NQN
	26	15	39	24	17	7
	+Qmax	-Qmax	+Qmax	-Qmax	+Qmax	-Qmax
	13	7	19	12	7	4

(See Appendixes C56-C60, for graphical representation of discharges)

Table 9.47: Analysis matrix for motor # 500BJ3

Condition	Phase-A	Phase-B	Phase-C
Can the graphical data be analysed?	Yes	Yes	Yes
If not, supply reason?	n/a		
Are any discharges centred at the classical discharge position of (45°/225°)?	Yes	Yes	Yes
Does this classical PD have polarity predominance?	Yes	Yes	Yes
Are the negative discharges predominant?	No	No	No
Are the positive discharges predominant?	Yes	Yes	Yes
Is the discharge angle shifted by 30° from the 45°/225° axis?	Yes	Yes	Yes
Does the two dimensional plot indicate a "hump", as normally associated with phase-phase PD?	No	No	No
Is the relationship between the affected phases, clearly visible on the LPD plot (for the correct phase rotation)?	n/c	n/c	n/c

Table 9.47: (Cont.)

Condition	Phase-A	Phase-B	Phase-C
Are the discharges shifted by 60°/120° from the 45°/225° axis?	No	Yes	No
Are the discharges occurring at the 0°/180°?	No	No	No

Conclusion

PD appears to be occurring on the surface of the coil.

9.2.2.10 Motor # 950AA3

Table 9.48: Nameplate data for motor # 950AA3

Make	Power	Stator Voltage	Stator Current	Speed
Siemens	950 kW	3300 V	200 A	1484 r/min

Table 9.49: Discharge magnitudes for motor # 950AA3

Load and temperature	Phase-A		Phase-B		Phase-C	
PD measured at 100% load, with the temperature of the stator winding at 67°C, 80°C and 81°C respectively.	+NQN	-NQN	+NQN	-NQN	+NQN	-NQN
	20	29	143	86	17	25
	+Qmax	-Qmax	+Qmax	-Qmax	+Qmax	-Qmax
	11	13	88	57	10	14

(See Appendixes C61-C65, for graphical representation of discharges)

Table 9.50: Analysis matrix for motor # 950AA3

Condition	Phase-A	Phase-B	Phase-C
Can the graphical data be analysed?	Yes	Yes	Yes
If not, supply reason?	n/a		
Are any discharges centred at the classical discharge position of (45°/225°)?	No	Yes	No
Does this classical PD have polarity predominance?	n/a	Yes	Yes
Are the negative discharges predominant?	n/a	No	n/a
Are the positive discharges predominant?	n/a	Yes	n/a
Is the discharge angle shifted by 30° from the 45°/225° axis?	Yes	Yes	Yes
Does the two dimensional plot indicate a "hump", as normally associated with phase-phase PD?	n/c	No	n/c
Is the relationship between the affected phases, clearly visible on the LPD plot (for the correct phase rotation)?	Yes	Yes	Yes
Are the discharges shifted by 60°/120° from the 45°/225° axis?	No	No	Yes
Are the discharges occurring at the 0°/180°?	Yes	No	No

Conclusion

PD appears to be phase-to-phase related:

- Phase-to-phase discharges can occur on the endwinding due to contamination. Contamination can lead to tracking which will eventually lead to a phase-to-phase failure.
- Inadequate spacing/ insulation between coils can lead to discharges between coils

causing a build-up of ozone.

- It is however not possible to determine if this is occurring between coils in the slot or on the endwinding.

9.2.2.11 Conclusion summary for motors tested in the plant

- Motors # 150CC3, 305AA2 and 380AB1 are random wound machines with extensive PD activity situated within the coil. All these motors have been rewound.
- Motor # 500BJ1 is a form coil machine operated in a very humid environment and is experiencing extensive electrical slot discharge activity.

9.3 Winding data

Table 9.51 summarises the winding data of machines tested in the plant.

Table 9.51: Winding data table for machines tested in the plant

Group no	Winding type	Impreg-nation type	Coils	Turns/ coil	Conductor size	Slot width
150CL2	Random	Dip	30	20	1x1.6, 1.32 & 2x1.7	n/a
150CL3	Random	Dip	30	20	1x1.6, 1.32 & 2x1.7	n/a
160BF1	Form coil	Resin Rich	48	14	4.25 x 1.96	12.5
160BF2	Form coil	Resin Rich	48	14	4.25 x 1.96	12.5
160BF3	Form coil	Resin Rich	48	14	4.25 x 1.96	12.5
160BF10	Form coil	Resin Rich	48	14	4.25 x 1.96	12.5
180CC4	n/a	Dip	90	24	3.35 x 2	12
180CC6	n/a	Dip	90	24	3.35 x 2	12
250BC1	Random	Dip	48	11	6 x 1.7	n/a
250BC2	Random	Dip	48	11	6 x 1.7	n/a

Table 9.51: (Cont.)

Group no	Winding type	Impreg-nation type	Coils	Turns/ coil	Conductor size	Slot width
250BC3	Random	Dip	48	11	6 x 1.7	n/a
250BC4	Random	Dip	48	11	6 x 1.7	n/a
305AA2	Form coil	VPI	72	6	3.98 x 2 x 2	11.9
380AB1	Form coil	VPI	72	6	8 x 2	11.9
435AA3	Form coil	VPI	90	6	5.65 x 2.8	n/a
435AA5	Form coil	VPI	90	6	5.65 x 2.8	n/a
500BJ1	Form coil	Resin Rich	48	7	5.6 x 2.8	15
500BJ2	Form coil	Resin Rich	48	7	5.6 x 2.8	15
500BJ3	Form coil	Resin Rich	48	7	5.6 x 2.8	15
950AA3	Form coil	Resin Rich	n/a	n/a	n/a	n/a

CHAPTER 10 – CONCLUSIONS AND RECOMMENDATIONS

10.1 Findings

10.1.1 The relationship between PD magnitudes and type testing

10.1.1.1 Routine PD testing performed at the Test Floor

Of the twenty-one machines tested at the Test Floor, three machines (14%) had no significant PD activity that could be analyzed. The average maximum Qmax values (positive or negative) were 271 mV. PD measurements were taken at an average load and temperature of 108% and 64°C, respectively.

10.1.1.2 PD testing in a plant environment

Twenty machines were tested in a plant environment. Fifty percent of these machines had no significant PD discharge activity. The average maximum Qmax values were 158 mV. PD measurements were taken at an average load and temperature of 83% and 45°C, respectively. The disparity in discharge activity between a machine tested at the Test Floor, and that tested in the plant, could be attributed to the difference in average load and thus temperature.

10.1.2 Relationship between PD magnitudes and coil construction types

Table 10.1 summarizes the PD discharge activities measured in motors with form coil windings with a resin-rich type impregnation system

Table 10.1: Form coil windings with a resin-rich type impregnation system

Group no	Load	Temp.	+NQN	-NQN	+Qmax	-Qmax	Original/ rewound
160BF1	100%	68	5	6	3	3	Original
160BF2	90%	56	50	31	42	24	Original
160BF3	100%	85	12	10	0	0	Original
160BF8	70%	30	n/a	n/a	n/a	n/a	Original
160BF10	70%	54	n/a	n/a	n/a	n/a	Original
160BF11	100%	74	5	2	3	0	Original
200DP2	100%	70	75	18	50	12	Original
500BJ1	80%	43	1025	690	672	442	Original
500BJ2	100%	30	34	18	23	17	Original
500BJ3	100%	63	39	24	19	12	Original
950AA3	100%	80	143	86	88	57	Original

Discharge values for resin-rich type windings are very low. The average PD magnitude is 95 mV. According to results provided by Iris Power Engineering [15, p. 9], it can be seen that up to the year 2001, 90% of the 4 kV machines in their database had Qmax magnitudes of less than 262 mV.

Table 10.2 summarizes the PD discharge activities measured in motors with form coil windings with a vpi type impregnation system

Table 10.2: Form coil windings with a vpi type impregnation system

Group no	Load	Temp.	+NQN	-NQN	+Qmax	-Qmax	Original/ rewound
185CD1	100%	80	57	26	40	0	Original
300AA3	100%	n/a	137	143	39	73	Original
400KW	100%	74	118	91	51	46	Original
435AA5	100%	40	24	15	14	7	Original
220AA5	150%	55	77	66	25	49	Rewound
250BB4	150%	59	68	60	25	28	Rewound
305AA2	100%	n/a	787	463	390	234	Rewound
380AB1	100%	73	893	667	455	330	Rewound
380XX1	100%	67	952	795	540	463	Rewound
435AA3	90%	36	1	1	0	0	Rewound
585AA2	70%	35	297	191	142	68	Rewound

The average PD magnitude is 178 mV. As can be seen from the column above, most of the Qmax magnitudes have a value below 262 mV. Only three of the rewound vpi machines have values exceeding that of the Iris database.

Table 10.3 summarizes the PD discharge activities measured in motors with random wound windings with a Resin-Rich type impregnation system

Table 10.3: Random wound windings with a dip type impregnation system

Group no	Load	Temp.	+NQN	-NQN	+Qmax	-Qmax	Original/ rewound
150CL2	100%	n/a	n/a	n/a	n/a	n/a	Original
240AB3	100%	43	49	44	26	26	Original
250BC1	70%	48	n/a	n/a	n/a	n/a	Original
250BC2	95%	29	n/a	n/a	n/a	n/a	Original
250BC3	150%	87	117	67	63	43	Original
250BC4	75%	58	8	1	6	0	Original
160BB3	150%	60	1314	1747	689	738	Rewound
175BD3	100%	90	1300	1156	878	719	Rewound
150CL3	100%	n/a	401	434	158	193	Rewound
400CE1	100%	57	1525	1219	915	919	Rewound

Discharge values for original random wound dipped machines were very low. Rewound machines had an average PD magnitude of 682 mV.

10.1.3 Correlation between discharge patterns for 3,3 kV machines and established failure mechanisms for higher voltage machines

10.1.3.1 Phase-to-phase related discharges

A large number of the machines (46%), which had significant PD to analyse, showed definite phase-to-phase dependant PD (As can be seen from the LPD plots).

Phase-to-phase related PD would have an expected influence on two failure mechanisms of 3,3 kV machines:

- End-winding contamination
- Inadequate spacing between coils

Phase-to-phase discharges can also occur between coils in the slot (Also identified during the dissection of motor # 250BB3).

10.1.3.2 End-winding contamination

End-winding contamination will normally lead to phase-to-phase discharges (As the end-winding is the knuckle portion of the coil that extends beyond the stator core, and thus away from earth). As was seen in 10.1.3.1, nearly 50% of the discharge activity analysed, was phase-to-phase related. It is however difficult to determine (with certainty), if a machine with phase-to-phase discharge activity is suffering from end-winding contamination.

Motor # 380AB1 had the characteristic "hump" associated with end-winding discharging [3, p. 66] as well as the 30° shift, from the classical position, in discharge phase angle. Motors # 500BJ2 & 500BJ3 has the same symptoms and operates in a very humid environment (It drives main water supply pumps, situated two stories below level, next to the river).

10.1.3.3 Inadequate spacing between coils

Motor # 250CG2 was used for special temperature rise tests at the Test Floor. The machine was expected to be discharging between phases, due to the close proximity of the phase to each other on the endwinding.

The phase-to-phase relationship on the LPD plot is not as well recognisable as for some of the other machines. However, the physical evidence found after the machine was dissected (Figure 8.6), indicated that the machine was discharging between phases on the endwinding.

10.1.3.4 Electrical slot discharge and semicon/grading coating interface deterioration

More than 80% of the machines tested (with discharge activity) at the Test Floor experienced an increase in PD activity with an increase in temperature. The majority of these machines experienced a bigger increase in positive discharges than in negative discharges, indicating that discharging is occurring on the surface of the coil.

Some of the machines (e.g., 400CE1, 400KW GEC & 585AA2) are discharging at the classic phase position, indicating possible slot discharge.

Very few of these machines are fitted with semicon or a grading coating. The increase in the discharge activity due to an increase in temperature could therefore be attributed to discharging in the slot due to the absence of a semicon layer.

10.1.3.5 Improper impregnation

In order to determine without a doubt if a winding was improperly impregnated, the following actions would have to be taken:

- The complete insulating process would have to be inspected for; compatibility of resins and tapes, adherence to minimum requirements for vacuum and pressure cycles where applicable.
- The winding would have to be dissected.

It would be difficult to determine if a machine had high PD due to improper impregnation, if the machine were tested after it was operating for more than a year with a new winding. PD activity could have increased due to thermal deterioration. Motors # 305AA2 and 380AB1 were tested approximately two weeks after it was rewound. There appear to be limited discharging occurring between phases, with the PD activity mainly centred at the classic position (45°/225°). The cavities causing these discharges could possible be attributed to improper impregnation.

10.1.3.6 Loose coils

None of the machines showed any of the expected changes of discharge activity with load.

10.1.3.7 Thermal deterioration

Thermal deterioration is such a long-term failure, that it can normally not be detected in a period of two years.

10.2 Conclusions

- Partial discharge measurement techniques can be used to diagnose certain faults on 3,3 kV machines. It is more effective to determine the condition of random wound motors than form coil motors.
- 3,3 kV machines, under normal operating conditions, experience partial discharge levels that are much lower than that experienced by higher voltage machines.
- The majority of discharge activity in 3,3 kV machines appears to be phase-to-phase related.
- In certain cases (when phase-to-phase discharge is not totally predominant) *end-winding contamination*, *electrical slot discharge and inadequate spacing between coils* could be detected.
    - There is no evidence that *loose coils, thermal deterioration and improper impregnation* can be detected on 3,3 kV motors by using PD measurement techniques.
- Resin-rich machines experience the lowest levels of PD.
- Random wound machines experienced the highest levels of PD.
- Machines that were still fitted with their original windings, had lower levels of PD than rewound machines.

10.3 Final statement and recommendation

This paper proves that although 3,3 kV motors are not subjected to the same amount of PD exposure than the higher voltage motors, the winding design as far as *semiconductor layers, stress relieving tapes and coil spacing* is concerned, should be treated in the same manner as the higher voltage machines.

The industry standard to neclect these protective measures on 3,3 kV motors should be reconsidered.

List of references

1. IEEE 1434 – 2000, IEEE Guide to the Measurement of Partial Discharges in Rotating Machinery.

2. Kreuger, F.H. Partial Discharge Detection in High Voltage Equipment, Butterworths, Londen, 1998.

3. Warren, V. PD Seminar – Volume 1; PD Theory, PD Detection, PD Interpretation and Failure Mechanisms, Proc. Iris Rotating Machine Conference, New Orleans, LA, June 2000.

4. Stone, G.C., Sedding, H.G. and Griffith, G. Experience with on-line Partial Discharge Testing of Motors and Generators, EPRI Utility Motor and Generator Predictive Maintenance and Refurbishment Conference, San Fransisco, December 1993.

5. Sedding, H.G. Basics of Rotating Machine Partial Discharge Testing, Canadian Electrical Association – Fourth International Conference on Generator and Motor Partial Discharge Testing Proceedings, Houston, Texas, May 22-24, 1996.

6. TGA – B: USER MANUAL, Chapter 5, Iris Power Engineering, January 1998.

7. Stone, G.C., Goodeve, T.E., Sedding, G. and McDermid, W. Unusual PD Pulse Phase Distributions in Operating Rotating Machines, IEEE Transactions on Dielectrics and Electrical Insulation, Vol 2 No 4, pp.567-577, 1995.

8. Fenger, M. PD Seminar – Advanced PD Interpretation, Proc. Iris Rotating Machine Conference, New Orleans, LA, June 2000.

9. McAllister, I.W. and Crichton, G.C. Partial Discharge Transients: The Field Theory Approach, Gaseous Dielectrics VIII, Christophorou, L.G. and Olthoff, J.K. eds., Plentum Press, New York, 1988.

10. Gao, G.G., Steinhauser, M. and Chen, W. Using a New PD Measurement Tool to Evaluate the Insulation Life of Adjustable Speed Drive (ASD)-fed Motors, Proc. Iris Rotating Machine Conference, New Orleans, LA, June 2000.

11. Iranaga, H. Practical Analysis of the Problems in the Stator Windings of Industrial Motors Associated to Repair Processes, Proc. Iris Rotating Machine Conference, New Orleans, LA, June 2000.

12. Woodburn, D.R. Stress Control in the Termination of Medium Voltage Power Cables, 29th A.G.M. of the Eastern Cape AMEU, Port Alfred, RSA, June 1986.

13. Warren, V., McDermid, W. and Haines, G. PDA/PPA Testing of Asphaltic-mica Insulation Systems Hydraulic Generating Units, CEA Fourth Motor and Generator PD Conference, Houston, TX, June 1996.

14. Cabanas, M.F., Melero, M.C., Orcajo, G.A., Rodriquez, J.M.C. and Sariego, J.S. Maintenance and Diagnostic Techniques for Rotating Electric Machinery, Marcombo, Barcelona,1999.

15. Warren, V. Partial Discharge Testing: A Progress Report, Proc. Iris Rotating Machine Conference, San Antonio, TX, June 2002.

16. Stone, G.C. Techniques for On-line Partial Discharge testing of Motors and Generators, CEA/Ontario Hydro Conference on Partial Discharge Testing, Toronto, Canada, April 1994.

17. Tétreault, S. Experience with On-Line PD Testing on 4 kV Motors, Iris Rotating Machine Conference, Dallas, Texas, March 1998.

18. Stone, G.C., Campbell, S.R., Sedding, H.G. & Levine, J. A Continuous On-Line Partial Discharge Monitor for Medium Voltage Motors, CEA Fourth Motor and Generator PD Conference, Houston, TX, June 1996.

19. Sasic, M. and Bertenshaw, D. On-Line Partial Discharge Monitoring on MV Motors – Case Studies on Improved Sensitivity Couplers and Interpretation Methods, Adwell International Ltd. Toronto, Canada.

20. Tétreault, S., Stone, G.C. and Campbell, S. Monitoring Partial Discharges in 4 kV Motors, IEEE Petroleum and Chemical Conference, September 1997.